A LOCALIZED, QUANTITATIVE DRUG DELIVERY TOOL FOR NEUROTRANSMISSION STUDIES

Natalie Rios Herr

A dissertation submitted to the faculty of the University of North Carolina at Chapel Hill in partial fulfillment of the requirements for the degree of Doctor of Philosophy in the Department of Chemistry

Chapel Hill
2010

Approved by:

R. Mark Wightman

Royce W. Murray

Gary L. Glish

Regina M. Carelli

Clyde W. Hodge

ABSTRACT

Natalie Rios Herr

A LOCALIZED, QUANTITATIVE DRUG DELIVERY TOOL FOR NEUROTRANSMISSION STUDIES

(under the direction of R. Mark Wightman)

Iontophoresis is the movement of charged molecules in solution under applied current using pulled multibarrel glass capillaries drawn to a sharp tip. The technique is commonly used in neuroscience as a localized drug delivery tool to target select brain regions. A major limitation of the technique is its non-quantitative nature and inherent variability between probes. In this dissertation, iontophoretic delivery has been coupled to fast-scan cyclic voltammetry for real-time monitoring of ejections. The ejection of charged and neutral species has been characterized with carbon-fiber microelectrodes coupled to iontophoresis barrels to reveal the mechanisms underlying drug delivery: iontophoretic and electroosmotic forces. With the use of the neutral, electroactive molecule 2-(4-nitrophenoxy) ethanol (NPE), which is only transported by electroosmotic flow (EOF), electroosmosis (EO) was identified as the major contributor to observed variability from probe to probe. In addition, differences in mobility for charged compounds were positively correlated to differences in electrophoretic mobility as determined by capillary electrophoresis (CE). Thus, CE can be used to predict the rate of transport for compounds that cannot be electrochemically monitored. With this information, quantitative iontophoresis is possible for electrochemically inactive drugs by using a marker molecule. This approach was validated *in vivo* in a well-understood

biological system. Carbon-fiber/iontophoresis probes were used to measure and modulate electrically evoked dopamine release in the striatum of anesthetized rats. Dopamine release in this brain region is highly regulated by autoreceptors and the dopamine transporter. Iontophoretic ejections of an autoreceptor antagonist and a dopamine transporter inhibitor demonstrate that this technique can be used to locally modulate presynaptic release. Additionally, the experiments demonstrate that use of an internal marker molecule do not interfere with the biological results. The final chapters of this dissertation focus on the use of quantitative iontophoresis in novel applications, such as presynaptic regulation of norepinephrine and dopaminergic signaling in awake animals performing behaviors related to drug addiction.

ACKNOWLEDGEMENTS

They say it takes a village to raise a child, and certainly the same can be said for completing a dissertation. I am thankful that I found such a village to help me make this body of work possible. I would like to start by thanking my advisor, Mark Wightman, for his guidance, support, and encouragement throughout the past five years. His depth of knowledge and enthusiasm for discovery has been instrumental to my development as a scientist, and I certainly look forward to our continued interactions as I pursue my own scientific career. I would like to give a special thanks to Dr. Andrew Seipel for providing me the initial iontophoresis training that laid the foundation for the work presented in this dissertation. I am also thankful for my collaborators from the Wightman lab that have contributed to various aspects of this work. Kevin B. Daniel, an honors undergraduate student that I had the pleasure of mentoring, provided experimental help for Chapters 2 and 3. Anna M. Belle, the lucky girl accepting my iontophoresis baton, helped with Chapter 3. Dr. Jinwoo Park and Dr. Zoe McElligott performed some of the experiments presented in Chapter 4. Finally, Dr. Catarina Owesson-White was my collaborator on the freely-moving experiments presented in Chapter 5. I would also like to acknowledge help from the UNC Electronics Facility and the UNC Physics Machine Shop, as well as funding from the NIH, Society for Neuroscience, and NSF.

In addition to being my collaborators, current and past members of the Wightman have been my friends throughout this process, and I am sincerely grateful for having had the opportunity to work with such a great group of people. I am especially thankful to have met Leslie Sombers, Parastoo Hashemi, Zoe McElligott, Catarina Owesson-White,

and Paul Walsh. You all have given me an unconditional friendship which has been key to the completion of this dissertation, so Thank You!

Finally, to my family: thank you for the years of support and encouragement you have given me. To my mother, thank you instilling in me an appreciation for hard work, education, good morals, and love of family and friends. To my father, thank you for teaching me to approach life with curiosity, and to find ways to make things better. To my mother-in-law, Ilene, and grandma, Sandy, thank you for accepting me so wholeheartedly into your family, and being such supporters of me.

And to my biggest supporter, the one that I so eagerly embarked on this graduate school ride with, my husband Joshua Herr: can you believe it's over? I can. And as I think back on the past 5 years, and then the past 9 years, I know that I owe a great deal to you. You have an incredible ability to make me realize that things can be taken one step at a time, and that with your support, and that of our friends, great things are possible. I look forward to our next ride, and the ones after that, and know that just how you helped us through this ride, you'll be there to support, encourage, and guide us through the rest!

TABLE OF CONTENTS

LIST OF TABLES

.

LIST OF FIGURES

LIST OF ABBREVIATIONS AND SYMBOLS

A/D	analog to digital
ACh	acetylcholine
AP	acetaminophen
AP	anterior-posterior
BNST	bed nucleus of the stria terminalis
C	coulomb
CE	capillary electrophoresis
CNS	central nervous system
D/A	digital to analog
DA	dopamine
$[DA]_{max}$	maximal dopamine overflow
DAT	dopamine transporter
DC	direct current
dl	dorsolateral
dm	dorsomedial
DMI	desipramine
DOPA	3,4-dihydroxyphenylalanine
DV	dorsal-ventral
E	applied electric-field,
EC_{5o}	concentration to obtain 50% maximal effect
EO	electroosmosis
EOF	electroosmotic flow
EPI	epinephrine

F	Faraday's constant (96,485 C/mol)
FSCV	fast-scan cyclic voltammetry
GABA	□-aminobutyric acid
HPLC	high pressure liquid chromatography
HQ	hydroquinone
Hz	hertz
i	current (A)
i.p.	intraperiotoneal injection
ICSS	intracranial self-stimulation
IDA	idazoxan
kg	kilogram
L	distance from the inlet to the detection point
LC	locus coeruleus
L_t	total length of capillary
M	molar
M	moles (iontophoretic flux)
MFB	medial forebrain bundle
mg	milligram
min	minutes
ML	medial-lateral
mm	millimeter
mM	millimolar
ms	millisecond
μA	microamperes

µm	micrometer
MSN	medium spiny neuron
N	nomifensine
n	transport number
nA	nanoamperes
NAc	nucleus accumbens
NE	norepinephrine
NET	norepinephrine transporter
nM	nanomolar
NPE	2-(4-nitrophenoxy) ethanol
PEEK	polyetheretherketone
q	iontophoretic flux
Q	quinpirole
q_D	diffusional efflux
R	raclopride
s	seconds
SEM	scanning electron microscopy
t	time
$t_{1/2}$	time required for signal to decay 50%
t_r	retention time
TRIS	tris(hydroxymethyl)aminomethane buffer
UA	uric acid
UV	ultra violet
v	ventral

V	volts
vm	ventral medial
VTA	ventral tegmental area
z	valence charge
ε	permittivity
ζ	zeta-potential formed at the glass capillary-solution interface
v_{eo}	velocity of electroosmotic flow
v_{ep}	rate of migration
v_{obs}	observed linear velocity
η	solution viscosity
μ_{eo}	electroosmotic mobility
μ_{ep}	electrophoretic mobility

Chapter 1

Iontophoresis and its contribution to the study of neurotransmission

Iontophoresis, also known as ionophoresis and microelectrophoresis, is the movement of ions and molecules under the influence of an applied current. The capillaries used for this technique are pulled to a fine tip making them ideal for localized ejection of drugs in biological systems. Iontophoresis has found a niche in neuroscience for the local application of neurotransmitters and drugs to discrete brain regions. It offers significant advantages over other drug delivery methods such as systemic injections, microinjection, and pressure ejection. For example, when a drug is administered systemically it non-selectively targets all regions of the brain possibly activating neuronal circuitry not under study, and thus confounding interpretation of the measured results. Additionally, metabolism of drugs in the periphery can reduce the drug's effects in the brain, and some drugs are unable to pass the blood-brain barrier (Stone, 1985). Microinjection and pressure ejection are two localized drug delivery tools which overcome the above disadvantages of systemic injections, but suffer from their own limitations. When compared to iontophoresis, microinjection and pressure ejection offer much less control over drug delivery, show problems with diffusive leakage, and the volume associated with delivery often causes damage to the tissue (Curtis and Nastuk, 1964). Iontophoresis offers fine control of drug delivery; diffusive leakage can be controlled with retaining currents (or by using high resistance pipettes) and tissue damage is minimal because there is little volume associated with the ejection. The technique is not, however, without disadvantages, and chief among them is the inability

to quantify drug delivery. The experiments carried out in this dissertation are aimed at eliminating these disadvantages and applying iontophoresis to the quantitative study of dopaminergic and norepinephrine neurotransmission in the rat brain.

This chapter will be divided into two main sections. The first will give an introduction to the basic principles of iontophoresis, and include an historical account on the development of iontophoresis. It will conclude with a summary of previous attempts made to quantify drug delivery and how the specific aims in this dissertation have led to quantitative iontophoresis. The second section will focus on neurotransmission of dopamine and norepinephrine in the rat brain. Particular emphasis will be placed on the basic principles of dopaminergic and norepinephrine neurotransmission as it related to signaling in the striatum and bed nucleus of the stria terminalis (BNST). It will close by summarizing the advantages of using iontophoresis and how the development of quantitative iontophoresis will facilitate future studies.

PART 1: IONTOPHORESIS

Basic principles of iontophoresis

Iontophoretic drug delivery relies on the movement of ions under the influence of an applied current. Single or multi-barrel glass pipettes are pulled to a sharp tip, where each barrel is about 1 μm in diameter. Individual barrels are loaded with a drug solution prepared in NaCl to ensure adequate ion flow and an outward current is applied to a glass capillary. A potential difference is established between the ejecting solution and the outside buffer such that ions move in the direction opposite their charge. If a positive current is applied to the capillary, cations will be ejected out of the pipette; similarly, if a negative current is applied, anions will be ejected out of the pipette (Curtis and Nastuk, 1964; Stone, 1985). Figure 1.1 shows a schematic diagram of an iontophoresis probe

containing ions X^+ and Y^-. In the right panel, a positive current is applied to the barrel, causing X^+ to be ejected into solution, and Y^- to be retained. A negative current is applied to the barrel on the left panel, and the ions move in opposite directions to that shown in the right panel.

In addition to the movement of ions due to the application of a current, there is also a significant contribution from electroosmosis (EO), as will be described in detail in Chapter 2. Transport by EO is due to the presence of an electrical double-layer on the surface of the glass capillaries. The glass surface has negative charges on it which attract positive charges. When a potential is applied to the glass capillary, the cations on the surface are attracted to the anode. When a positive current is applied to the capillary, the bulk of the solution will move out of the capillary, carrying with it cations, anions, and neutrals alike. Since this a bulk flow of solution, charged molecules as well as neutral molecules are transported with equal efficiency, unlike when transport is due to the migration of ions. To accurately describe drug delivery by iontophoresis, a distinction must be made between transport that is due to the migration of ions and that due to bulk flow. In this dissertation, the migration of ions will be termed electrophoretic and the movement due to bulk flow will be termed electroosmotic. Thus, observed iontophoresis ejections are due the combination of electrophoretic and electroosmotic processes.

Iontophoresis probes are normally constructed from multi-barrel glass, allowing one of the barrels to serve as a recording electrode. In some cases the barrel is filled with 4-5 mM NaCl and is used to measure voltage changes in response to the application of a drug. For *in vitro* preparations, such as that of the neuromuscular junction, fluctuations in membrane potentials are measured. Measurements by the recording electrode in the CNS are usually of the electrical properties of single neurons,

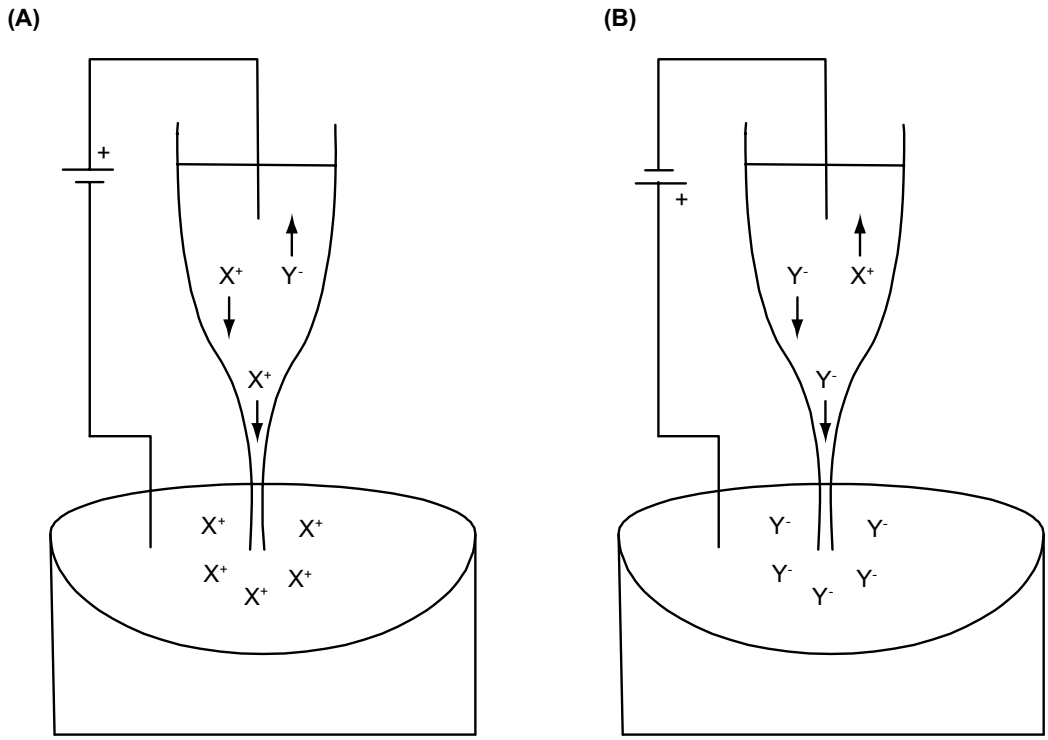

Figure 1.1 Schematic diagram of an iontophoretic barrel containing a salt solution of X+Y-. (A) Positive current is applied to the solution to initiate migration of cations (X+) out of the barrel. (B) A negative current is applied to retain cations (X+), and thus control diffusive leakage. A negative current may also be used to eject a drug which is an anion (Y-) in solution.

with a technique known as extracellular single-unit recordings. Fine metal wires (few microns in diameter) are normally used for extracellular single-unit recordings, and in this case, the wire is inserted into the center barrel and insulated by the surrounding glass. Tungsten and platinum alloys are the most common types of metal used for these measurements. The coupling of a recording electrode to multiple iontophoresis probes allows for quick comparison of the differences or similarities in the measured results due to the application different drugs.

Origin of iontophoresis in neurobiology

Modern neurobiology, as it is studied today, relies on three unifying principles. The oldest and most established principle stems from the work of the neuroanatomist Santiago Ramon y Cajal and is called the "neuron doctrine." This work established the anatomical significance of neurons, showing that neurons are cells, with dendrites, axons, and cell bodies that contain a nucleus. Additionally, it showed that neurons form specialized connections (termed synapses by Sherrington) with other neurons, and that the location and nature of these connections is indicative of the function of a neuron. The electrical properties of neurons are the basis of the second important principle for studying neurons. Alan Hodgkin and Andrew Huxley's seminal experiments in squid giant axons led to the discovery that rapid potential changes at a cell body propagate down an axon to communicate with other neurons downstream. This signal, called an action potential, relies on the opening and closing of ion channels located on neurons, and is a very fast form of communication between neurons. The final principle is that of chemical synaptic transmission. After an action potential propagates down an axon, chemical messengers, termed neurotransmitters, are released which interact with receptors on other neurons. This form of neuronal communication was best demonstrated by the work of Otto Loewi and Sir Henry Dale, who showed that when the

vagus nerve of the frog heart is stimulated it releases chemicals that when put on a non-innervated heart exert the same physiological changes as the stimulation. Later work established that acetylcholine (ACh) was responsible for the observed effects, and it was noted as the first discovered neurotransmitter.

This discovery led to major changes in the study of neurobiology, as scientist became interested in identifying new neurotransmitters and understanding the functional actions of neurotransmitters. It also led to years of heated debates regarding whether synaptic transmission was chemical or electrical in nature. The division between the two camps has become known as the “soup versus spark” controversy, and lasted roughly from 1936 to 1952. Mounting evidence in support of the chemical hypothesis culminated with the finding that synaptic inhibition was mediated chemically by Sir John Eccles, a key proponent of the electrical hypothesis. At this time it became widely accepted that synaptic transmission was chemically mediated, although, later experiments showed that at some cells, electrical transmission occurs. Nonetheless, chemical synaptic transmission, termed neurotransmission henceforth, is the dominating mechanism for neuronal communication, and much research since the 1950s has focused on understanding its principles.

Research on neurotransmission during the years following the “soup versus spark” controversy focused on the actions of ACh at the frog neuromuscular junction, and how the release of ACh affected the muscle’s permeability to different ions. Experiments were carried out in which ACh was applied to the junction by perfusion or diffusion from a microelectrode. However, it was quickly accepted that this form of ACh application was too slow and crude to accurately correlate to the synaptic release of ACh. A need grew for a method to deliver ACh to the junctions locally and quickly. In 1953, William Nastuk published what is widely accepted to be the first account of

iontophoresis (Hicks, 1984). The paper describes the use of pulled glass capillaries filled with ACh that were electrically controlled to deliver ACh directly onto the neuromuscular junction. A recording electrode was placed in close proximity to the pulled glass capillary to measure changes in membrane potential. The work showed that as the pipette approached the end-plate region of the neuromuscular junction, depolarization slowly occurred. It also showed that application of a positive current to the barrels caused the muscle to depolarize and application of a negative current repolarized the muscle (Nastuk, 1953). From these experiments, iontophoresis was born, and later refined by del Castillo and Katz (Del Castillo and Katz, 1955).

Studies on the neuromuscular junction and the initial development of iontophoresis

It was suspected (and supported by indirect findings) that along the neuromuscular junction the end-plate regions would respond with increased sensitivity to ACh as compared to nerve-free regions. The development of iontophoresis made direct testing of this hypothesis possible, and del Castillo and Katz published a paper definitively showing that end-plate regions were more responsive to iontophoretic application of ACh than nerve-free regions (Del Castillo and Katz, 1955). Additionally, they showed that intracellular application of ACh caused no effect, leading them to conclude that receptors are located only on the outer surface of the end-plate. These experiments not only provided valuable insight to the mechanisms of ACh at neuromuscular junctions, but also introduced other researchers to the advantages of iontophoresis and its usefulness for mapping end-plate potentials (Axelsson and Thesleff, 1959; Miledi, 1960; Katz and Miledi, 1964; Peper and McMahan, 1972).

Del Castillo and Katz continued their studies, and published a series of papers describing both advances on the understanding of how ACh (and its agonists and

antagonists) acted at the neuromuscular junction, and how iontophoresis was used in these studies (Del Castillo and Katz, 1956, 1957a, b, c; Del Castillo and Katz, 1957d). The body of this work opened up a whole new area of research using iontophoresis, and it was soon expanded to the CNS and other families of neurotransmitters.

Iontophoresis in the central nervous system

The technique of iontophoresis as it is used today is essentially the same as that described in the paper by David Curtis and Rosamund Eccles, which is the first account of using iontophoresis in the CNS. Using five-barrel pipettes pulled to a fine tip, they loaded four of the barrels with drugs, and the central barrel, filled with 4M NaCl, served as the recording electrode. Each barrel was individually controlled, with positive currents applied to cause ejection and retaining currents applied in between ejections to minimize leakage effects. Importantly, they determined that Renshaw cells can be locally modulated by iontophoresis, and that there is a differential response between some drugs when administered systemically versus iontophoretically. This led them to the conclusion that the blood-brain barrier may have been causing some drugs to seem unresponsive, and that by using iontophoresis this problem was circumvented since application occurs directly onto the receptor sites (Curtis and Eccles, 1958).

From 1960s into the 1980s, largely thanks to the papers published by Curtis, iontophoresis was increasingly used in the CNS to study the pharmacological activity of various drugs at cells in specific brain regions. Research quickly moved beyond studying ACh and into studying all known neurotransmitters and the receptors that they activate. There was particular interest in sensitivity variations from cell to cell, pharmacology of new antagonists, and the mechanism of action. Some of the most commonly studied neurotransmitters with iontophoresis include glutamate, GABA,

acetylcholine, norepinephrine, dopamine, and serotonin. Part 2 of this chapter will discuss neurotransmission of dopamine and norepinephrine.

Quantification of iontophoretic drug delivery

Early on, from del Castillo and Katz's very first papers on iontophoresis, a critical analysis of the practical considerations necessary to use the technique effectively had taken place. The advantages of the technique were immediately apparent: it allows for rapid and local application of ACh, easily simulating the actions of synaptic ACh release to map receptor distributions. They also, however, noted the drawbacks, chiefly that an incomplete understanding of how drug delivery occurred made it difficult to interpret some of the results. In their own words,

> "… the time course and amplitude of the potential change varied a great deal, depending upon such variable factors as the resistance of the ACh pipette and the distribution and accessibility of the receptive spots on the fibre" (Del Castillo and Katz, 1955).

In future papers they noted variability in the electrical properties of the iontophoresis barrels (most likely changes in tip resistance) which led to changes in the magnitude of current and the distance between the tip and tissue necessary to elicit a response with ACh application (Del Castillo and Katz, 1957d). These same findings have been continuously referred to in the literature up to the present-day, and accounts for the technique's eventual decline in popularity (Curtis and Nastuk, 1964; Bradley and Candy, 1970; Bloom, 1974; Hicks, 1984).

Due to the variations observed in neuronal response, a new area of research developed focused on understanding how iontophoretic drug delivery occurred. The first efforts were put toward developing a theory that could predict drug ejection, both as it

traveled down an iontophoretic barrel and once out of the barrel. To describe transport within the barrel, a modified form of Faraday's Law was used where the iontophoretic flux (moles), M, is defined as:

$$M = n\frac{it}{ZF} \tag{1-1}$$

where n is the transport number, i is the current applied (A), t is the ejection time (s), z is valence charge, and F is the Faraday constant (96,485 C/mol) (Purves, 1979). The transport number, n, is determined empirically and refers to the percentage of the total current that the ion carries during ejection. From this simple relationship, it is expected that the amount of delivered material can be predicted by knowing the transport number and the applied current and ejection time, which are controlled by the experimenter. Unfortunately, in practice, this is not the case, as great variability in ejection exists from barrel to barrel. This is likely due to additional contributions in delivery from electroosmosis which is not included in equation 1, and is the focus on Chapter 2.

Determination of transport numbers

Despite the incomplete description of delivery given by equation 1-1, much research was focused on determining the transport number for all the neurotransmitters and drugs most commonly used. This was done by measuring the amount of material delivered *in vitro* using a variety of detection schemes, including bioassays, electrochemistry, and most commonly, radiolabeling assays (Krnjevic and Phillis, 1963b, a; Bradley and Candy, 1970; Purves, 1977; Armstrong-James et al., 1980; Kruk et al., 1980; Armstrong-James et al., 1981). The quantities of material detected were highly variable from barrel to barrel leading to high variability in re ported transport numbers. To account for this, researchers took the average of many electrodes to determine the transport number, although different researchers still obtained different transport

numbers. For example, the transport number determined for norepinephrine ranges from 0.09 to 0.35 over 6 different published reports (Krnjevic et al., 1963; Bradley and Candy, 1970; Hoffer et al., 1971; Barasi and Roberts, 1977; Sasa et al., 1978; Bradshaw et al., 1981). Interestingly, Bradley and Candy found that they obtained significantly different transport numbers for 5-hydroxytryptamine (serotonin) when they used small versus large tip iontophoresis probes (Bradley and Candy, 1970). This seems indicative of the effect electroosmosis and spontaneous diffusion had on the measured transport numbers, and highlights the ineffectiveness of equation 1-1. As will be seen in Chapter 2, electroosmosis contributes significantly to observed iontophoretic ejections. Additionally, increases in tip diameter positively correlate with increases in the amount of electroosmosis observed, further suggesting that this mechanism may account for their observed variability.

Effects of retaining currents

Recognizing that equation 1-1 is an incomplete description of iontophoretic transport within the barrel, Purves derived an expression for iontophoretic flux (q) which included a factor for what he termed "diffusional efflux, q_D" shown in equation 1-2 (Purves, 1979)

$$q = \frac{q_F}{\exp\left(\frac{q_F}{q_D}\right) - 1} \tag{1-2}$$

where q_F is equal to M from equation 1-1. Although this modified equation still does not accurately predict iontophoretic delivery, development of this equation led to a critical analysis of retention currents applied in between ejections, which affect diffusional efflux. From these studies it was noted that the observed ejection is a function of the magnitude of the retention current applied as well as the duration and frequency for which it was applied. A lag in rise-time to reach steady state will be increased with increased

retention time and magnitude, highlighting the importance of knowing the "history of the pipette" (Purves, 1977, 1979, 1980). Intuitively, this makes sense, since application of current opposite in polarity to the ejecting current will cause ions to migrate up the barrel, depleting the solution at the tip of ions for ejection. Because of this, low retention currents are typically applied (5 nA or less of opposite polarity to the ejecting current), and often a "warm-up" period is necessary to replenish the solution at the tip of ions. A warm-up period consists of at least 2 or 3 cycles of ejection and retention to achieve fast rise and decay time courses during experiments. The need to reach an equilibrium between ejection and retention is crucial considering the nature of the experiments typically performed with iontophoresis. For example, one use of iontophoresis is to study receptor-drug interactions, which would be greatly affected by a variable time course in drug delivery.

Other factors affecting iontophoretic delivery

In addition to transport numbers and diffusional efflux, the literature is laced with other factors not included in equations 1-1 or 1-2 that are thought to contribute to iontophoretic delivery (Stone, 1985). Factors such as the concentration of the drug solution and the dimensions of the barrels have obvious implications on the observed ejection. The acidity of the drug solution will affect the solubility of the drug, and will also affect the amount of EOF since there will be more anions on the glass surface at lower pHs. The concentration of drug in solution and the dimensions of the barrel are not expected to affect delivery due to ion migration, but will have a significant effect on diffusional efflux and electroosmosis since both cause a bulk flow of solution. Thus, using higher concentrated drug solutions as well as barrels with larger tips, will lead to larger observed ejections.

Some other factors mentioned include the method used for filling the barrels and the age of the constructed electrode. One can see how these factors may influence drug delivery, but not many reports exist which specifically document their effects. Additionally, the medium into which compounds are iontophoresed will also affect delivery, but this more likely a consequence of transport away from the tip, than the ejection itself. Transport away from the tip has been modeled as diffusion from a point source, and factors such as volume fraction and tortuosity of the brain have been included (Rice and Nicholson, 1995). The extracellular volume fraction of the brain is given the symbol α, and is defined as the fraction of the total brain volume that is extracellular space. In the brain, tortuosity, given the symbol λ, is a measure of how much the movement of substances is hindered by cellular components such as cell bodies or processes.

Real-time monitoring of iontophoretic delivery

Despite the efforts of many researchers, complete understanding of iontophoretic delivery has not been achieved. This is in part due to the complex mechanisms involved in delivery that will undoubtedly influence attempts to quantify delivery based on theory. For this reason it seems that the best alternative for quantifying iontophoretic drug delivery is to monitor drug delivery in real-time. The pioneering design by Millar and co-workers couples iontophoretic barrels to carbon-fiber microelectrodes, for real-time monitoring of electroactive compounds using fast-scan cyclic voltammetry (Armstrong-James et al., 1981). In addition to being able to monitor ejection of electroactive compounds, this design is advantageous because the carbon-fiber microelectrode can also be used to monitor extracellular single-unit activity, as well as the release of electroactive neurotransmitters such as dopamine and norepinephrine.

Specific aim 1

The first aim of this dissertation is to use carbon-fiber iontophoresis probes to gain a better understanding of iontophoretic drug delivery, with particular emphasis on electroosmosis and iontophoretic variability. It is hypothesized that inherent variability in the construction of iontophoresis barrels leads to variability in electroosmotic flow (EOF), ultimately causing variability in the observed iontophoretic ejection. Furthermore, the relative rate of transport of anions or cations, as it compares to transport of a neutral EOF marker molecule will remain the same across barrels. Thus, quantification of iontophoretic delivery for electroinactive drugs is possible by monitoring the rate of EOF and knowing the relative rate of transport for the drugs which can be obtained by capillary electrophoresis. The results and conclusions for this aim are given in Chapter 2.

Specific aim 2

The second aim of this dissertation is to establish a methodology for quantifying the delivery of electroinactive drugs which is compatible with *in vivo* experiments already carried out in the Wightman lab. To accomplish the goal of this aim it was first necessary to test the methodology in a well understood biological system. For this purpose, regulation of dopaminergic autoreceptors and uptake in the striatum of urethane anesthetized rats was chosen, since it has been extensively studied in the Wightman lab (Garris et al., 1994b; Garris et al., 1994a; Jones et al., 1995; Mickelson et al., 1998; Garris et al., 2003; Kita et al., 2007). Part 2 of this introduction will explain dopaminergic neurotransmission and highlight previous findings that will be used to confirm functionality of the iontophoresis method. The results and conclusions from these experiments are given in Chapter 3.

PART II: INTRODUCTION TO NEUROTRANSMISSION OF DOPAMINE AND NOREPINEPHRINE

Neurotransmission is the process by which neurons communicate with one another, though a combination of electrical and chemical signals. The basic structure of a neuron is shown in Figure 1.2. A typical neuron is made up of three basic parts: a cell body, dendrites, and an axon. Similar to other cells in the body, a neuron has a cell body containing a nucleus and all the essential organelles necessary for cellular function. Unique to neurons is the axon and the elaborate arborization of dendrites that originate in the cell body. Dendrites are responsible for receiving information from other neurons, while axons are responsible for sending information. The transfer of information occurs at the synapse, which is where an axon and dendrite meet. Signals are sent through axons in the form of electrical impulses, called action potentials. At the synapse, the axonal ending, called the presynaptic terminal, releases its neurotransmitter onto the dendrites of the post-synaptic cell which furthers neuronal communication.

Dopamine (DA) and norepinephrine (NE) belong to a class of neurotransmitters called catecholamines which contain a catechol moiety and a side chain of ethyl amine. The synthesis of catecholamine neurotransmitters occurs at the terminals of catecholamine neurons and is shown in Figure 1.3. It begins with tyrosine and is terminated with either the synthesis of DA, NE, or epinephrine (EPI), depending on the specialization of the neuron. After synthesis, the catecholamines are packaged into vesicles for subsequent release into the extracellular space in a Ca^{2+}-dependent process which initiates when an action potential depolarizes the presynaptic terminal. The depolarization causes voltage-gated Ca^{2+} channels to open allowing vesicles to fuse with the presynaptic membrane in a process called exocytosis. In this process, vesicles are directed, tethered, and docked to the plasma membrane for a final priming step before

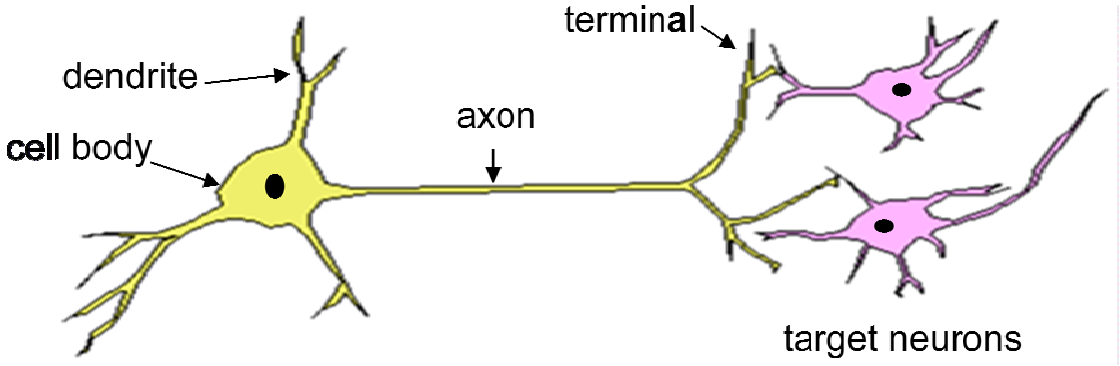

Figure 1.2. Schematic of a typical dopamine neuron. Dendrites, which receive input signals, originate in the cell body of a neuron. An axon transmits electrical signals to terminals which relay information in the form of chemical messengers to their target neurons.

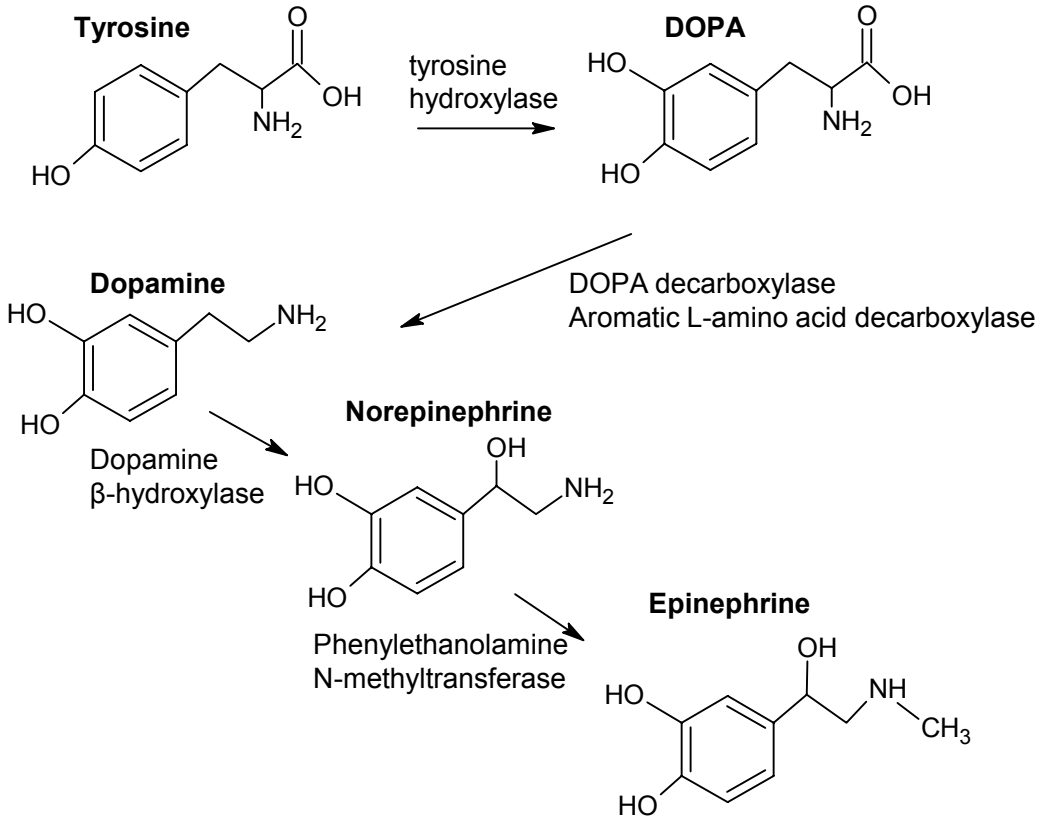

Figure 1.3. Synthesis of catecholamine neurotransmitters. Catecholamine synthesis begins with tyrosine. Tyrosine hydroxylase is the rate-limiting enzyme in the synthesis of catecholamines and is responsible for converting tyrosine to DOPA. Dopamine is synthesized from DOPA, and synthesis of norepinephrine and epinephrine occurs from dopamine at dendritic terminals.

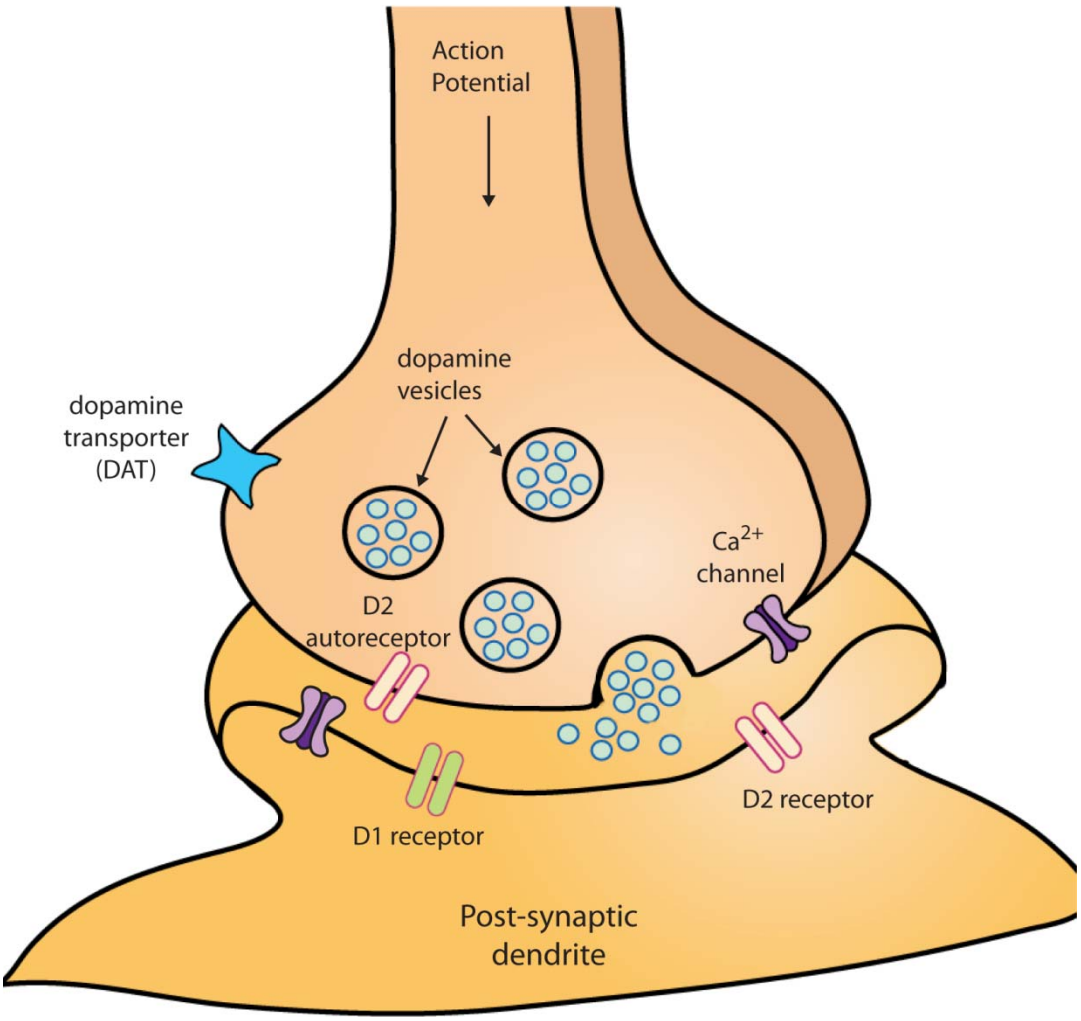

Figure 1.4. Drawing of a dopamine synapse. DA terminals synthesize, package, and process DA for release. Upon invasion of an action potential into the DA terminal, vesicles fuse with the plasma membrane and release their contents in a Ca^{2+}-dependent process called exocytosis. Once released, DA diffuses across the synaptic cleft (and often times outside of the cleft) to reach its targets. Pre-synaptically, DA release is modulated by D2 autoreceptors. Levels of DA in the extracellular space are regulated by the dopamine transporter, which is responsible for recycling DA back into the terminal. Post-synaptically, DA exerts its effects on either D1-like or D2-like receptors.

undergoing fusion and release. Once released, the catecholamine neurotransmitters diffuse in the synaptic cleft to reach their target receptors which may be pre or post-synaptically located. Figures 1.4 shows the basic structure of a DA synapse. NE synapses contain the same basic elements as the DA synapse, but also contain dopamine β-hydroxylase inside vesicles to convert DA to NE. Instead of DAT and D2 autoreceptors, NE terminals express the norepinephrine transporter (NET) and α_2-adrenergic autoreceptors. Post-synaptically they express α- or β-adrenergic receptors.

Dopamine neurotransmission

Dopamine is the most abundant catecholamine in the brain and is involved in many key functions such as locomotion, learning, cognition, and the processing of rewarding stimuli. It has been extensively implicated in drug addiction due to its involvement in motivation and reward. A common model for studying reward-seeking, and by extension drug addiction, is intracranial self-stimulation (ICSS). In ICSS, animals are taught to press a lever to deliver an electrical stimulation to the brain which they find rewarding. These types of experiments established a clear role for DA in reward-seeking behavior, as animals learn to press quicker and press more frequently for stimulations to certain brain regions containing mainly DA neurons (Wise, 2004). However, despite decades of DA research on reward, the exact mechanisms by which DA influences reward-seeking behavior remain unclear. Technological advances continue to further our understanding of DA neurotransmission, and the work presented in this dissertation is aimed at continuing this advancement.

Tools for studying dopamine neurotransmission in vivo

Dopamine neurotransmission can be studied either presynaptically at terminals that release DA, or post-synaptically at the cells to which DA terminals synapse to. Presynaptic release of DA can be studied with a variety of techniques, of which

microdialysis and voltammetry are the most common. Microdialysis is a sampling method that relies on the diffusion of small molecules into a dialysis membrane implanted in the brain region of interest. The dialysate, which is the solution removed from the brain, is externally analyzed using techniques such as liquid chromatography and capillary electrophoresis. This method of detection offers excellent chemical selectivity, and allows multiple analytes to be examined at once. However, despite recent advance, the time-scale of detection (10's of s) remains much slower than the time-scale at which neurotransmitter release occurs (ms) (Robinson et al., 2008; Perry et al., 2009). Due to their catechol moiety, catecholamines are electroactive and can be detected at modest potentials. Electrochemical methods offer increased temporal resolution over microdialysis, but less chemical selectivity. In a recent review, Robinson et al discuss the available tools for studying neurotransmission, including the advantages and disadvantages of both electrochemical and non-electrochemical approaches (Robinson et al., 2008).

Fast-scan cyclic voltammetry at carbon-fiber microelectrodes has emerged as the preferred electrochemical tool for *in vivo* monitoring of dopamine. Carbon-fiber microelectrodes consist of a glass-encased carbon fiber that is ~5 μm in diameter and cut to a length of 50-100 μm. The small dimensions of the probe limit the tissue damage caused by implantation, and allow for mapping of microenviornments within brain regions (Wightman et al., 2007). In the experiments presented in this dissertation, a triangular waveform from -0.4 V to +1.3 V, versus a Ag/AgCl reference electrode is applied at 400 V/s and a frequency of 10 Hz. Due to the presence of a large background current, electrochemical measurements are background subtracted so oxidative and reductive processes of the analyte can be better visualized. For instance, DA is oxidized at +0.6 V and reduced at 0.2 V. The current measured due to the oxidation and

reduction of DA is directly proportional to the concentration of DA found at the site of detection. Thus, FSCV provides a method for the detection of DA release that is quantitative and has high temporal and spatial resolution.

Post-synaptic effects of DA neurotransmission *in vivo* are studied using electrophysiology, namely, extracellular single-unit recordings. As described in Part I of this Chapter, single-unit recordings measure the electrical properties of single neurons that are less than ~50 μm from the recording electrode. Fine metal wires (few microns in diameter) encased in glass are normally used as the recording electrode in these experiments. However, carbon-fiber microelectrodes may also be used for single-unit recordings. This approach offers the significant advantage of being able to monitor pre-synaptic and post-synaptic events in the same experiments. Additionally, as will be the focus of this dissertation, carbon-fiber microelectrodes can also be coupled to iontophoretic drug delivery, making this approach even more advantageous.

Dopamine signaling in the striatum

DA neuron cell bodies are located in the substantia nigra, ventral tegmental area (VTA), and hypothalamus. From there, these neurons project into several areas of the brain, including the prefrontal cortex, hippocampus, and striatum. Projections traveling through the medial forebrain bundle (MFB) innervate the striatum, a DA target involved in the processing of reward. The majority of the cell bodies found in the striatum are medium spiny neurons (MSNs), which contain GABA, the principal inhibitory neurotransmitter in the CNS. In addition to DA innervation, MSNs receive strong inputs from the cortex and thalamus releasing glutamate, the principal excitatory neurotransmitter in the CNS. Thus, the striatum has been proposed to be a processing center responsible for maintaining a smooth flow of signaling. DA in the striatum modulates glutamatergic signaling through dopamine receptors found post-synaptically

on MSN dendrites. However, unlike classical neurotransmission, DA neurotransmission is thought to be both synaptic and extrasynaptic. Morphological and functional evidence suggests that DA is a volume transmitter, that is, it diffuses in the extracellular space for a distance much larger than the synaptic cleft (Zoli et al., 1998). This means that DA modulation of striatal signaling occurs at a variety of sights post-synaptically. Electron microscopy experiments have revealed that DA acts at four anatomically distinct sites: inside the DA synapse, adjacent the DA synapse, inside cortical glutamatergic synapses, and at extrasynaptic sites (Schultz, 1998). A depiction of DA modulation at these sights is shown in Figure 1.5.

Several dopamine receptors have been cloned and are classified into two main subtypes: D1-like or D2-like. The D_1 and D_5 receptors make up the D1-like receptor family and are liked to G_s proteins that activate adenylyl cyclase. Conversely, D2-like receptors inhibit adenylyl cyclase and consist of D_2, D_3 and D_4 receptors. In the striatum, D1 and D2 receptors are found on MSNs, with estimates that ~80% of dopamine receptors are D1 and the other 20% are D2 (Schultz, 1998). Although some reports indicate that D1 and D2 receptors may be co-localized on MSNs, evidence suggests that the majority of MSNs are anatomically segregated. The differing projections have lead to the classification of “direct” and “indirect” striatonigral pathways. MSNs that project to the globus pallidus and substantia nigra express high levels of D1 receptors, and are part of the “direct” pathway. The “indirect” pathway, consisting of neurons that project to an external segment of the globus pallidus (which then project to the substantia nigra), express high levels of D2 receptors (Nicola et al., 2000). Perhaps to compensate for differences in receptor expression, D1 and D2 receptors exist primarily at different affinity states. Although D1 receptors are the most abundant, they are primarily in a low-affinity state, and require relatively high concentrations of DA (μM) for activation. D2

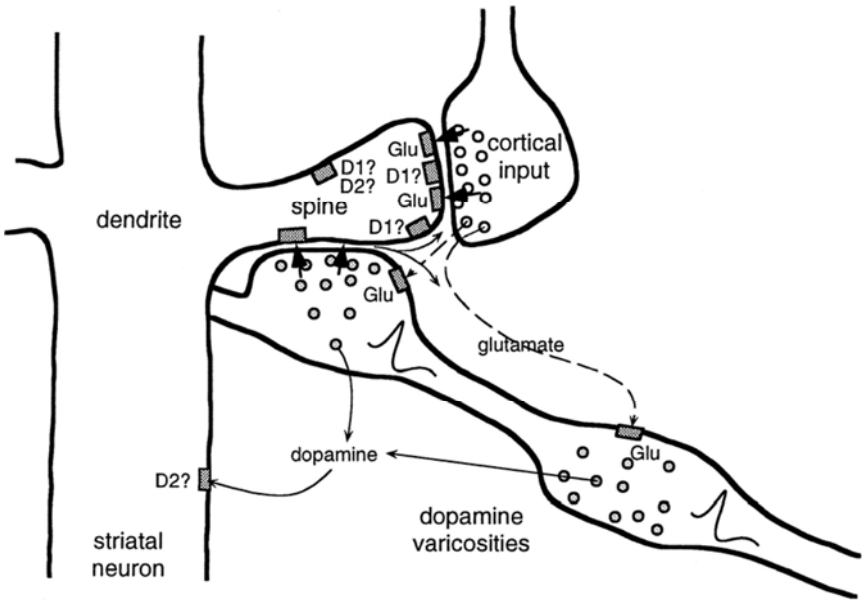

Figure 1.5. Targets of DA signaling in the striatum. DA terminals in the striatum synapse onto the necks of medium spiny neurons, which are GABAergic. MSNs also receive inputs from the cortex in by glutamatergic projections. DA release in the striatum serves to modulate striatal signaling by affecting multiple sites. Within the DA synapse, DA acts on either D1 or D2 receptors. DA will also diffuse out of the synaptic cleft to target adjacent DA targets, and targets within the cortical synapse. Extra-synaptic DA release can modulate signaling by activating D2 receptors found on more distant sites. Additionally, cortical inputs that release glutamate will affect DA release, thereby modulating striatal signaling. (Figure from ref (Schultz, 1998)).

receptors, on the other hand, are typically in a high affinity state and become activated by low concentrations of DA (nM) (Schultz, 1998).

In addition to being found post-synaptically on MSNs, D2 receptors are found presynaptically on DA terminals. These receptors, termed autoreceptors, serve to modulate the release of dopamine. Activation of D2 autoreceptors triggers a series of intracellular events resulting in the inhibition of tyrosine hydrolxylase, the enzyme necessary for dopamine synthesis. It also modulates K+ channels lowering release probability. The net result is a decrease in dopamine release which occurs on a time scale of seconds. Indeed, presynaptic autoinhibition of DA may impact striatal signaling by filtering baseline DA signals and only letting through higher frequency signals (Grace, 2000; Schmitz et al., 2003). Additionally, experiments in anesthetized rats have shown that the duration and range of DA action is directly linked to the activity of the dopamine transporter (DAT), which is responsible for reuptake of DA into the presynaptic terminal (Garris et al., 1994b).

Studying the role of DA in the striatum with iontophoresis

The complex signaling of DA in the striatum has lead many researchers to ask what the exact role of DA in the striatum is. Iontophoresis is uniquely suited for tackling this question because it allows for DA to be directly applied to MSNs. To this end, extracellular single-unit recording in anesthetized animals has been coupled to iontophoresis of endogenous DA. Results from these experiments were sometimes contradictory, but it is now generally accepted that iontophoretically applied DA inhibits MSN firing (White et al., 1995; Hu and White, 1997). However, since spontaneous firing of MSNs in anesthetized rats is generally low, the effects of iontophoretically applied DA was also examined on cells activated by iontophoretically applied glutamate or by stimulation of the cortical inputs . These experiments showed similar results to those

done without glutamate activation, where the application of DA lead to a general decrease in cell firing. It is important to note, though, that this effect has been reported to be dose-dependent, with low amounts of DA actually increasing cell firing, and higher doses decreasing firing (Hu and Wang, 1988; Williams and Millar, 1990; Hu and White, 1997). These findings support the idea that D1 and D2 receptors differentially modulate MSN signaling. Thus, low affinity D1 receptors may be responsible for inhibition, and high affinity D2 receptors may be responsible for activation of striatal signaling.

Work done in awake rats has generally confirmed results obtained from anesthetized rats and suggests that the role of DA in the striatum is to gate incoming glutamatergic signaling and control the level of spontaneous MSN firing or "noise" (Kiyatkin and Rebec, 1997, 1999a, b). Hence, DA is thought to act as a low-pass filter, effectively increasing the "signal-to-noise" of striatal signaling. However, recent evidence demonstrates that glutamate is co-released with DA from DA terminals, further complicating interpretation of the role of DA in the striatum (Stuber et al., ; Chuhma et al., 2009). Indeed, to tease apart the roles of DA and glutamate in the striatum selective and localized pharmacology will be needed. To this end, the use of carbon-fiber microelectrodes coupled to iontophoretic barrels offers several advantages over other recording and drug delivery techniques. First, carbon-fiber microelectrodes can be used to measure presynaptic DA events as well as post-synaptic changes in cell firing. Additionally, quantitative iontophoresis is now possible, thanks to the work presented in Chapters 1 and 2 of this dissertation. The use of this technique has been established in anesthetized rats, and has confirmed its utility for selective and local pharmacological intervention on pre-synaptic processes.

Specific Aim 3

In order to fully understand the role of DA in the striatum it is necessary to examine the system as a whole, including post-synaptic modulation and the resulting effects on behavior associated with striatal signaling. The focus of specific aim 3 is the transfer of quantitative iontophoresis for use in awake rats trained to perform ICSS. Although carbon-fiber microelectrodes coupled to iontophoresis have been previously used in behaving animals, these experiments have focused on post-synaptic events and have not been quantitative (Kiyatkin and Rebec, 1996, 1997, 1999a, b; Windels and Kiyatkin, 2006). Significant challenges are associated with using carbon-fiber iontophoresis probes in behaving rats for DA detection and quantitative iontophoresis. While several challenges have already been overcome, others remain, and are described in Chapter 4.

Norepinephrine neurotransmission

Norepinephrine (NE) belongs to the family of catecholamine neurotransmitters, and is synthesized from DA by the enzyme dopamine β-hydroxylase. It has been implicated in a diverse set of behaviors related to attention and arousal, including drug addiction. However, despite early studies suggesting a role for NE in drug addiction, DA has received the majority of attention. NE cell bodies in the brain are mainly located in the locus coeruleus (LC) and the lateral tegmental noradrenergic fields. The LC is considered the most important noradrenergic nucleus, and projects to various targets including the thalamus, hypothalamus, and cortex. The bed nucleus of the stria terminalis (BNST) is a small nuclei which is part of the extended amygdala and receives dense noradrenergic inputs from the LC as well as other noradrenergic nuclei. The BNST also receives DA inputs from the VTA and periaquaductal grey (PAG), and purportedly sends glutamatergic signals to the VTA. Thus, due to its anatomical

positioning, the BNST has been proposed to be act as a relay center between regions implicated in cognitive processing and those implicated in stress and reward.

NE terminals express α2-adrenergic presynaptic receptors which act as autoreceptors to control release. They also express the NE uptake transporter (NET) which is responsible for recycling released NE back into the terminal. Post-synaptically, α- or β-adrenergic receptors are found. The family of α-adrenergic receptors consists of α1 and α2; the β-adrenergic receptor family consists of β1, β2., and β3 . Unlike D1 and D2 receptors, the post-synaptic effects of α- or β-adrenergic receptor activation has not been extensively studied. On the presynaptic side, the field is just beginning to understand the physiological mechanism by which NE (or DA) affects neurons in the BNST (for review see McElligott and Winder 2009).

Tools for studying norepinephrine neurotransmission in vivo

All the techniques described above for studying DA can be used to study NE neurotransmission. Like DA, NE is electroactive, and can be monitored voltammetrically. The electrochemistry of DA and NE are almost identical, and thus the signals cannot be qualitatively distinguished. For studies involving DA in the striatum, this is typically not a problem since DA is the predominate neurotransmitter released and the area is sufficiently large that exact targeting with microelectrodes can be routinely done. The BNST, however, is a much smaller brain region, spanning just a few hundred microns in its smallest dimension, and contains both DA and NE, depending on the subnuclei being studied. To accurately study neurotransmission in this brain region precise electrode placement is necessary and pharmacology is needed to confirm the identity of the measured signal. A recent study from the Wightman lab showed that NE release from the BNST could be monitored using FSCV and carbon-fiber microelectrodes.

Specific Aim 4

The final goal of this dissertation is to use quantitative iontophoresis coupled to FSCV to probe the mechanisms underlying NE control in the BNST. Previous experiments have demonstrated that α2-adrenergic receptors control NE release. However, it is unknown if these effects are localized to terminal regions in the BNST, or if regulation occurs through a systemic effect. The use of quantitative iontophoresis coupled to FSCV provides evidence that control of NE release by α2-adrenergic receptors is presynaptic. The results from these experiments are shown in Chapter 4. Additionally, catecholamine content in the BNST is a mixture of DA and NE, making specific evaluation of the role of just NE or just DA difficult. The experiments presented in Chapter 4 will highlight the utility of using iontophoresis to quickly determine if the measured signal is mostly NE or DA.

OVERVIEW OF DISSERTATION

The understanding of neurotransmission has greatly increased due to the introduction of technological advancements. Yet, as our understanding increases it becomes apparent that neuronal circuitry is extremely complex, and that further advancements are necessary. The overarching goal of this dissertation is to further the functionality of *in vivo* voltammetric measurements of neurotransmission by coupling the measurements to a quantitative, selective, and localized drug delivery tool, iontophoresis. The first aims of this dissertation concern the development, characterization, and implementation of quantitative iontophoresis coupled to FSCV. The final aims are an attempt to highlight the experimental advantages of using this technique, while probing relevant neurotransmission questions that have been previously unanswered.

REFERENCES

Armstrong-James M, Millar J, Kruk ZL (1980) Quantification of noradrenaline iontophoresis. Nature 288:181-183.

Armstrong-James M, Fox K, Kruk ZL, Millar J (1981) Quantitative ionophoresis of catecholamines using multibarrel carbon fibre microelectrodes. J Neurosci Methods 4:385-406.

Axelsson J, Thesleff S (1959) A study of supersensitivity in denervated mammalian skeletal muscle. J Physiol 147:178-193.

Barasi S, Roberts MT (1977) Responses of motoneurones to electrophoretically applied dopamine. Br J Pharmacol 60:29-34.

Bloom FE (1974) To spritz or not to spritz: The doubtful value of aimless iontophoresis. Life Sciences 14:1819-1834.

Bradley PB, Candy JM (1970) Iontophoretic release of acetylcholine, noradrenaline, 5-hydroxytryptamine and D-lysergic acid diethylamide from micropipettes. Br J Pharmacol 40:194-201.

Bradshaw CM, Pun RY, Slater NT, Szabadi E (1981) A procedure for comparing the mobilities of unlabeled drugs used in microelectrophoresis experiments. J Pharmacol Methods 5:67-73.

Chuhma N, Choi WY, Mingote S, Rayport S (2009) Dopamine neuron glutamate cotransmission: frequency-dependent modulation in the mesoventromedial projection. Neuroscience 164:1068-1083.

Curtis DR, Eccles RM (1958) The excitation of Renshaw cells by pharmacological agents applied electrophoretically. J Physiol 141:435-445.

Curtis DR, Nastuk WL (1964) Micro-electrophoresis. In: Physical Techniques in Biological Research, pp 144-190. New York: Academic Press.

Del Castillo J, Katz B (1955) On the localization of acetylcholine receptors. J Physiol 128:157-181.

Del Castillo J, Katz B (1956) Localization of active spots within the neuromuscular junction of the frog. J Physiol 132:630-649.

Del Castillo J, Katz B (1957a) Interaction at end-plate receptors between different choline derivatives. Proc R Soc Lond B Biol Sci 146:369-381.

Del Castillo J, Katz B (1957b) A comparison of acetylcholine and stable depolarizing agents. Proc R Soc Lond B Biol Sci 146:362-368.

Del Castillo J, Katz B (1957c) The identity of intrinsic and extrinsic acetylcholine receptors in the motor end-plate. Proc R Soc Lond B Biol Sci 146:357-361.

Del Castillo L, Katz B (1957d) A study of curare action with an electrical micromethod. Proc R Soc Lond B Biol Sci 146:339-356.

Garris PA, Ciolkowski EL, Wightman RM (1994a) Heterogeneity of evoked dopamine overflow within the striatal and striatoamygdaloid regions. Neuroscience 59:417-427.

Garris PA, Ciolkowski EL, Pastore P, Wightman RM (1994b) Efflux of dopamine from the synaptic cleft in the nucleus accumbens of the rat brain. J Neurosci 14:6084-6093.

Garris PA, Budygin EA, Phillips PE, Venton BJ, Robinson DL, Bergstrom BP, Rebec GV, Wightman RM (2003) A role for presynaptic mechanisms in the actions of nomifensine and haloperidol. Neuroscience 118:819-829.

Grace AA (2000) Gating of information flow within the limbic system and the pathophysiology of schizophrenia. Brain Res Brain Res Rev 31:330-341.

Hicks TP (1984) The history and development of microiontophoresis in experimental neurobiology. Prog Neurobiol 22:185-240.

Hoffer BJ, Neff NH, Siggins GR (1971) Microiontophoretic release of norepinephrine from micropipettes. Neuropharmacology 10:175-180.

Hu XT, Wang RY (1988) Comparison of effects of D-1 and D-2 dopamine receptor agonists on neurons in the rat caudate putamen: an electrophysiological study. J Neurosci 8:4340-4348.

Hu XT, White FJ (1997) Dopamine enhances glutamate-induced excitation of rat striatal neurons by cooperative activation of D1 and D2 class receptors. Neurosci Lett 224:61-65.

Jones SR, Garris PA, Wightman RM (1995) Different effects of cocaine and nomifensine on dopamine uptake in the caudate-putamen and nucleus accumbens. J Pharmacol Exp Ther 274:396-403.

Katz B, Miledi R (1964) Further Observations on the Distribution of Actylcholine-Reactive Sites in Skeletal Muscle. J Physiol 170:379-388.

Kita JM, Parker LE, Phillips PE, Garris PA, Wightman RM (2007) Paradoxical modulation of short-term facilitation of dopamine release by dopamine autoreceptors. Journal of neurochemistry 102:1115-1124.

Kiyatkin EA, Rebec GV (1996) Dopaminergic modulation of glutamate-induced excitations of neurons in the neostriatum and nucleus accumbens of awake, unrestrained rats. Journal of Neurophysiology 75:142-153.

Kiyatkin EA, Rebec GV (1997) Iontophoresis of amphetamine in the neostriatum and nucleus accumbens of awake, unrestrained rats. Brain Res 771:14-24.

Kiyatkin EA, Rebec GV (1999a) Striatal neuronal activity and responsiveness to dopamine and glutamate after selective blockade of D1 and d2 dopamine receptors in freely moving rats. Journal of Neuroscience 19:3594-3609.

Kiyatkin EA, Rebec GV (1999b) Modulation of striatal neuronal activity by glutamate and GABA: iontophoresis in awake, unrestrained rats. Brain research 822:88-106.

Krnjevic K, Phillis JW (1963a) Acetylcholine-sensitive cells in the cerebral cortex. J Physiol 166:296-327.

Krnjevic K, Phillis JW (1963b) Iontophoretic studies of neurones in the mammalian cerebral cortex. J Physiol 165:274-304.

Krnjevic K, Laverty R, Sharman DF (1963) Iontophoretic release of adrenaline, noradrenaline and 5-hydroxytryptamine from micropipettes. Br J Pharmacol Chemother 20:491-496.

Kruk ZL, Armstrong-James M, Millar J (1980) Measurement of the concentration of 5-hydroxytryptamine ejected during iontophoresis using multibarrel carbon fibre microelectrodes. Life Sci 27:2093-2098.

Mickelson GE, Garris PA, Bunin M, Wightman RM (1998) In vivo and in vitro assessment of dopamine uptake and release. Adv Pharmacol 42:144-147.

Miledi R (1960) The acetylcholine sensitivity of frog muscle fibres after complete or partial devervation. J Physiol 151:1-23.

Nastuk WL (1953) Membrane potential changes at a single muscle endplate produced by transitory application of acetylcholine with an electrically controlled microjet. Fed Proc 102.

Nicola SM, Surmeier J, Malenka RC (2000) Dopaminergic modulation of neuronal excitability in the striatum and nucleus accumbens. Annual Review of Neuroscience 23:185-215.

Peper K, McMahan UJ (1972) Distribution of Acetylcholine Receptors in the Vicinity of Nerve Terminals on Skeletal Muscle of the Frog. Proceedings of the Royal Society of London Series B, Biological Sciences 181:431-440.

Perry M, Li Q, Kennedy RT (2009) Review of recent advances in analytical techniques for the determination of neurotransmitters. Anal Chim Acta 653:1-22.

Purves RD (1977) The release of drugs from iontophoretic pipettes. J Theor Biol 66:789-798.

Purves RD (1979) The physics of iontophoretic pipettes. J Neurosci Methods 1:165-178.

Purves RD (1980) Effect of Drug Concentration on Release from Ionophoretic Pipettes. Journal of Physiology-London 300:P72-P73.

Rice ME, Nicholson C (1995) Diffusion and Ion Shifts in the Brain Extracellular Microenvironment and Their Relevance for Voltammetric Measurements. In: Voltammetric methods in brain systems Voltammetric methods in brain systems, p 27. Totowa, N.J.: Humana Press.

Robinson DL, Hermans A, Seipel AT, Wightman RM (2008) Monitoring rapid chemical communication in the brain. Chem Rev 108:2554-2584.

Sasa M, Igarashi S, Fujiwara H, Inagaki C (1978) Comparison between fluorimetric and radiochemical assays of iontophoretically released noradrenaline from a seven-barreled micropipette. Jpn J Pharmacol 28:639-642.

Schmitz Y, Benoit-Marand M, Gonon F, Sulzer D (2003) Presynaptic regulation of dopaminergic neurotransmission. J Neurochem 87:273-289.

Schultz W (1998) Predictive reward signal of dopamine neurons. Journal of neurophysiology 80:1-27.

Stone TW (1985) Microiontophoresis and Pressure Ejection. London: John Wiley & Sons.

Stuber GD, Hnasko TS, Britt JP, Edwards RH, Bonci A Dopaminergic terminals in the nucleus accumbens but not the dorsal striatum corelease glutamate. J Neurosci 30:8229-8233.

White SR, Harris GC, Imel KM, Wheaton MJ (1995) Inhibitory effects of dopamine and methylenedioxymethamphetamine (MDMA) on glutamate-evoked firing of nucleus accumbens and caudate/putamen cells are enhanced following cocaine self-administration. Brain research 681:167-176.

Wightman RM, Heien ML, Wassum KM, Sombers LA, Aragona BJ, Khan AS, Ariansen JL, Cheer JF, Phillips PE, Carelli RM (2007) Dopamine release is heterogeneous within microenvironments of the rat nucleus accumbens. Eur J Neurosci 26:2046-2054.

Williams GV, Millar J (1990) Differential Actions of Endogenous and Iontophoretic Dopamine in Rat Striatum. The European journal of neuroscience 2:658-661.

Windels F, Kiyatkin EA (2006) Dopamine action in the substantia nigra pars reticulata: iontophoretic studies in awake, unrestrained rats. European Journal of Neuroscience 24:1385-1394.

Wise RA (2004) Dopamine, learning and motivation. Nat Rev Neurosci 5:483-494.

Zoli M, Torri C, Ferrari R, Jansson A, Zini I, Fuxe K, Agnati LF (1998) The emergence of the volume transmission concept. Brain Res Brain Res Rev 26:136-147.

Chapter 2

Electroosmotic flow and its contribution to iontophoretic delivery

INTRODUCTION

Iontophoresis is a technique in which substances are ejected from a micropipette under the influence of an electric field. It is popular among neuroscientists as it can be used for the delivery of specific drugs to highly localized regions of the brain without disrupting ongoing behaviors, a likely consequence of administering the drugs systemically (Overton and Clark, 1992; Shen et al., 1992; Pierce and Rebec, 1995; Kiyatkin and Rebec, 1996, 1997; Kiyatkin et al., 2000; Windels and Kiyatkin, 2006; Cheer et al., 2007). Despite the advantages of this approach, it is difficult to determine the amount of drug ejected, and thus the technique is typically considered to be non-quantitative (Bloom, 1974; Purves, 1980a). Ejections have been evaluated by correlating the potency of a drug (as determined by other preparations) to various ejection currents (Clarke et al., 1974). Although this methodology can produce adequate dose-response curves, it assumes that the drug acts with similar potency in the brain of an intact animal as in other preparations such as brain slices and cell cultures. This assumption is likely not valid due to the complex chemistry of the brain.

During iontophoresis, ejection of charged substances is a consequence of two processes: electroosmosis and migration (Curtis, 1964). As such, the observed rate of ejection is governed by the observed linear velocity (v_{obs}) that is defined by

$$v_{obs} = v_{eo} + v_{ep} \tag{2.1}$$

where v_{eo} is the velocity of electroosmotic flow and v_{ep} is the rate of migration. Each of these velocities is further dependent on the individual mobilities as defined by:

$$v_{eo} = \frac{-\varepsilon\zeta}{\eta}\mathrm{E} = \mu_{\mathrm{eo}}\mathrm{E} \tag{2.2}$$

$$v_{ep} = \mu_{ep}\mathrm{E} \tag{2.3}$$

where μ_{ep} and μ_{eo} are the mobilities of migration and electroosmosis, respectively, E is the applied electric-field, ε is the permittivity, ζ is the zeta-potential formed at the glass capillary-solution interface, and η is the solution viscosity.

The role of electroosmosis on the ejection of species from iontophoretic barrels has been controversial. Early experiments were unable to confirm a major contribution of electroosmosis (Krnjevic et al., 1963). In contrast, Szabadi and co-workers used radioactivity measurements to show that the neutral molecule glucose could be ejected iontophoretically with an efficiency that was 23% of the ejection of norepinephrine, a monovalent cation under their conditions (Bevan et al., 1981). Furthermore, electroosmosis has also been documented during transdermal iontophoresis (Scott et al., 1993; Volpato et al., 1995; Bath et al., 2000; Guy et al., 2000).

When electroosmosis is ignored, ejection is due solely to migration and the number of moles (M) ejected is defined as:

$$M = \mathrm{n}\frac{iT}{zF} \tag{2.4}$$

where n is the transport number (a number empirically determined that describes the percentage of total current that the compound of interest carries), i is the applied current, T is the time, z is the charge, and F is Faraday's constant (Stone, 1985). From this

relationship, one expects that if the transport number is known, quantitative predictions of the amount ejected can be made by controlling the applied current and time. In practice, great variability exists in the amount ejected from barrel to barrel despite using the same applied current, time, and solution conditions. Consequently, a direct measurement of the amount ejected is necessary for quantitative analysis, since the relationship given in equation (4) is an incomplete description of mass transport during iontophoresis.

Numerous approaches have been used to quantify iontophoresis directly using techniques such as fluorescence, radioactivity, and electrochemistry (Krnjevic et al., 1963; Bradley and Candy, 1970; Clarke et al., 1974; Dionne, 1976; Purves, 1977, 1979; Armstrong-James et al., 1980; Kruk et al., 1980; Purves, 1980b; Armstrong-James et al., 1981; Bevan et al., 1981; Gerhardt and Palmer, 1987; Rice and Nicholson, 1989; Fu and Lorden, 1996; Bunin et al., 1998). For example, ion-selective microelectrodes were used to monitor ejections of acetylcholine from nearby iontophoretic pipettes. This was done by measuring changes in potential at the ion-selective electrodes due to the introduction of acetylcholine to the bath solution. The study showed that the rate of acetylcholine ejection varied for different iontophoresis barrels, thus requiring calibration for each pipette barrel (Dionne, 1976). Purves did extensive work using a cationic fluorescent molecule, quinacrine, which showed similar results. He also showed that release from iontophoretic pipettes is time-dependent and is influenced by “the history of the pipette” – meaning it is affected by the retaining current applied previous to ejection (Purves, 1977, 1979; Purves, 1980a; Purves, 1980b). Carbon-fiber microelectrodes have been used to effectively monitor the ejection of catecholamines in vitro and in vivo, but this technique is limited to electroactive substances (Armstrong-James et al., 1980; Kruk et al., 1980; Armstrong-James et al., 1981).

In the present work, we further examined the role of electroosmosis in iontophoresis using carbon-fiber microelectrodes to monitor the ejection of electroactive compounds as described by Millar et al (Armstrong-James et al., 1980; Kruk et al., 1980; Armstrong-James et al., 1981). By using neutral and charged compounds with distinct electrochemical signals we monitored the rate of ejection for each separately. This approach allowed us to determine the relative contribution of electroosmosis to the ejection of various charged compounds. Our findings indicate that electroosmosis plays a significant role, accounting for over 30% of the total ejection observed for cationic compounds and 80% for anionic compounds. For each compound tested, the rate of electroosmotic flow (EOF) relative to the observed ejection remained constant, suggesting that the variability in the absolute amount ejected from different pipette barrels is due to changes in the amount of EOF present. Furthermore, differences in iontophoretic mobility were correlated with differences in electrophoretic mobility, as determined by capillary electrophoresis.

MATERIALS AND METHODS

Chemicals.

Unless noted, all chemicals were purchased from Sigma-Aldrich (St. Louis, MO) and used as received. Solutions were prepared using doubly distilled deionized water (Megapure system, Corning, NY). A physiological buffer solution, pH 7.4, (15 mM TRIS, 126 mM NaCl, 2.5 mM KCl, 25 mM $NaHCO_3$, 2.4 mM $CaCl_2$, 1.2 mM NaH_2PO4, 1.2 mM $MgCl_2$, 2.0 mM Na_2SO_4) was used in all electrochemical experiments.

Iontophoresis Probes.

Multi-barrel (3 or 5) probes were constructed by fusing a single-barrel glass capillary (A-M Systems, Carlsborg, WA) to a multi-barrel (2 or 4) glass capillary that

contain filaments that aid in filling the barrel by capillary action (A-M Systems, Carlsborg, WA and Stoelting Co., Wood Dale IL). The single barrel was loaded with a carbon fiber (T-650, Thornel, Amoco Corp., Greenville, SC). The capillaries were bundled together with heat shrink and were tapered to a tip of about 1 μm in diameter using a micropipette puller (Narashige, Tokyo, Japan) with a two-step twist and pull process. The protruding carbon fiber was cut to a length between 30 and 50 μm. Before use, barrels containing the carbon fiber were backfilled with electrolyte (4 M potassium acetate, 150 mM potassium chloride) and fitted with wires for electrical contact. A silver/silver chloride electrode served as the reference. Empty barrels for iontophoresis were filled with analyte solutions prepared in 5 mM NaCl at pH 5.8. An electron micrograph and drawing of the assembly with 2 and 4 iontophoretic barrels is shown in Figure 2.1.

Data Acquisition.

Cyclic voltammograms were acquired using data-acquisition hardware and local software written in LabVIEW (National Instruments, Austin, TX). The cyclic voltammetry waveform was generated and the voltammetric signal was acquired with an A/D, D/A board, the PCI-6052E (National Instruments). A PCI-6711E D/A board (National Instruments) was used to synchronize waveform application, data acquisition, and to trigger the iontophoretic current applied and the loop injector in the flow injection apparatus. The voltammetric waveform was input into a custom-built instrument for application to the electrochemical cell and current transduction (University of North Carolina at Chapel Hill, Department of Chemistry Electronics Facility). After collection,

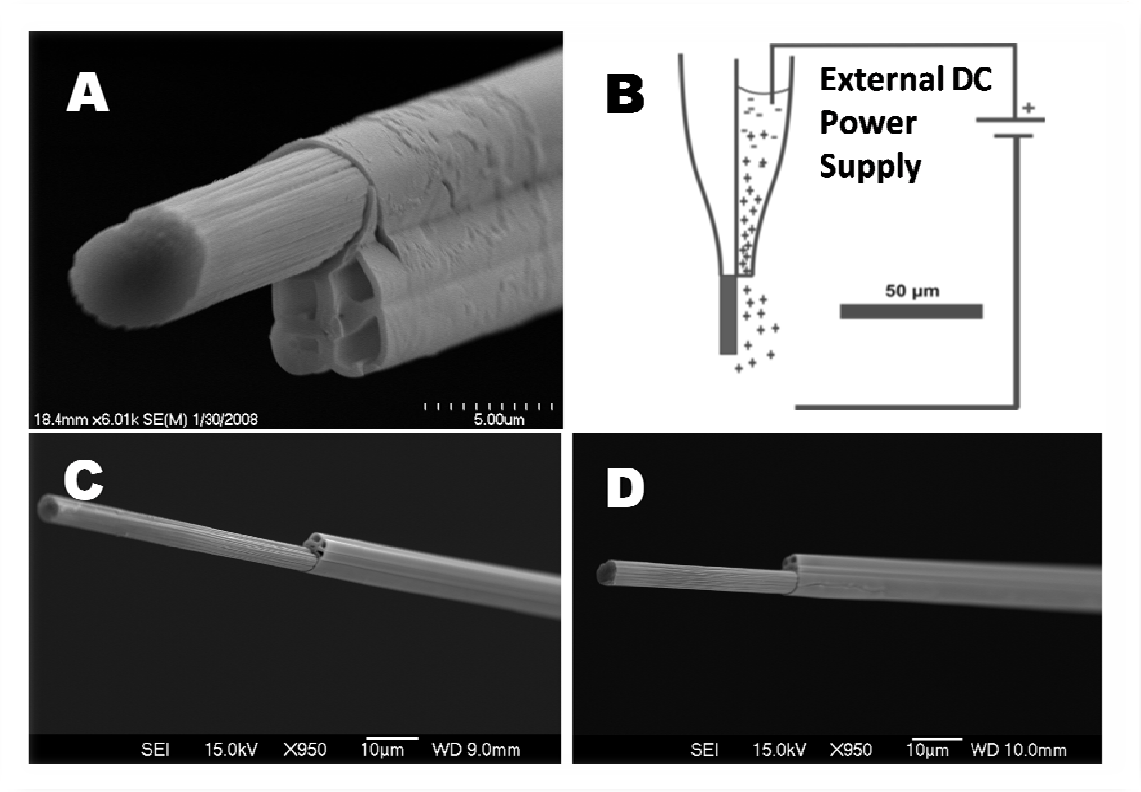

Figure 2.1. SEM images and schematic of carbon-fiber iontophoresis probe. A) Close up showing the empty iontophoretic barrels of a 5-barrel probe. B) a DC power source is used to apply positive or negative current to solution-filled barrels for iontophoretic ejection. C-D) Carbon-fiber iontophoresis probes made by fusing a single barrel containing a carbon fiber to either 4 (shown in C) or 2 (shown in D) empty barrels.

background subtraction, signal averaging, and digital filtering (low pass filtered at 1 kHz) were all done under software control.

For most experiments, a triangular waveform was applied with a scan rate of 200 V s^{-1} with a rest potential of -0.7 V versus Ag/AgCl between scans, an initial scan to -1.3 V, followed by an excursion to 1.0 V, and a scan to the rest potential. The scans were repeated every 100 ms. These parameters were chosen to maximize separation of peaks for the analytes being studied.

Iontophoresis Ejections.

Multi-barrel iontophoresis probes with a carbon-fiber microelectrode (Figure 2.1) were used to eject and detect the analytes that were made up as 10-12 mM solutions in 5 mM NaCl at pH 5.8 unless otherwise noted. Positive currents (average of 5 to 40 nA) delivered by a constant current source designed for iontophoresis experiments (Neurophore, Harvard Apparatus, Holliston, MA) were used to eject the various analytes. For each barrel, an appropriate ejection current was determined by first performing 30 second test ejections until a signal sufficient for analysis was measured (average of -5 to -30 nA at the reduction potential of NPE). In some of the experiments, a retaining current of -5 nA was applied between ejections. For all remaining experiments, a current of 0 nA was applied between ejections.

Flow Injection Apparatus.

The electrode was positioned at the outlet of a six-port rotary valve[37]. A loop injector was mounted on an actuator (Rheodyne model 7010 valve and 5701 actuator) that was used with a 12-V DC solenoid valve kit (Rheodyne, Rohnert Park, CA) to introduce the analyte to the surface of the electrode. The linear flow velocity (1.0 cm s^{-1})

was controlled with a syringe infusion pump (Harvard Apparatus model 940, Holliston, MA).

Special considerations were necessary because oxygen can be detected with the waveform used. Therefore, PEEK® tubing (Upchurch Scientific, Oak Harbor, WA) and glass syringes were used to limit oxygen interference, and all solutions were degassed with nitrogen before use.

HPLC Experiments.

Iontophoretic ejections were made into a 500 µL volume of 0.1 N perchloric acid. HPLC injections (10 µL) were made onto a reverse phase column (C-18, 5 µm, 4.8 x 250 mm, Waters symmetry 300). The mobile phase (prepared in HPLC grade water) contained 0.1 M citric acid, 0.1 mM EDTA, and 1 mM hexyl sodium sulfate, pH 3.5 and 10% organic modifier (methanol). Analytes were detected with a thin-layer radial electrochemical flow cell (BASi, West Lafayette, IN USA), with the working electrode at 0.7 V vs. the Ag/AgCl reference. Data was collected using a custom written LabVIEW program (Courtesy of Professor James Jorgensen, UNC-CH). Peak areas were calculated using statistical moments regression (Igor Version 5.0). Differences in detection efficiency were normalized for by using a response ratio for each analyte.

Capillary Electrophoresis Experiments.

These were performed using a HP^{3D}CE system (Agilent Technologies) equipped with an on-column diode-array detector, an auto-sampler and a 30 kV power supply. CE Chemstation (Agilent Technologies) was used for CE control, data acquisition and handling. The separation was performed in a 50 µm fused silica capillary 96.0 cm in total length, and 87.5 cm to the UV detector. All experiments were carried out in cationic mode (the anode at the inlet and cathode at the outlet). Samples were run at a

concentration of 2 mM in 17 mM PBS (phosphate buffered saline, made up of 0.25% monosodium phosphate and 0.04% disodium phosphate) with a pH of 5.8 to keep constant with the buffer conditions used for the iontophoresis experiments. UV detection was measured at 195 and 240 nm. The electrophoretic mobility was calculated as:

$$\mu_{ep} = \left(\frac{L}{t_r}\right)\left(\frac{L_t}{V}\right) \quad (5)$$

where L is the distance from the inlet to the detection point, t_r is the time required for the analyte to reach the detection point, V is the applied voltage, and L_t is the total length of the capillary (Skoog et al., 2007).

RESULTS AND DISCUSSION

Construction of carbon-fiber iontophoresis probes.

Initially, probes were constructed using only multi-barrel glass by loading one barrel with a carbon fiber and then pulling the assembly to a fine tip. Although this approach provided adequate results, it had two disadvantages. First, multi-barrel glass comes either with or without filaments. The filaments are needed for backfilling solutions into the barrels for iontophoresis. However, when the carbon fiber is placed in one of these filament-containing barrels, it can reduce the quality of the carbon fiber- glass seal which will increase the magnitude of the cyclic voltammetric background current. Second, some of these probes exhibited electrical cross-talk between the iontophoresis barrels and the barrel containing the carbon-fiber. We believe this is due to the thin glass that separates the barrels, which when filled with ionic solutions, allows capacitive coupling.

To remedy these problems, we modified our construction techniques by using multi-barrel, filament glass for iontophoresis, and then fusing a separate single barrel

capillary to it (without a filament) for electrochemical detection. This improved the carbon-fiber glass seal and electrical crosstalk was much less likely to be seen. This procedure allows fabrication of any number of configurations using 2, 3, and 4-barrel glass, and we have seen no difference in performance. Images of a 2 and 4-barrel capillary fused to single capillary containing a carbon-fiber microelectrode are shown in Figure 2.1.

Quantitative iontophoresis of electroactive compounds.

We were able to monitor iontophoretic ejections in real-time by coupling iontophoresis with fast-scan cyclic voltammetry (Figure 2.1). Figure 2.2 shows consecutive ejections of 10 mM dopamine with an applied iontophoretic current of 10 nA and a retaining current of -5 nA. The ejections are fairly reproducible and show fast time responses. As seen from the cyclic voltammogram, the expected signature peak from the oxidation of dopamine occurs at around 0.6 V. After calibration, the oxidation current was converted to dopamine concentration, which shows that for 10 nA of iontophoretic current, the signal at the carbon-fiber surface is equivalent to that found in a 5 μM dopamine solution. In reality, the concentration along the electrode length varies with the concentration (10 mM) of dopamine within the barrel at the micropipette tip, to progressively lower concentrations down the length of the cylindrical electrode. This concentration profile approximates the dilution expected for ejection from a point source (Nicholson et al., 1979).

To characterize the role of electroosmosis in iontophoretic ejections, we chose a neutral, electroactive compound to serve as a marker for EOF. Considerations such as pK_a, solubility in water, and lack of voltammetric overlap with dopamine limited the

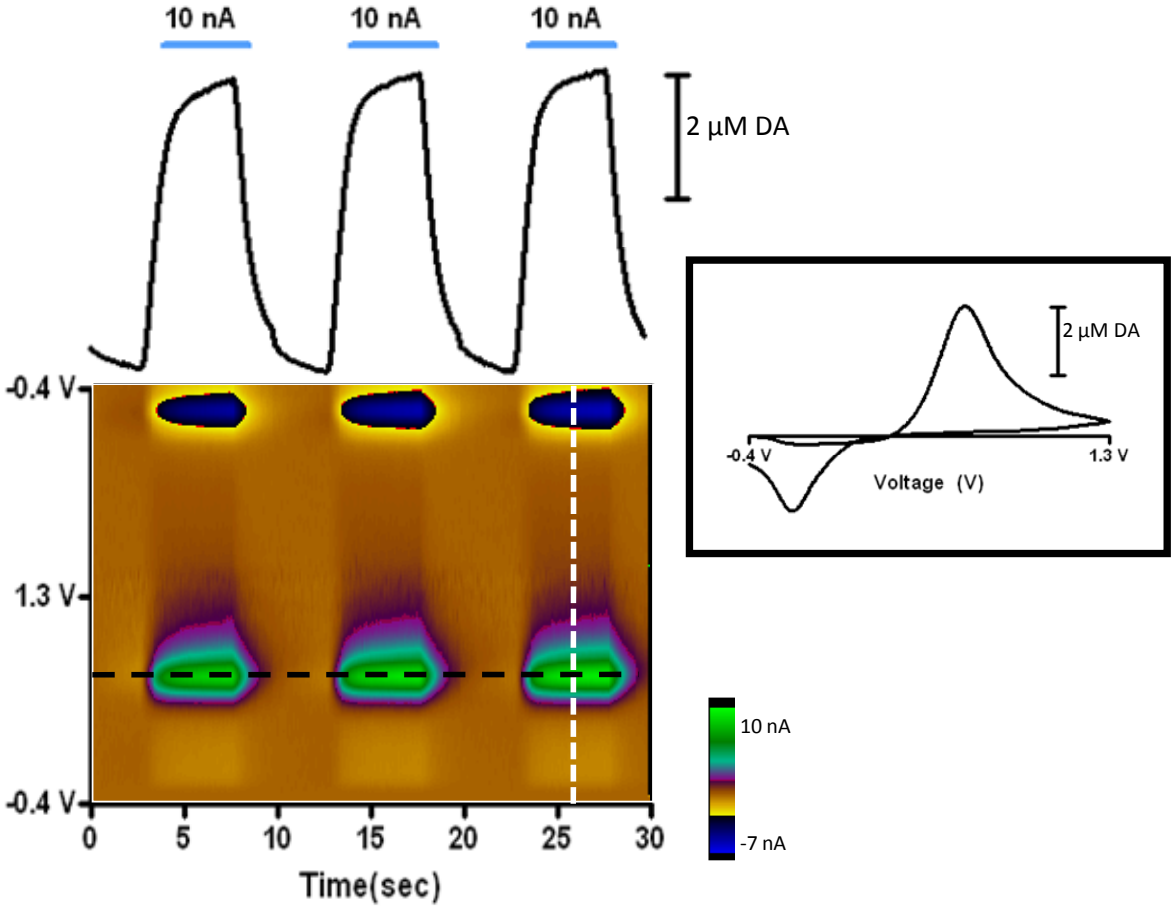

Figure 2.2. Analysis of consecutive iontophoretic ejections of dopamine. Carbon-fiber iontophoresis probes were used to eject a solution of dopamine cations at pH 5.8 into a solution of TRIS buffer at pH 7.4. Upper left: Solid line represents the concentration of dopamine measured at its oxidation potential of 0.6 V vs. time trace obtained for three consecutive 10 nA ejections at times indicated by the horizontal bars. Lower left: Color representation of the iontophoretic ejections shown, with applied voltage at the carbon fiber plotted vs. time and the current measured in response to dopamine ejection plotted in false color. Right: Cyclic voltammogram obtained at the time indicated by the white dashed line in the color plot.

options available. The pK_a determines whether the molecule is neutral at the pH values used during experimentation. Solubility in water is essential because it is the preferred solvent for making up drug solutions typically used in iontophoresis; other solvents can affect EOF and may also be toxic when used in biological experiments. The EOF marker must be voltammetrically different from dopamine so that the signals from each can be resolved. With all of these prerequisites in mind, we chose 2-(4-nitrophenoxy) ethanol as the EOF marker for the experiments performed with FSCV (Figure 2.3).

Figure 2.4 illustrates iontophoretic ejections of a mixture of dopamine and NPE at equal concentrations (10 mM). The pH of this solution is 5.8, at which NPE is neutral and dopamine is a monocation. Ejection of both of these compounds confirms that EOF plays a role in iontophoresis since the only mechanism for ejection of NPE is electroosmosis. Much like the results for dopamine, ejections of NPE are reproducible and rapid. As seen from the cyclic voltammogram, the oxidation of dopamine can be seen at around 0.6 V, whereas the reduction of NPE can be seen at about -1.2 V, facilitating the quantification of both species. Because dopamine is charged, its ejection should be due to iontophoretic forces and electroosmosis; consistent with this expectation more dopamine (~14 μM) than NPE (~6 μM) is detected at the electrode surface.

Variability in iontophoresis.

Although ejections are reproducible for a given barrel (demonstrated in Figures 2.2, 2.3, and 2.4), there is substantial variability when ejections from various barrels are compared to one another for a given iontophoretic current. The top panel of Figure 2.5 shows NPE ejections from 5 different iontophoretic barrels containing the same solution (10 mM NPE). The apparent concentration recorded with the cylindrical electrode is

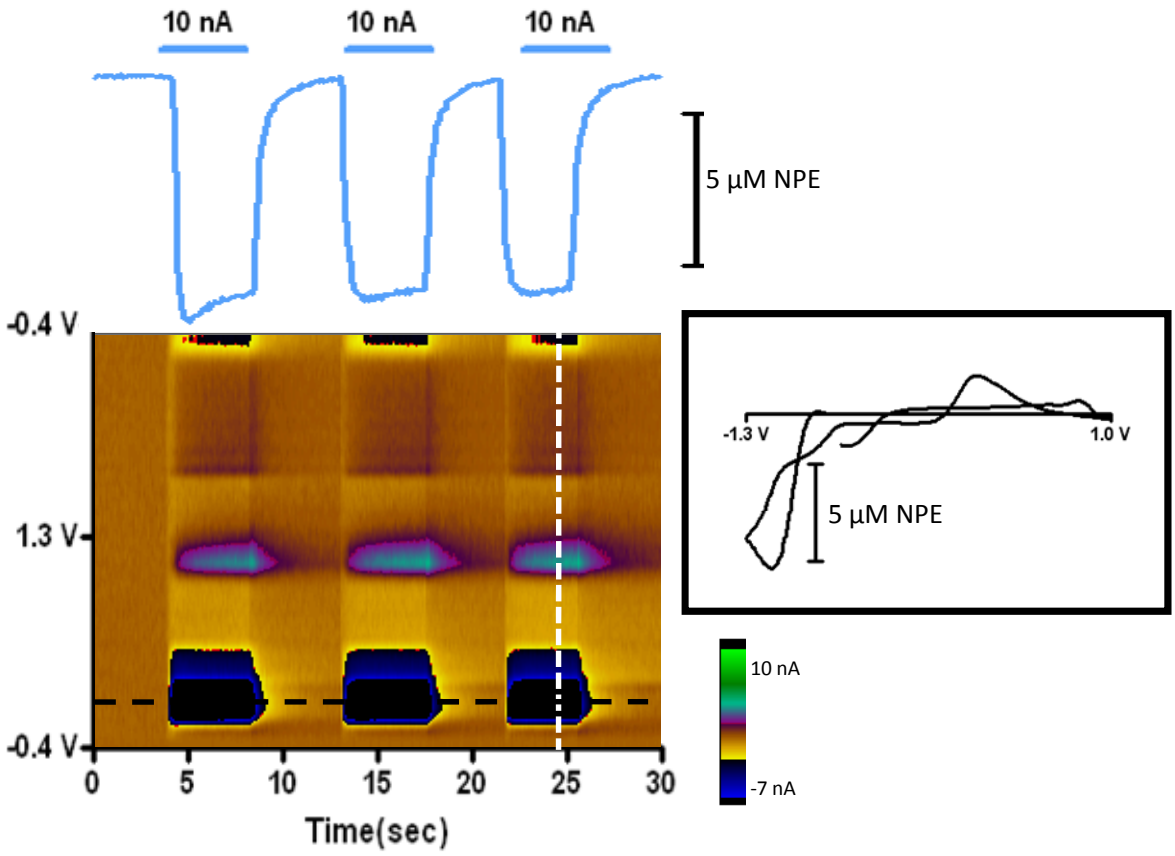

Figure 2.3. Analysis of consecutive iontophoretic ejections of a neutral marker compound, NPE. Carbon-fiber iontophoresis probes were used to eject a solution of NPE at pH 5.8 into a solution of TRIS buffer at pH 7.4. Upper left: The solid line represents [NPE] at -1.2 V (light blue solid line) measured vs. time trace obtained for three consecutive 10 nA ejections at times indicated by the horizontal bars. Lower left: Color representation of the iontophoretic ejections shown, with applied voltage at the carbon fiber plotted vs. time and the current measured in response to NPE ejection plotted in false color. Right: Cyclic voltammogram obtained at the time indicated by the white dashed line in the color plot.

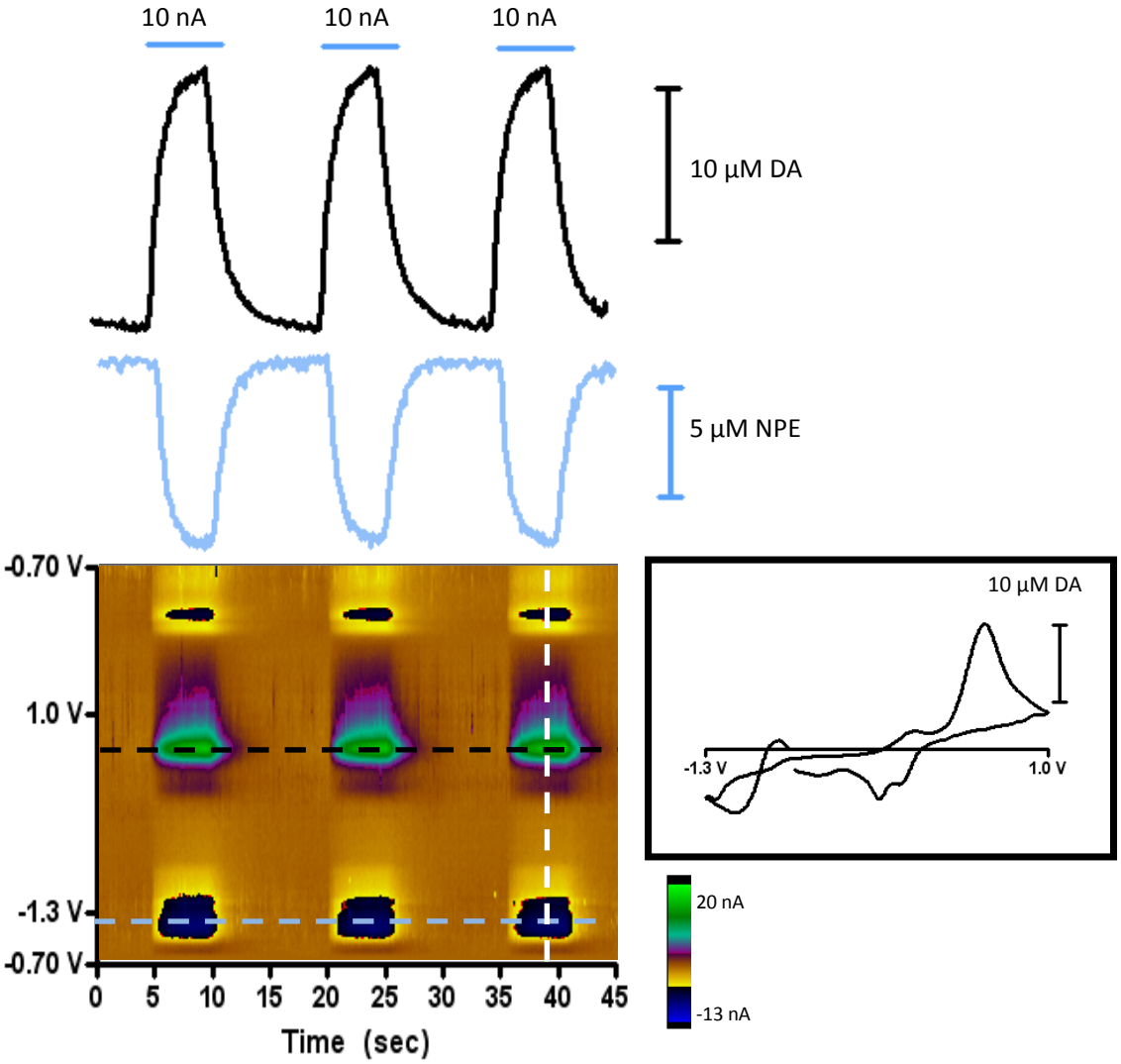

Figure 2.4. Analysis of consecutive iontophoretic ejections of dopamine and NPE. Carbon-fiber iontophoresis probes were used to eject a mixture of dopamine and NPE at pH 5.8 into a solution of TRIS buffer at pH 7.4. Upper left: The solid lines represent [DA] at 0.6 V (black) and [NPE] at -1.2 V (light blue) measured vs. time trace obtained for three consecutive 10 nA ejections at times indicated by the horizontal bars. Lower left: Color representation of the iontophoretic ejections shown, with applied voltage at the carbon fiber plotted vs. time and the current measured in response to dopamine and NPE ejection plotted in false color. Right: Cyclic voltammogram obtained at the time indicated by the white dashed line in the color plot.

linear with ejection current. The difference in the slope of the 5 lines indicates that each barrel is ejecting at a different rate.

Previous experiments by Bradley and Candy compared the amount of ejected cations for large and small diameter pipette tips (Bradley and Candy, 1970). Their results showed that the larger diameter pipettes ejected more for a fixed ejection current than small diameter pipettes. To examine whether this is the cause of variability in our experiments, the tip diameter of the iontophoretic barrels used was estimated from scanning electron microscope (SEM) images of the probes that were employed. One of the barrels contained a carbon fiber, while one of the other barrels was used to eject either dopamine or NPE. The concentration of dopamine or NPE detected during ejection followed similar behavior, and showed a correlation with the diameter of the ejection tip (Figure 2.5). Since the ejection of both neutral and charged species depends on the electric field (E) at the tip (equations 2 and 3), the variation likely arises because E is a function of the tip geometry. However, because we have not characterized the collection of ejected amounts with different dimensions of the iontophoretic barrel, a quantitative interpretation cannot be made. Even so, it is clear that the variability in tip dimensions leads to variability of the ejected amounts.

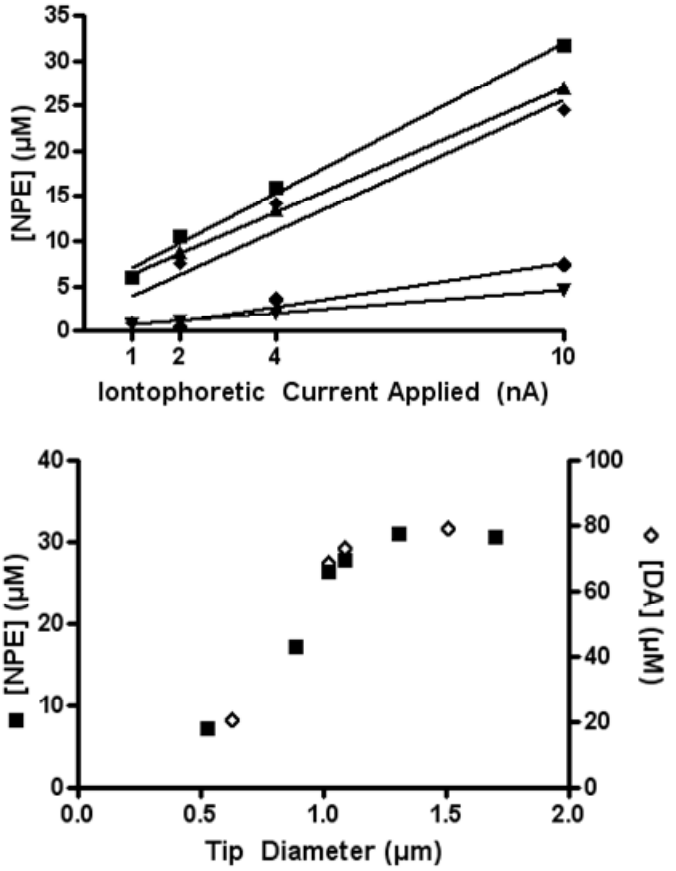

Figure 2.5. Variability of iontophoretic ejections for different barrels. Upper: 5 different probes were used to eject a mixture of dopamine and NPE at currents ranging from 1 - 10 nA into TRIS buffer. Each line represents the linear dependence of applied current to the amount of NPE ejected, as well as the difference in ejection efficiency for each barrel. (Dopamine showed an identical relationship, although not shown here). Lower: Different probes were used to eject dopamine or NPE into TRIS buffer using a 10 nA ejection current. After the ejections, SEM images of the probes were obtained to estimate the tip diameter of the iontophoresis probes. Plotted is the relationship between the amount of NPE (solid squares) and dopamine (empty diamonds) ejected at 10 nA and the diameter of tip.

Quantification of electroosmosis and migration.

The concentrations measured at the electrode surface are directly related to the flux at the iontophoretic tip and indicate the individual contributions from iontophoresis and electroosmosis. The pH of the solution in the barrel is critical because it will determine the charge of the compound in solution and the extent to which the silanol surface groups on the glass capillaries are ionized. To demonstrate the importance of the latter, the relative iontophoretic delivery of dopamine, a cation at pH values below pH ~7.4, and NPE, a marker for EOF, were compared from solutions of pH 5.8 and 4.0. Decreasing the pH increases protonation of the silanol groups and should decrease the ζ potential, thus decreasing the contribution of EOF. Consistent with this, the relative amount of dopamine ejected was greater at pH 4.0 due to the decreased transport of NPE by EOF.

To characterize the role of electroosmosis for other molecules, NPE was used as the marker for EOF at pH 5.8, and it was paired with a set of neutral and charged molecules that exhibit electrochemistry similar to that of dopamine shown in Figures 2.2 and 2-4. Acetaminophen (AP) and hydroquinone (HQ), which are both neutral at pH 5.8, traveled at the same speed as the EOF marker, NPE. As expected, charged molecules uric acid, norepinephrine, and dopamine, moved at rates that were significantly different from EOF. It might seem surprising that uric acid, an anion at the pH used, can be ejected with a positive current. This arises because electroosmosis effectively competes with the iontophoretic mobility that carries uric acid in the opposite direction. Norepinephrine and dopamine, which are cations, have transport rates that are enhanced by their respective iontophoretic mobilities. Importantly, over a series of at least 5 barrels, the ratio between each compound tested and NPE remained reasonably constant as indicated by the standard deviations. That is, the fraction of the observed

ejection due to EOF did not vary, despite fluctuations in the absolute amount of compounds ejected. Thus, consistent with the results in Figure 2.5(B), variations in EOF arising from differences in the tip diameter are the origin of the variability in the amounts ejected of both neutral and charged compounds.

Carbon-fiber iontophoresis probes were used to deliver a mixture consisting of a charged compound (10 mM) and the EOF marker, NPE (10 mM), into 1X TRIS buffer (pH 7.4). The values given are the average of at least 6 different barrels for each of the compounds tested. For each barrel, 25 consecutive ejections were averaged at ejection currents ranging from 1 nA to 100 nA as needed to deliver concentrations of NPE in the 5-50 μM range.

The differences in mobility observed in our iontophoresis experiments match differences in electrophoretic mobilities observed in published data (Wallingford and Ewing, 1987) and are confirmed by our own experiments as demonstrated in Figure 2.6. As such, it is possible to use electrophoretic mobility data in conjunction with iontophoresis data to make predictions of the rate of transport relative to EOF for compounds that are not electroactive, but that can be detected in the UV. Such compounds include quinpirole and raclopride, both of which are important drugs frequently studied in our laboratory. Such an approach has been used to characterize transdermal iontophoresis and the zeta potential of brain slices in rats (Abla et al., 2005; Guy et al., 2008). Although our experiments were run in the presence of 5 mM NaCl, electroosmosis is still an effective transport mechanism with much higher ionic strength.

Since iontophoretic ejections generate high, localized concentrations of analyte near the point of ejection, there was concern that quantitative measurements of the amount ejected may be convoluted due to differences in electrode response along its

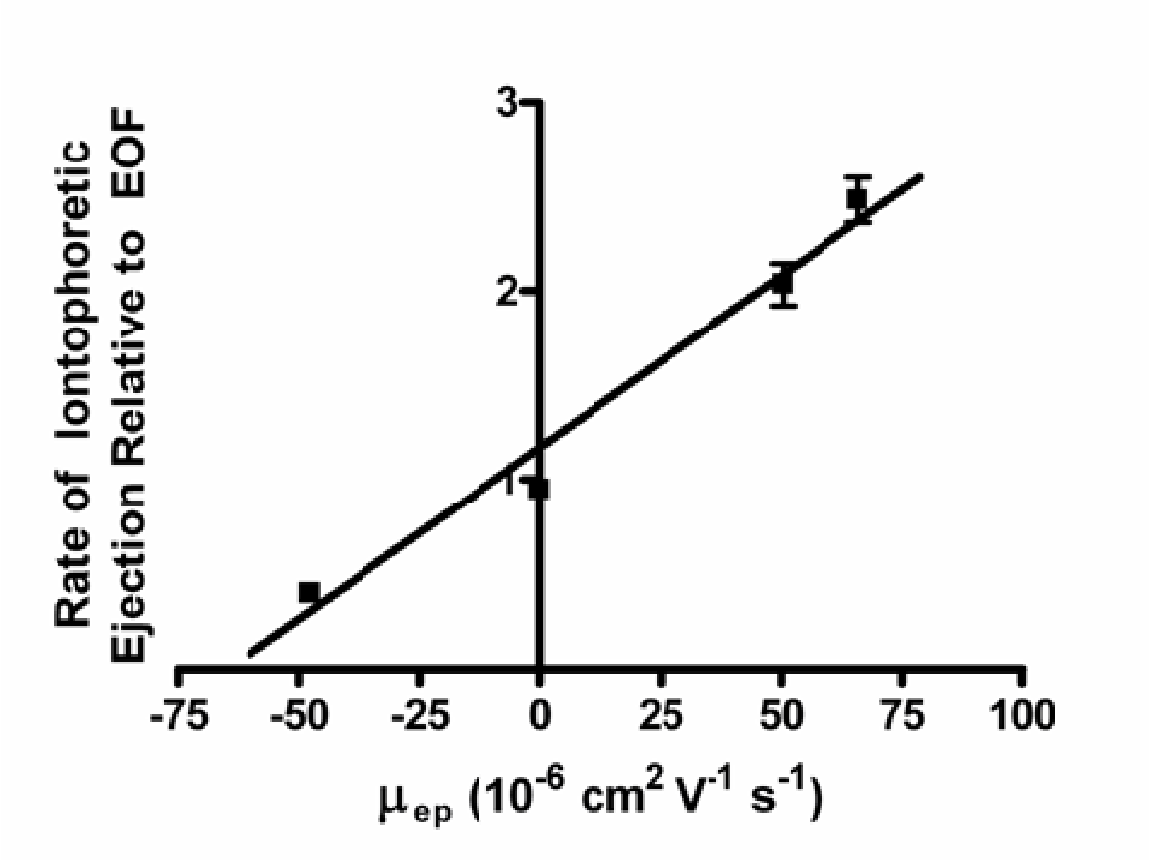

Figure 2.6. Correlation between iontophoretic and electrophoretic mobility. Iontophoretic mobility was determined as a ratio of the amount ejected by iontophoretic and electroosmotic forces to the amount ejected by electroosmotic forces only. This was done by ejecting a mixture of a charged compound (DA, NE, or UA) with a neutral marker, NPE. The amount of the charged compound ejected corresponded to the amount ejected by iontophoretic and electroosmotic forces, and the amount of NPE ejected was taken as the rate of EOF. Electrophoretic mobilities were obtained for each of these compounds using Equation 5 and plotted against the rate of transport relative to EOF given in Table 2.1.

Table 2.1. Rate of iontophoretic delivery of charged compounds relative to EOF as measured by FSCV.

Compound Ejected by Iontophoresis	**Concentration Ejected Relative to NPE**
Dopamine (pH 4.0)	3.56 ± 0.27
Dopamine (pH 5.8)	2.57 ± 0.30
Norepinephrine (pH 5.8)	2.04 ± 0.27
Hydroquinone (HQ) (pH 5.8)	1.01 ± 0.02
Acetaminophen (AP) (pH 5.8)	0.95 ± 0.06
Uric Acid (pH 5.8)	0.49 ± 0.18

length. To ensure that this would not present a problem, we used HPLC as an independent measure to confirm the results obtained with our carbon-fiber iontophoresis probes. With HPLC we can separate a mixture post-ejection, and quantitatively determine how much was ejected by oxidizing at +0.7 V vs. Ag/AgCl. For these experiments, 10 minute iontophoretic ejections of AP and HQ were made into a known volume of perchloric acid (500 µL). Analysis of the mixture showed that the rate of transport for HQ relative to AP was 1.04 ± 0.21. This result is expected for two neutrals, and is in agreement with those obtained with the carbon-fiber iontophoresis probe measurements using NPE.

Effects of retaining currents.

Traditionally, a retaining current is applied between ejections during iontophoresis to control for diffusive leakage. Given the tip size of our iontophoresis probes, we hypothesized that retaining current may not be necessary. To test this, we performed a series of dopamine ejections at various retaining currents. Initially the barrel was held at -10 nA for 6 minutes, and then the current was progressively increased to more positive currents and held at that current for another 6 minutes. During each of these ejection currents, the amount of dopamine and NPE ejected was monitored. If the electrodes were leaking between ejections, it is predicted that some ejection would be seen when the current was changed from -10 nA to -5 nA to -2 nA to 0 nA, since at each transition there would be less retaining current to control for leakage. As seen in Figure 2.7 this was not the case. In each of those transitions, no ejection was observed. Ejection was only observed when the current switched from 0 nA to 3 nA, indicating that no retention current is necessary, and holding at 0 nA is sufficient.

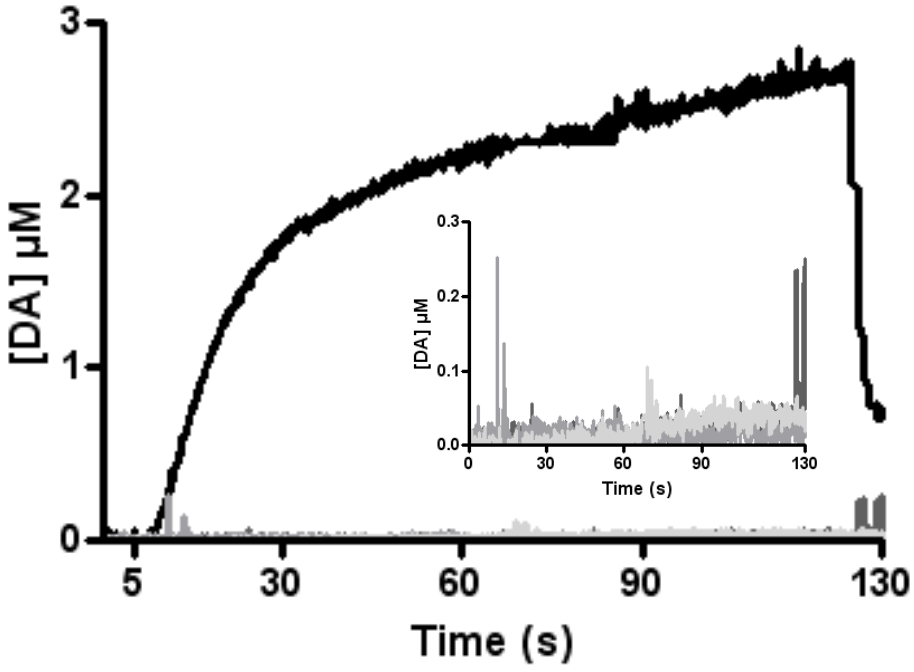

Figure 2.7. Effects of retention current on iontophoretic ejections. Carbon-fiber iontophoresis probes were used to ejected dopamine cations after the application of retaining currents ranging from -10 nA to 0 nA. Each retaining current was applied for 6 minutes prior to the application of a higher ejection current for 6 minutes. The solid lines (amplified in the inset) represent the amount of dopamine ejected after the application of -10 nA retaining current followed by -5 nA (dark gray) ejection current, -5 nA retaining current followed by -3 nA ejection current (gray), and -3 nA retaining current followed by 0 nA (light gray). The black solid line shows the amount of dopamine ejected after holding the barrel at 0 nA for 6 minutes and then applying +3 nA for ejection current.

Considerations for *in vivo* use.

Carbon-fiber microelectrodes have been routinely used to study fluctuations of catecholamines in the brain of anesthetized and freely-moving rats (Robinson et al., 2008). Carbon-fiber iontophoresis probes have also been used to deliver drugs to localized regions, and subsequently detect the changes induced in catecholamine release with electrochemistry[1]. However, quantitation of the amounts ejected has remained a challenge, except in the rare cases when the drugs used are electroactive. Since electroosmosis seems to be the transport mechanism most affected by the variations present from barrel to barrel, it makes sense to use a marker for EOF as an indicator of the variability present. In addition, because the relationship between EOF and migration of charged compounds remains constant, the marker for EOF can be used as an internal standard to calibrate for the amounts of non-electroactive drugs ejected.

This methodology can be readily used *in vivo* with any electroactive neutral molecule, such as NPE, acetaminophen, or hydroquinone. It is important to keep in mind that the electrochemistry of some of these compounds may overlap with that of catecholamines. As such, if the experiment requires continuous ejection and detection of released cathecholamines, it would be advantageous to use NPE which does not overlap. Toxicity remains a concern, although given the localized nature of iontophoretic ejections and the effects of dilution, it is expected that this is minimal.

CONCLUSIONS.

A long-standing disadvantage of iontophoresis has been its non-quantitative nature. Using carbon-fiber iontophoresis probes we have shown that the main challenge with quantitating iontophoretic ejections is the variability observed from barrel to barrel due to varied tip dimensions which affects electroosmosis. Using NPE, AP, or HQ as

neutral markers for EOF, it is now possible to quantitate this variability. In addition, the positive correlation observed between electrophoretic mobility and iontophoretic mobility relative to our EOF markers enables us to extend this methodology and make quantitative predictions for compounds that are not electroactive, but that can be measured by other detection schemes used with CE such as UV or fluorescence. We plan to use this approach for quantitative iontophoresis applications in the study of neurotransmitter release and modulation in the brain of anesthetized and freely-moving rats.

REFERENCES

Abla N, Geiser L, Mirgaldi M, Naik A, Veuthey JL, Guy RH, Kalia YN (2005) Capillary zone electrophoresis for the estimation of transdermal iontophoretic mobility. J Pharm Sci 94:2667-2675.

Armstrong-James M, Millar J, Kruk ZL (1980) Quantification of noradrenaline iontophoresis. Nature 288:181-183.

Armstrong-James M, Fox K, Kruk ZL, Millar J (1981) Quantitative ionophoresis of catecholamines using multibarrel carbon fibre microelectrodes. J Neurosci Methods 4:385-406.

Bath BD, Scott ER, Phipps JB, White HS (2000) Scanning electrochemical microscopy of iontophoretic transport in hairless mouse skin. Analysis of the relative contributions of diffusion, migration, and electroosmosis to transport in hair follicles. J Pharm Sci 89:1537-1549.

Bevan P, Bradshaw CM, Pun RY, Slater NT, Szabadi E (1981) Electro-osmotic and iontophoretic release of noradrenaline from micropipettes. Experientia 37:296-297.

Bloom FE (1974) To spritz or not to spritz: The doubtful value of aimless iontophoresis. Life Sciences 14:1819-1834.

Bradley PB, Candy JM (1970) Iontophoretic release of acetylcholine, noradrenaline, 5-hydroxytryptamine and D-lysergic acid diethylamide from micropipettes. Br J Pharmacol 40:194-201.

Bunin MA, Prioleau C, Mailman RB, Wightman RM (1998) Release and uptake rates of 5-hydroxytryptamine in the dorsal raphe and substantia nigra reticulata of the rat brain. J Neurochem 70:1077-1087.

Cheer JF, Aragona BJ, Heien ML, Seipel AT, Carelli RM, Wightman RM (2007) Coordinated accumbal dopamine release and neural activity drive goal-directed behavior. Neuron 54:237-244.

Clarke G, Forrester PA, Straughan DW (1974) A quantitative analysis of the excitation of single cortical neurones by acetylcholine and L-glutamic acid applied micro-iontophoretically. Neuropharmacology 13:1047-1055.

Curtis DR (1964) Micro-electrophoresis. In: Physical Techniques in Biological Research (Nastuk WL, ed), pp 144-190. New York: Academic Press.

Dionne VE (1976) CHARACTERIZATION OF DRUG IONTOPHORESIS WITH A FAST MICROASSAY TECHNIQUE. In, pp 705-717.

Fu JJ, Lorden JF (1996) An easily constructed carbon fiber recording and microiontophoresis assembly. In, pp 247-251.

Gerhardt GA, Palmer MR (1987) CHARACTERIZATION OF THE TECHNIQUES OF PRESSURE EJECTION AND MICROIONTOPHORESIS USING INVIVO ELECTROCHEMISTRY. In, pp 147-159.

Guy RH, Kalia YN, Delgado-Charro MB, Merino V, Lopez A, Marro D (2000) Iontophoresis: electrorepulsion and electroosmosis. J Control Release 64:129-132.

Guy Y, Sandberg M, Weber SG (2008) Determination of zeta-potential in rat organotypic hippocampal cultures. Biophys J 94:4561-4569.

Kiyatkin EA, Rebec GV (1996) Dopaminergic modulation of glutamate-induced excitations of neurons in the neostriatum and nucleus accumbens of awake, unrestrained rats. Journal of Neurophysiology 75:142-153.

Kiyatkin EA, Rebec GV (1997) Iontophoresis of amphetamine in the neostriatum and nucleus accumbens of awake, unrestrained rats. Brain Res 771:14-24.

Kiyatkin EA, Kiyatkin DE, Rebec GV (2000) Phasic inhibition of dopamine uptake in nucleus accumbens induced by intravenous cocaine in freely behaving rats. Neuroscience 98:729-741.

Krnjevic K, Mitchell JF, Szerb JC (1963) Determination of iontophoretic release of acetylcholine from micropipettes. J Physiol 165:421-436.

Kruk ZL, Armstrong-James M, Millar J (1980) Measurement of the concentration of 5-hydroxytryptamine ejected during iontophoresis using multibarrel carbon fibre microelectrodes. Life Sci 27:2093-2098.

Nicholson C, Phillips JM, Gardner-Medwin AR (1979) Diffusion from an iontophoretic point source in the brain: role of tortuosity and volume fraction. Brain Res 169:580-584.

Overton P, Clark D (1992) IONTOPHORETICALLY ADMINISTERED DRUGS ACTING AT THE N-METHYL-D-ASPARTATE RECEPTOR MODULATE BURST FIRING IN A9-DOPAMINE NEURONS IN THE RAT. Synapse 10:131-140.

Pierce RC, Rebec GV (1995) Iontophoresis in the neostriatum of awake, unrestrained rats: differential effects of dopamine, glutamate and ascorbate on motor- and nonmotor-related neurons. In, pp 313-324.

Purves R (1980a) Ionophoresis - Progress and Pitfalls. Trends in Neurosciences 3:245-247.

Purves RD (1977) The release of drugs from iontophoretic pipettes. J Theor Biol 66:789-798.

Purves RD (1979) The physics of iontophoretic pipettes. J Neurosci Methods 1:165-178.

Purves RD (1980b) Effect of Drug Concentration on Release from Ionophoretic Pipettes. Journal of Physiology-London 300:P72-P73.

Rice ME, Nicholson C (1989) Measurement of nanomolar dopamine diffusion using low-noise perfluorinated ionomer coated carbon fiber microelectrodes and high-speed cyclic voltammetry. Anal Chem 61:1805-1810.

Robinson DL, Hermans A, Seipel AT, Wightman RM (2008) Monitoring rapid chemical communication in the brain. Chem Rev 108:2554-2584.

Scott ER, White HS, Phipps JB (1993) Iontophoretic transport through porous membranes using scanning electrochemical microscopy: application to in vitro studies of ion fluxes through skin. Anal Chem 65:1537-1545.

Shen RY, Asdourian D, Chiodo LA (1992) MICROIONTOPHORETIC STUDIES OF THE EFFECTS OF D-1 AND D-2 RECEPTOR AGONISTS ON TYPE-I CAUDATE-NUCLEUS NEURONS - LACK OF SYNERGISTIC INTERACTION. In, pp 319-329.

Skoog DA, Holler FJ, Crouch SR (2007) Principles of instrumental analysis, 6th Edition. Belmont, CA: Thomson Brooks/Cole.

Stone TW (1985) Microiontophoresis and Pressure Ejection. London: John Wiley & Sons.

Volpato NM, Santi P, Colombo P (1995) Iontophoresis enhances the transport of acyclovir through nude mouse skin by electrorepulsion and electroosmosis. Pharm Res 12:1623-1627.

Wallingford RA, Ewing AG (1987) Capillary zone electrophoresis with electrochemical detection. Anal Chem 59:1762-1766.

Windels F, Kiyatkin EA (2006) Dopamine action in the substantia nigra pars reticulata: iontophoretic studies in awake, unrestrained rats. European Journal of Neuroscience 24:1385-1394.

Chapter 3

Probing pre-synaptic regulation of dopamine release with iontophoresis

INTRODUCTION

Iontophoresis was first developed by W.L. Nastuk, a student of A.L. Hodgkin, who was interested in how the actions of acetylcholine (ACh) on the neuromuscular junction were altered with changes in the ionic composition of the extracellular bath solution (Hicks, 1984). His previous studies with intracellular pipette recordings led him to the discovery that if pipettes were pulled to a coarse tip and then filled with ACh, some would slowly diffuse out. He expanded on this observation and decided to electrically control delivery of ACh through the glass pipettes, and thus iontophoresis was born in 1953 (Nastuk, 1953). Recognizing that fast and controlled delivery of ACh could be used to search and map end-plate regions on the neuromuscular region, many researchers, including del Castillo and Katz, used it to study the actions of ACh on synaptic sites (Del Castillo and Katz, 1955, 1956; Axelsson and Thesleff, 1959; Miledi, 1960). The first studies using iontophoresis in the central nervous system were made by Eccles and Curtis who were interested in studying Renshaw cells and used the first account of a multi-barrel iontophoresis probe to locate and modulate cells (Curtis and Eccles, 1958; Curtis et al., 1960; Curtis and Koizumi, 1961).

Throughout the remainder of the 1950s and into the 1970s, iontophoresis grew in popularity, and important contributions concerning the advantages and disadvantages of iontophoretic drug delivery were made (Krnjevic et al., 1963a; Krnjevic et al., 1963b;

Crawford and Curtis, 1964; Curtis and Nastuk, 1964; Bradley and Candy, 1970; Bloom, 1974; Simmonds, 1974; Freedman et al., 1975; Purves, 1977, 1979). The technique was (and is) favored for studying receptor dynamics *in vivo* because drugs can be quickly, selectively, and locally delivered to the site (or sites) of action. Traditional methods of pharmacological intervention such as intraperitoneal or intravenous delivery affect the entire brain and can confound interpretation of the measured results. Furthermore, only drugs that can pass the blood-brain barrier can be used for system drug delivery, and even then, metabolism of the drug may reduce its effects (Bloom, 1974). Iontophoresis circumvents all of these problems, making it very attractive for pharmacological neurobiology studies.

However, despite the clear advantages of iontophoresis, challenges with reproducibility and quantitation of drug delivery have prevented the technique from being more widely used (Del Castillo and Katz, 1955; Krnjevic et al., 1963b; Curtis and Nastuk, 1964; Bloom, 1974; Purves, 1977, 1979; Purves, 1980a; Purves, 1980b; Armstrong-James et al., 1981; Stone, 1985). A major drawback of iontophoresis as it has been previously used is that there is no way to differentiate between an unresponsive site and a faulty drug ejection. Recently, we modified the design of Millar and co-workers, coupling iontophoresis barrels to carbon-fiber microelectrodes to allow the concentrations of electroactive compounds delivered by iontophoresis to be monitored with fast-scan cyclic voltammetry (Armstrong-James et al., 1981). While characterizing iontophoretic delivery, we found that electroosmosis contributes significantly to the observed drug delivery. Electroosmosis is due to ionizable silanol groups on the glass capillary surface which attract cations in solution to form an electrical double layer. When a positive current is applied to the capillary, the cations along the wall migrate toward the anode (outside of the capillary), creating a bulk movement of solution, termed

electroosmotic flow (EOF). Thus, iontophoretic delivery is governed by the traditional mechanism attributed to iontophoresis, ion migration, and EOF. In addition, we showed that an electroactive neutral molecule could serve as an internal standard to monitor the variability in the amount of drug delivered from different barrels. These insights into the iontophoresis technique enable quantitative delivery of electroactive and electroinactive drugs by monitoring the ejection of an electroactive EOF marker (Herr et al., 2008).

Although fast-scan cyclic voltammetry has been previously combined with iontophoresis for neurophysiology experiments, it has not been used to modulate pre-synaptic release of neurotransmitters (Kiyatkin and Rebec, 1996, 1997; Rebec, 1998; Kiyatkin and Rebec, 1999b, a; Kiyatkin et al., 2000; Kiyatkin and Rebec, 2000). In this chapter, the use of quantitative iontophoresis for the modulation of dopamine release in the striatum of anesthetized rats is demonstrated. Ejections are characterized *in vivo* with particular emphasis on leakage and the time course of drug ejection. In addition, the effects on dopamine release upon application of two electroactive marker molecules, AP and 2-(4-nitrophenoxy) ethanol (NPE) are tested to ensure that our method of quantitation does not alter the biological system. Expanding on previous work, he relative mobilities of drugs of pharmacological interest that are not electroactive are quantified. Finally, it is demonstrated that dopamine neurotransmission can be locally modulated at terminals by affecting D2 autoreceptors and the dopamine transporter.

MATERIALS AND METHODS

Chemicals.

Unless noted, all chemicals were purchased from Sigma-Aldrich (St. Louis, MO) and used as received. Chemical structures of the species used are shown in Figure 3.5. Solutions were prepared using deionized water. A physiological buffer solution, pH 7.4,

(15 mM TRIS, 126 mM NaCl, 2.5 mM KCl, 25 mM $NaHCO_3$, 2.4 mM $CaCl_2$, 1.2 mM NaH_2PO4, 1.2 mM $MgCl_2$, 2.0 mM Na_2SO_4) was used in all calibration experiments.

Animals and surgery.

Male Sprague-Dawley rats (225-350g; Charles River, Wilmington, MA) were anesthetized with urethane (1.5 g/kg, i.p.) and placed in a stereotaxic frame (Kopf, Tujunga, CA). Holes were drilled in the skull on the right hemisphere for the working and stimulating electrodes at coordinates selected from the atlas of Paxinos and Watson (Paxinos and Watson, 2005). An Ag/AgCl reference electrode was inserted in the left hemisphere. The carbon-fiber iontophoresis probe was placed in the striatum (AP +1.2 mm, ML +2.0 mm, and DV -4.5 to -6 mm). The stimulating electrode was placed in the medial forebrain bundle (AP -2.8mm, ML +1.7 mm, and DV -8.5mm). The carbon-fiber and stimulating electrodes were individually adjusted in the dorsal-ventral coordinate to locate the optimal locations for stimulated dopamine release.

Electrical Stimulation.

An untwisted bipolar stimulating electrode (Plastics One, Roanoke, VA) was used to stimulate dopaminergic neurons using a pair of linear constant current stimulus isolators (model NL80A, NeuroLog System, Digitimer Ltd, UK). The stimulation train consisted of 40 biphasic pulses (± 300 μA, 2 ms/phase unless otherwise noted) applied at 60 Hz. The pulses were generated by a computer and applied between the cyclic voltammograms to avoid electrical interference.

Iontophoresis Probes.

A glass capillary (Part # 624503, 0.60 mm o.d., 0.4 mm i.d., 4” long, A-M Systems, Sequim, WA) was loaded with a carbon fiber (T-650, Thornel, Amoco Corp., Greenville, SC) that served as the working electrode. This capillary containing the carbon fiber was

then inserted into one barrel of a 4-barrel capillary (Part # 50644, 1 mm o.d., 0.75 mm i.d., 4barrel GF pipettes, 4" long, Stoelting Co., Wood Dale IL). The four barrel assembly contained glass filaments (GF) in each barrel that aid in filling the barrel by capillary action. The capillaries were bundled together with heat shrink and tapered to a sharp tip using a micropipette puller (Narashige, Tokyo, Japan) with a two-step pull process. The protruding carbon fiber was cut to a length between 30 and 50 μm by careful use of a scalpel under a 10X microscope objective. The resulting probe consists of a glass-encased carbon fiber that is 5-7 μm in diameter and 3 iontophoretic barrels each about 1 μm in diameter. Before use, the barrel containing the carbon fiber was backfilled with electrolyte (4 M potassium acetate, 150 mM potassium chloride) and fitted with wires for electrical contact. The remaining barrels for iontophoresis were filled with solutions containing reagents to be ejected.

Electrochemical Data Acquisition and Presentation.

Cyclic voltammograms were acquired using data-acquisition hardware and locally software written in LabVIEW (National Instruments, Austin, TX). The cyclic voltammetry waveform was generated and the voltammetric signal was acquired with a computer interface board, the PCI-6052E (National Instruments). A PCI-6711E D/A board (National Instruments) was used to synchronize waveform application, data acquisition, and to trigger the iontophoretic current applied and the loop injector in the flow injection apparatus. The voltammetric waveform was input into a custom-built instrument for application to the electrochemical cell and current transduction (University of North Carolina at Chapel Hill, Department of Chemistry Electronics Facility). After data collection, background subtraction, signal averaging, and digital filtering (low pass filtered at 2 kHz) were all done under software control.

For all experiments, a triangular waveform was applied with a scan rate of 400 V s^{-1} with a rest potential of -0.4 V versus a Ag/AgCl reference electrode between scans, a linear scan to 1.3 V, followed by a scan back to the rest potential. The scans were repeated every 100 ms, and collection was typically for 15- 60 s. This large amount of data is presented as a color plot, with the applied voltage plotted on the ordinate, time on abscissa, and measured current in false color.

Iontophoresis Ejections.

Characterizations studies involving the effects of the neutral marker molecule on stimulated dopamine release were done with solutions made up at 10 mM concentrations of acetaminophen, 2-4(nitrophenoxy) ethanol, in 5 mM NaCl. The effects of saline were studied with 5 mM NaCl solutions. For studies involving the modulation of stimulated dopamine release, each barrel of the iontophoresis assembly was filled with either raclopride tratrate salt, nomifensine maleate salt, or quinpirole hydrochloride and the EOF marker, usually AP, at concentrations of ~10 mM each, in 5 mM NaCl at pH 5.8. These concentrations of drug and supporting electrolyte were chosen for the following reasons: for the following reasons. Electrolyte is needed to facilitate conductivity and to ensure adequate and reproducible EOF without it being so high that EOF is suppressed (Cazes, 2001). Therefore 5 mM NaCl was chosen as a compromise between the two limits. Traditionally, drug concentrations are higher than used here and barrels are sometimes loaded with drugs at concentrations of 250 mM. However, given that we are able to electrochemically monitor drug ejection, we determined that 10 mM is sufficiently concentrated to get observable ejection, and observe effects on stimulated dopamine release. Ejection currents were delivered by a constant current source designed for iontophoresis (Neurophore, Harvard Apparatus, Holliston, MA). For each barrel, an ejection current (between 5 to 40 nA) was selected by evaluating ejections (30 s

duration) that gave a measurable voltammetric signal for the EOF marker (average peak current of 5 to 30 nA at the peak potential in the voltammogram). A current of 0 nA was applied between ejections.

To minimize electrical cross-talk between the electrochemical and iontophoretic electrodes, both systems had a common ground. The reference electrode served as the return for the iontophoresis currents and was tied to ground. The potential of the working electrode was controlled by applying the voltage to the non-inverting input of the current transducer.

Calibrations.

The response of the carbon fiber electrode in the iontophoresis probe was calibrated in a flow injection analysis system after *in vivo* use (Kristensen et al., 1986). The probe was positioned at the outlet of a six-port rotary valve. A loop injector was mounted on an actuator (Rheodyne model 7010 valve and 5701 actuator) that was used with a 12-V DC solenoid valve kit (Rheodyne, Rohnert Park, CA) to introduce the analyte to the surface of the electrode. The linear flow velocity (1.0 cm s^{-1}) was controlled with a syringe infusion pump (Harvard Apparatus model 940, Holliston, MA). The voltammetric current was measured at the peak potential for each analyte that was evaluated at 4 concentrations.

Capillary Electrophoresis Experiments.

A home-built CE system equipped with an absorbance detector and a 30 kV power supply was employed. Absorbance traces were collected using a custom written LabVIEW program (Courtesy of Professor James Jorgensen, UNC-CH). Separations were carried out in a 50 μm diameter fused silica capillary, 96.0 cm in total length, with the UV detector placed 87.5 cm from the inlet. Experiments were done in cationic mode

(the anode at the inlet and cathode at the outlet). Samples were run at a concentration of 2 mM in 17 mM PBS (phosphate buffered saline, made up of 0.25% monosodium phosphate and 0.04% disodium phosphate) with a pH of 5.8 as in the iontophoresis experiments. UV detection was measured at 195 and 240 nm and electrophoretic mobilities were calculated as previously described (Herr et al., 2008).

Histology.

After animal experiments were complete, pontamine sky blue was loaded into one of the empty iontophoresis barrels to mark electrode location. The dye was ejected by applying 40 nA of current for 20 min. The animals were euthanized and brains were removed from the skull and stored in 10 % formaldehyde for at least 3 days. Brains were coronally sectioned into 40-50 μm thick slices with a cryostat and visualized under a stereoscope equipped with a camera.

RESULTS AND DISCUSSION

Characterization of iontophoretic delivery in vivo

Traditionally, iontophoretic ejection of substances with constant current has been considered as continuous electrical migration of an ion out of the pipette tip followed by diffusion into the surrounding environment (Rice and Nicholson, 1995). Theoretical and experimental calculations predict that migration out of the pipette tip will be influenced by the prior history of the pipette including the magnitude of the retaining current applied and the frequency of previous ejections (Purves, 1977, 1979). Our previous work showed that the iontophoretic barrels we construct have sufficiently small leakage that it is immeasurable by the adjacent carbon-fiber microelectrode (Herr et al., 2008). However, we observe that the first few ejections have diminished ejection efficiency, presumably due to leakage during the time for implantation and stabilization of the

electrode (~ 1 hour). This is shown in Figure 3.1, where the local AP concentration was monitored at the peak current of its oxidation during fast-scan cyclic voltammetry as it was ejected into the striatum of an anesthetized rat. The time course during 30 s ejections is shown in Figure 3.1(A). The voltammetric response increases when the iontophoretic current is initiated. The response continues to increase as the ejection continues and reaches a steady state. If we note the exact length of each electrode, using a model for simple diffusion we can estimate the rise time for ejections. Interestingly, however, our measured-time course predicts that there is an additional mechanism that is *slowing* diffusion, which we do not fully understand.

As shown, the time to reach a steady state is longer for the first ejection than the subsequent ones. This delay is the likely cause of the "warm-up phenomenon" noted in previous studies where initial iontophoretic ejections elicited little to no biological response, but with subsequent ejections the response grew in over time (Freedman et al., 1975). For this reason, before beginning biological studies, we "warm up" the electrode by continuously ejecting for 2-5 min into an area of the brain that is of not of interest. Figure 3.1(B) shows the reproducibility of ejections after the "warm-up" period. Ten consecutive ejections for a single barrel show a similar steady state level when compared to the first ejection after the warm-up period (n = 5). However, to take advantage of the finely controlled drug delivery enabled by iontophoresis, we are interested in monitoring the biological effects of a single 30 s ejection, and thus may not always reach this steady state at the site of interest, as will be evident later.

For a substance monitored by cyclic voltammetry with the carbon fiber, the amplitude of the voltammetric current is expected to increase as the ejected substance diffuses from the ejection point down the length of the fiber and to remain constant once the diffusion distance exceeds the electrode length. The concentration measured is

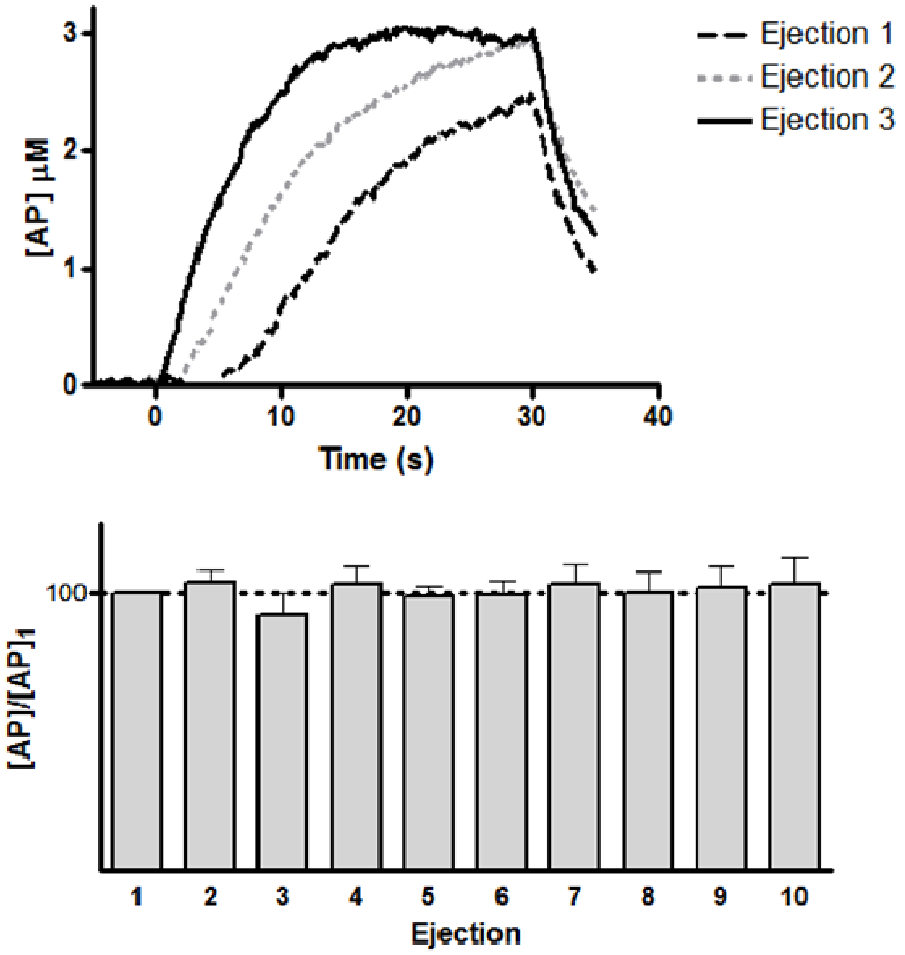

Figure 3.1. Temporal profile of consecutive iontophoretic ejections. A) Current vs. time trace for the first 3 ejections of AP in the rat brain. Ejection current was turned on at t = 0 s and off at t=30 s. Ejection 1 shows a characteristic delay in rise time, consistent with a "warm-up" period for ejections. Subsequent ejections, 2 and 3, have less of a delay, and ejection 3 reaches steady state. B) 10 consecutive ejections into PBS buffer after "warm-up" period. $[AP]/[AP]_1$ represents the amount of AP measured at steady state compared to the amount measured from the first ejection after the "warm-up" period.

actually the average concentration along the length of the electrode determined by a gradient started at the iontophoretic tip, where the concentration is close to that in the barrel (10 mM). For example, an electrode with a length of 30 μm (as in Figure 3.1) reports a current that is proportional to a uniform concentration of 3 μM across the surface of the electrode once steady state is reached. When the iontophoretic current is turned off, the analyte quickly diffuses away from the electrode. Within 120 s, the iontophoresed substance can still be detected voltammetrically, but it has diluted to a concentration that is ~2% of its steady-state value during ejection.

Effects of EOF marker on stimulated dopamine release

A common way to probe presynaptic factors that regulate neurotransmitter release is to examine the effects of added pharmacological agents on electrically evoked release (Limberger et al., 1991; Benoit-Marand et al., 2001; Phillips et al., 2002). For example, the role of autoreceptors can be probed by examining stimulations before and after addition of receptor antagonists. However, before the iontophoretic method was used with electrical stimulation to probe presynaptic events at dopaminergic terminals, we had to ensure that delivery of the neutral marker substances did not affect dopamine release. In these experiments, AP or NPE was delivered for 30 s, followed by a wait-period of 120 s before electrical stimulation of the medial forebrain bundle (MFB). Figure 3.2 shows the results of a typical experiment in a urethane anesthetized rat. A carbon-fiber/iontophoresis probe was lowered into the striatum and a stimulating electrode was lowered into the MFB. Stimulated release (60 Hz, 40 pulses) was evoked every 120 s until ten consecutive maximal stimulations showed a similar maximal concentration (typically requiring 15 stimulations). A representative baseline trace and color plot are shown in Figure 3.2(A). To test the effects of the EOF marker on dopamine release, AP was iontophoretically applied for 30 s at a location that exhibited reproducible stimulated

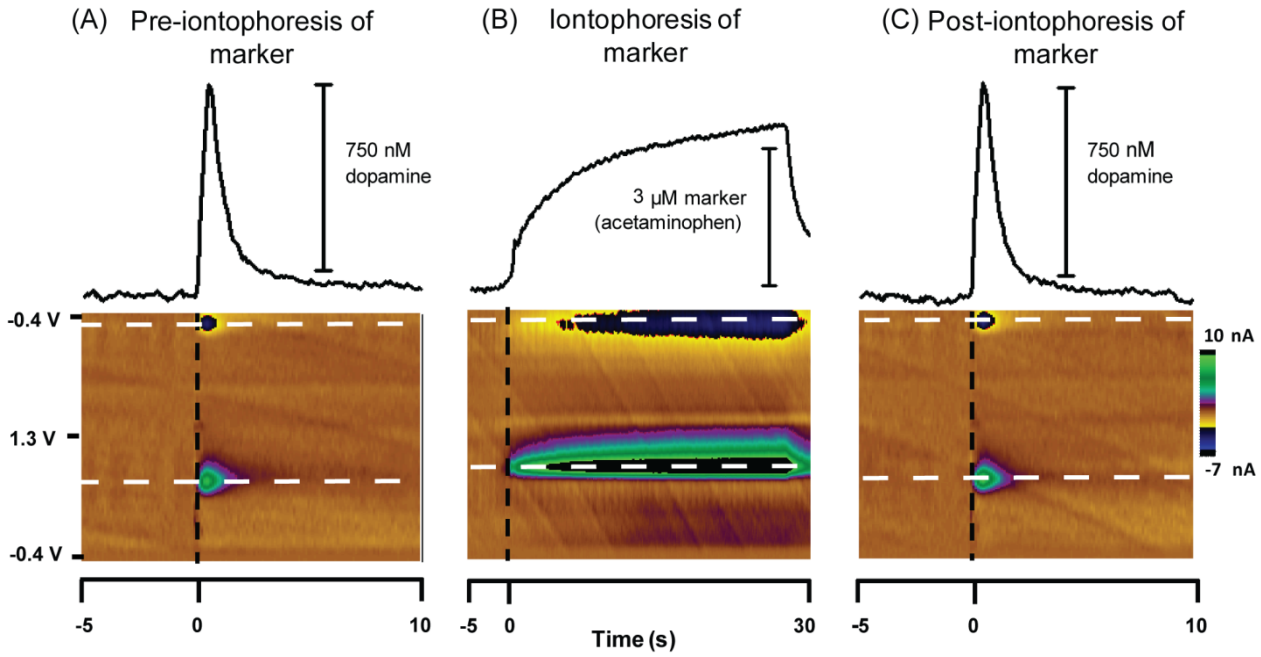

Figure 3.2. Effect of AP on stimulated dopamine release. The top panels show current as a function of time while the lower panels are two dimensional color plots where current is shown in false color on the potential vs. time axes. The white dashed lines on the color plots indicate the voltages at which oxidation (lower lines) and reduction (top lines) is occurring. (A) A representative baseline current trace and color plot for the stimulated release of dopamine. The black dashed line (t=0) indicates time of stimulation. (B) Representation of iontophoretic ejection of 3 µM AP. The black dashed line (t=0) indicates the application of a positive current to the barrel. (C) Current trace and color plot for stimulated release after ejection seen in B. The black dashed line (t=0) indicates time of stimulation. There is no change in the extracellular concentrations of dopamine seen in A and C elicited with a stimulation indicated by the black dashed line and t=0 for each trace.

release. The amount of AP delivered was monitored electrochemically, and the concentration vs. time trace and color plot are shown in Figure 3.2(B). Stimulation was repeated 120 s after AP delivery, and the maximum amplitude of released dopamine and its time course remained the same. From the concentration of AP during its iontophoresis, 3 μM, we can estimate the concentration at the time of the stimulation to be 60 nM (2% of the steady state level). Stimulations were continued at 2 min intervals for 30 min, and there was no significant change in the amount of dopamine released or rate of uptake (Fig 2C, $n = 9$, $p > 0.01$). The same experiment was performed for NPE, with no measurable difference observed from control ($n=4$, $p > 0.01$).

Current artifacts on stimulated dopamine release

It is often noted in iontophoretic literature that current artifacts can be seen neurophysiologically due to the introduction of Na^+ and Cl^- that are in the drug solution (Curtis and Nastuk, 1964; Stone, 1985). Although in our experiments we are not monitoring cell firing, and are instead monitoring presynaptic release of dopamine, we wanted to ensure that current artifacts were not affecting our measured results. For these experiments, just as in the previous set of experiments, we adjusted the position of the carbon-fiber/iontophoresis assembly so that it was in a location in the striatum that showed robust dopamine release. After establishing reproducible stimulated release of dopamine, we iontophoretically ejected NaCl (5 mM in the barrel, made up in deionized water) for 30 sec. Although NaCl is not electroactive, by applying a large constant current (greater than 100 nA) we are able to detect a change in our background signal (~4 nA in this example) that evolves with time (Figure 3.3). The current is an indirect effect of the iontophoresis and its time course indicates that it reflects a change in the electrical double layer formed at the carbon fiber electrode. While we cannot quantify the amount of NaCl delivered from this signal, it does serve to confirm that ejection

occurred. Stimulated dopamine release was then measured 120 s after the NaCl ejection was terminated to ensure that it did not alter presynaptic release dynamics. The results from this experiment indicate that stimulated dopamine release is unaffected by large ejections of NaCl and are shown in Figure 3.3 ($n=4$, $p>0.05$). The NaCl ejected with large currents does alter the double layer of the carbon fiber, although this is not seen with the lower ejection currents typically used.

Marking of electrode placement by iontophoresis of a dye

When dealing with small brain structures it is crucial to know the location of the electrode. A common way to verify electrode placement is to remove the brain after the experiment is over for histology. For experiments using carbon-fiber microelectrodes, one approach is to electrolytically lesion the electrode. This has the shortcoming that the carbon-fiber is destroyed during this process and cannot be calibrated after the *in vivo* experiment. An alternate approach is to remove the electrode after the experiment for calibration and insert a tungsten wire to electrically mark the location of the previous electrode. Iontophoresis barrels provide a more convenient and precise method to mark electrode placement. Figure 3.4 shows the marking of electrode placement by delivering pontamine sky blue dye iontophoretically for 20 min at 40 nA once the experiment was over. The length of ejection was chosen to ensure that a large enough spot was produced, given that iontophoresis is such a localized drug delivery mechanism. By using one of the empty barrels to deliver a dye, the electrode placement can be accurately determined while keeping the carbon-fiber intact for post-calibration. Many other dyes can be used, such as alcian blue, methyl blue, fast green, and lucifer yellow, making the procedure compatible with any other immunohistochemistry that may be done post-experiment (Stone, 1985).

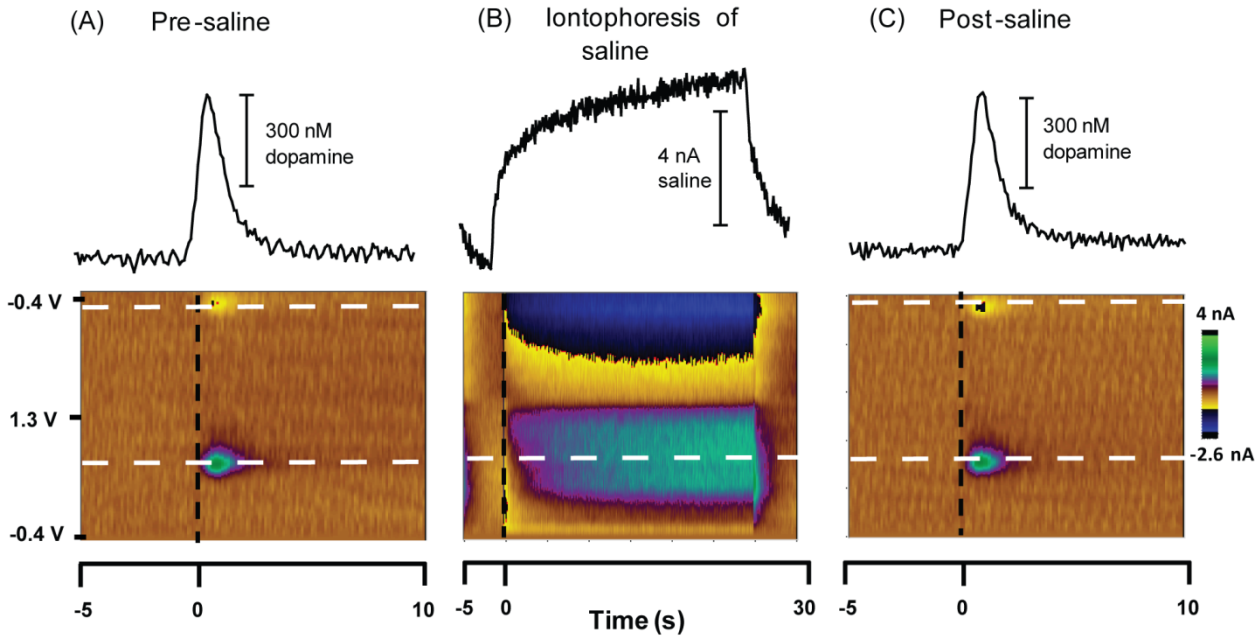

Figure 3.3. Effect of saline on stimulated dopamine release. The top panels show current as a function of time while the lower panels are two dimensional color plots where current is shown in false color on the potential vs. time axes. The white dashed lines on the color plots in (A) and (C) indicate the voltages at which oxidation (lower lines) and reduction (top lines) is occurring, whereas in (B) the dashed white line indicates the potential change observed due to the ejection of NaCl. (A) A representative baseline current trace and color plot for the stimulated release of dopamine. The black dashed line (t=0) indicates time of stimulation. (B) Representation of iontophoretic ejection of saline with high applied current. The black dashed line (t=0) indicates the application of a positive current to the barrel. (C) Current trace and color plot for stimulated release after ejection seen in B. The black dashed line (t=0) indicates time of stimulation. There is no change in the extracellular concentrations of dopamine seen in A and C elicited with a stimulation indicated by the black dashed line and t=0 for each trace.

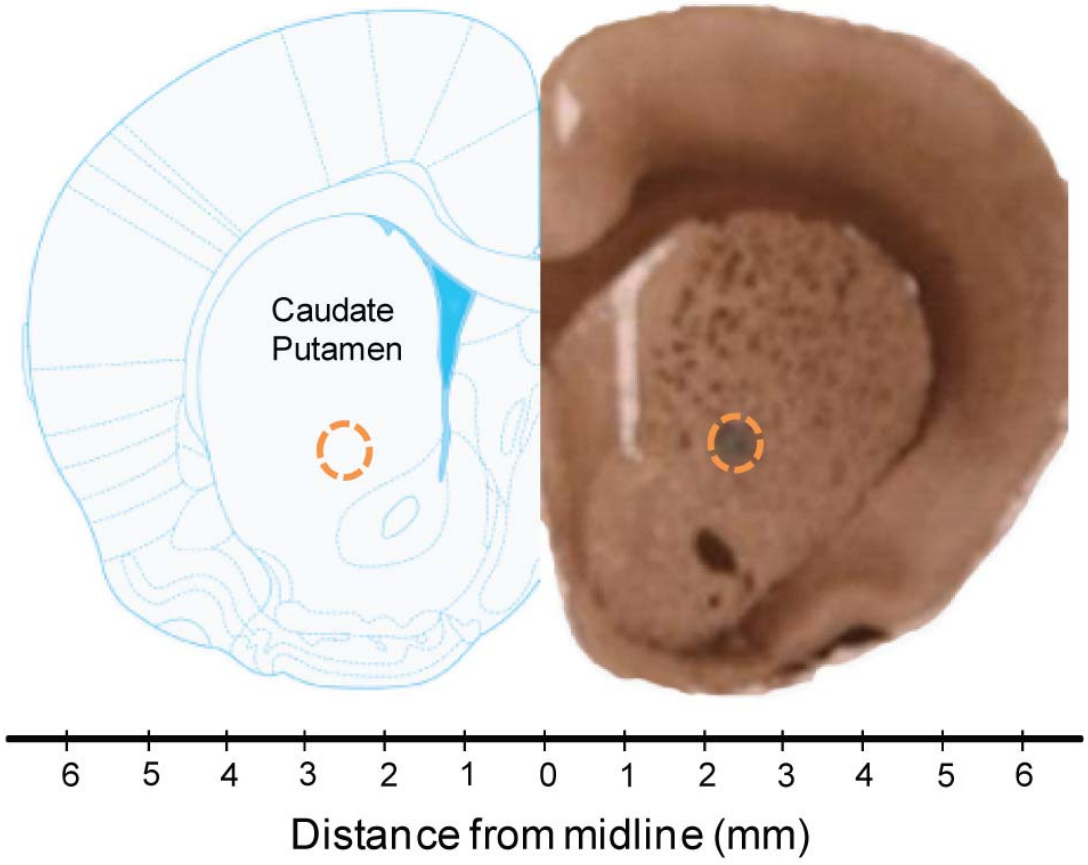

Figure 3.4. Confirmation of electrode placement into the striatum using iontophoresis of pontamine sky blue dye. After a 20 min ejection, the spot is 600 µm in diameter. Left side of the figure shows region of interest labeled and circled with a dashed line. On the right, the spot from the ejection of dye can be seen in the circled region of interest.

Quantitative iontophoresis of non-electroactive drugs

In our previous work, relative iontophoretic mobilities at capillary tips were obtained for electroactive molecules by measuring the ejected amounts at the adjacent carbon-fiber microelectrode (Herr et al., 2008). We found that neutral molecules such as AP can be ejected, establishing a role for EOF. We also established the role of EOF by demonstrating that iontophoretic and electrophoretic mobilities measured via capillary electrophoresis are linearly correlated, further demonstrating that at the tip of an iontophoresis pipette delivery is governed by both the migration of ions in an electric field and electroosmotic flow. To obtain the iontophoretic mobility of electroinactive molecules such as the dopaminergic drugs raclopride, quinpirole, and nomifensine (structures shown in Figure 3.5), the electrophoretic mobility through a capillary column was measured with UV detection. Retention times were used to compute the electrophoretic mobilities for dopamine, raclopride, quinpirole, nomifensine (all monocations), AP (a neutral molecule), and uric acid (a monoanion). The electrophoretic mobilities were then used to compute the relative iontophoretic mobilities as shown in Figure 3.6. Thus, raclopride is ejected at a rate 1.68 times as fast as AP whereas quinpirole and nomifensine are ejected at a rate 2.18 and 2.24 times as fast as AP, respectively. With the knowledge of these ratios, the amount of an electroinactive molecule that is ejected can be calculated by the measured co-ejection of a neutral, electroactive molecule from the same barrel. Note that the relative mobilities are in agreement with the expected charge computed from the relevant pK_as and the size of the molecules.

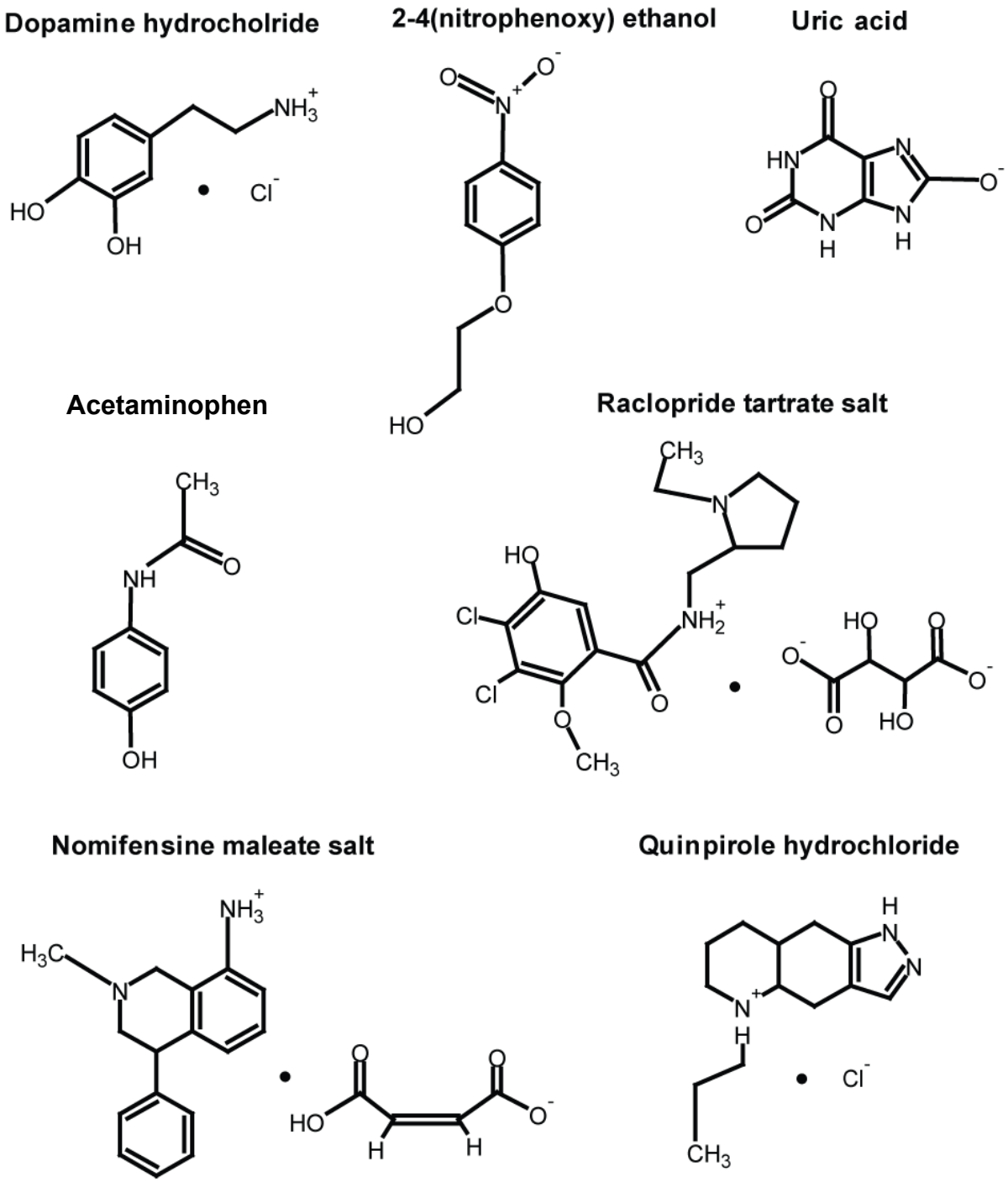

Figure 3.5. Chemical structures of compounds used for study. Shown are compounds as they exist in the iontophoretic ejection solution at pH 5.8 given their pKas obtained on Scifinder. All solutions were made up as 10 mM in 5 mM NaCl to ensure adequate electroosmotic flow and for buffering of the ionic strength.

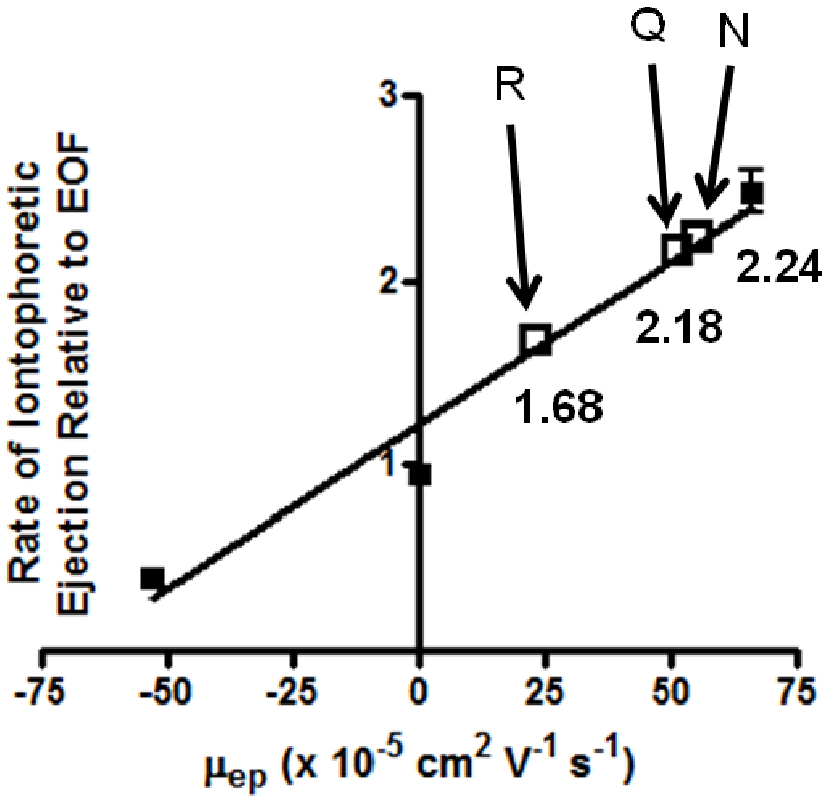

Figure 3.6. Correlation of electrophoretic mobility to iontophoretic transport rate for dopamine drugs. The electrophoretic mobilities of the electroactive compounds uric acid, AP, and DA (■) are positively correlated to previously reported iontophoretic rates. The linear regression from this correlation was used to determined iontophoretic rates relative to AP for raclopride (R), quinpirole (Q), and nomifensine (N) (□) based on their electrophoretic mobilities calculated by capillary electrophoresis.

With an average ejection and an electrode with a length of 30 μm, the average concentration of AP across the carbon fiber is 3 μM for the example shown in Figure 3.2. However, the concentration at the portion of the carbon fiber closest to the iontophoresis tip is very near that placed inside the barrel (10 mM). Such high concentrations of drug could alter the sensitivity of the electrode to dopamine. To evaluate this, we first calibrated a series of carbon-fiber iontophoresis probes to determine their sensitivity to dopamine. We then loaded one of the iontophoresis barrels with the EOF marker (AP), or AP plus a drug of interest. While monitoring the response of AP with the carbon-fiber microelectrode, we continuously ejected the mixture into buffer for 40 min with a pump current sufficient to deliver approximately 10 μM of AP. After the 40 min ejection and monitoring period, we calibrated the carbon-fiber electrodes' sensitivity to dopamine again and determined the ratio of the electrodes' post iontophoresis sensitivity to pre-iontophoresis sensitivity. The results from these experiments are presented in Table 1. AP and NPE, which are both neutral and can be used as EOF markers, did not significantly alter the electrodes' response to dopamine. Pharmacological agents, such as nomifensine, quinpirole, and raclopride, have slight effects on the electrodes' response to dopamine. Note, however, that the ejection times used during these iontophoresis experiments (40 min per ejection) were considerably longer than would be used in most *in vivo* experiments (normally 30 s per ejection). Given the small effect observed, even with these prolonged iontophoresis conditions, the results demonstrate that iontophoresis of these drugs during *in vivo* experiments will not affect our dopamine measurements.

Modulation of neurotransmitter release using quantitative iontophoresis

Dopamine release from terminals in the striatum is regulated by D2-autoreceptors (Benoit-Marand et al., 2001). Quinpirole, a D2-agonist, has been shown to decrease

Table 3.1. Effect of iontophoresis on the sensitivity of carbon-fiber microelectrodes for dopamine detection.

Solution Ejected by Iontophoresis	Post Ionto/Pre Ionto Sensitivity (nA/nM)
AP	1.00 ± 0.10
AP + NPE	1.01 ± 0.07
AP + Nomifensine	0.86 ± 0.08
AP + Quinpirole	0.91 ± 0.08
AP + Raclopride	0.87 ± 0.07

stimulated dopamine release in slices (Kennedy et al., 1992), and we wanted to show *in vivo* modulation with iontophoretic application of quinpirole. For these experiments we adjusted the position of the carbon-fiber/iontophoresis assembly so that it was in a location in the striatum that showed robust dopamine release (Moquin and Michael, 2009). After establishing reproducible stimulated release of dopamine, we iontophoretically ejected quinpirole and AP from the same barrel for 30 sec. The local AP concentration was monitored by fast-scan cyclic voltammetry. The stimulation was repeated 120 s after the iontophoretic delivery terminated when AP had diminished to ~2 % of its concentration during iontophoretic application. From the AP concentration we can calculate that the local quinpirole concentration at the time of the stimulation was 87 nM. This value is near the EC_{50} (60 nM) for quinpirole measured in brain slices (Joseph et al., 2002).

Consistent with autoreceptor regulation, dopamine release was diminished (representative example in Figure 3.7). This experiment was repeated in 6 different rats with a different iontophoretic assembly in each animal. In these experiments the amount of current used for ejection was adjusted so that the same amount of AP (and thus quinpirole) was ejected in each animal. The release amplitude was 63 ± 5% (n = 6) of its pre-drug value. The small error associated with these measurements highlights the advantage of using an electroactive marker, since it allows for adjustment to the applied iontophoretic current so that uniform amounts of quinpirole are ejected. Thus, compensation can be made for the variability inherent to each iontophoretic barrel. Because autoreceptors and uptake processes appear to be linked, we also examined the clearance rates of dopamine after stimulation. While a trend towards faster uptake rates was observed after quinpirole ejections, there was not a statistically significant decrease in $t_{1/2}$.

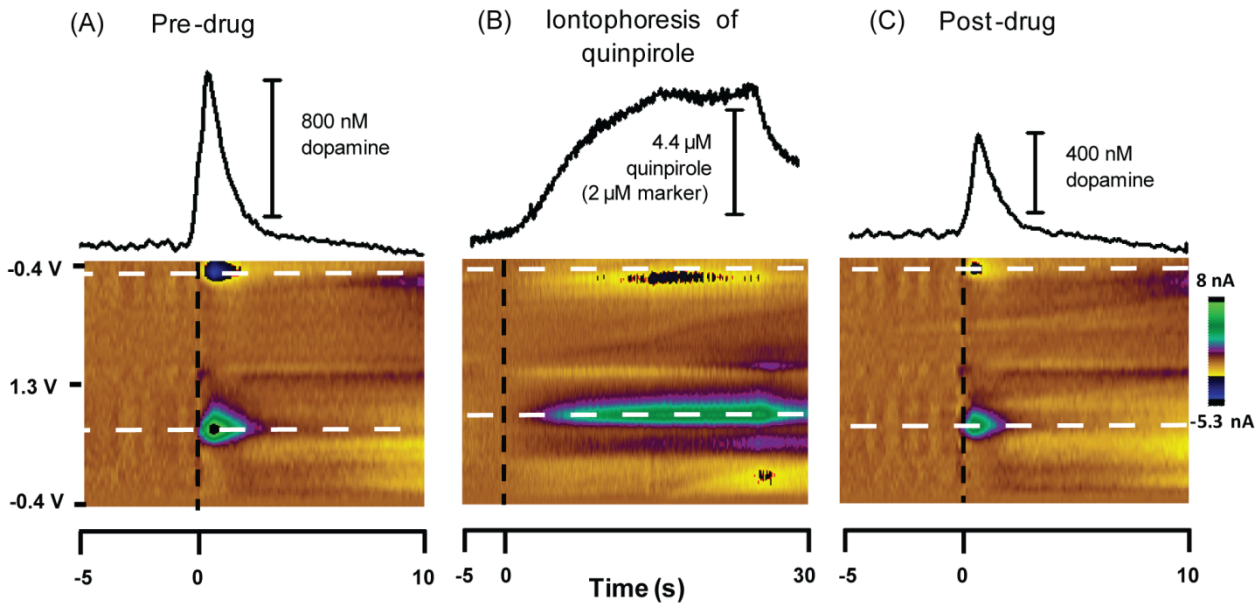

Figure 3.7. Stimulated dopamine release in an anesthetized animal before and after a localized ejection of solution containing both AP and quinpirole. The top panels show current as a function of time while the lower panels are two dimensional color plots where current is shown in false color on the potential vs. time axes. The white dashed lines on the color plots indicate the voltages at which oxidation (lower lines) and reduction (top lines) is occurring. (A) A representative baseline current trace and color plot for the stimulated release of dopamine. The black dashed line indicates the time of stimulation (B) Representation of iontophoretic ejection of AP and quinpirole. The black dashed line (t=0) indicates the application of a positive current to the barrel. The measured signal is due solely to AP, and is used to estimate the concentration of quinpirole. Here, 2 µM AP is the average concentration across the electrode, and is equivalent to 4.4 µM quinpirole. (C) Current trace and color plot for stimulated release 120 s after ejection seen in B. At the time of stimulation (black dashed line), the concentration of AP has decreased to 2% of its original value, corresponding to a decrease in quinpirole concentration to 88 nM. The extracellular concentration of dopamine seen in C is less than half the concentration initially seen in A. In both A and C the time of stimulation is indicated by the black dashed line and t=0 for each trace.

Stimulations were repeated at 2 min intervals and the amplitude returned to its original value within 3-5 stimulations after the initial iontophoretic application. In addition, when the electrode was lowered 400 μm, release similar to that seen in the absence of drug was observed. Since the amounts introduced by iontophoresis are microscopic, it would not be expected to exert an effect over a region much larger than that immediately around the electrode. It is worth noting that most iontophoresis experiments done previously used ejections much longer than 30 s, some delivering drug for 10's of min (Cheer et al., 2007). Such ejections seem unnecessary in light of the results presented here. Indeed, the ability to make multiple injections at the same or different sites enables multiple concentrations of drugs to be examined in a single animal. Systemic doses do not allow this type of flexibility, clearly highlighting one of the major advantages of iontophoresis.

Modulation of other dopaminergic presynaptic processes

Similar experiments were done with raclopride, a D2-receptor antagonist, which can block dopamine autoreceptor function, leading to an increase in release, as well as nomifensine, a dopamine re-uptake inhibitor that increases the amount of time required for dopamine to clear the synapse. The results from these experiments showed that raclopride increased stimulated dopamine release to 270 ± 40% (n=5) of its pre-drug value. Raclopride also caused a decrease in re-uptake rate, as indicated by the increased $t_{½}$, from 0.63 ± 0.03 s to 0.96 ± 0.05 s. This result is consistent with previous work where systemic injections of a D2-antagonist affected both release and uptake (Benoit-Marand et al., 2001; Wu et al., 2002) and further supports the idea that autoreceptor antagonists increase evoked DA levels by decreasing uptake in a complex signaling process. Similarly, nomifensine delivery resulted in a 187 ± 13% increase in stimulated dopamine release and an increased $t_{½}$ from 0.63 ± 0.03 s to 1.36± 0.05 s

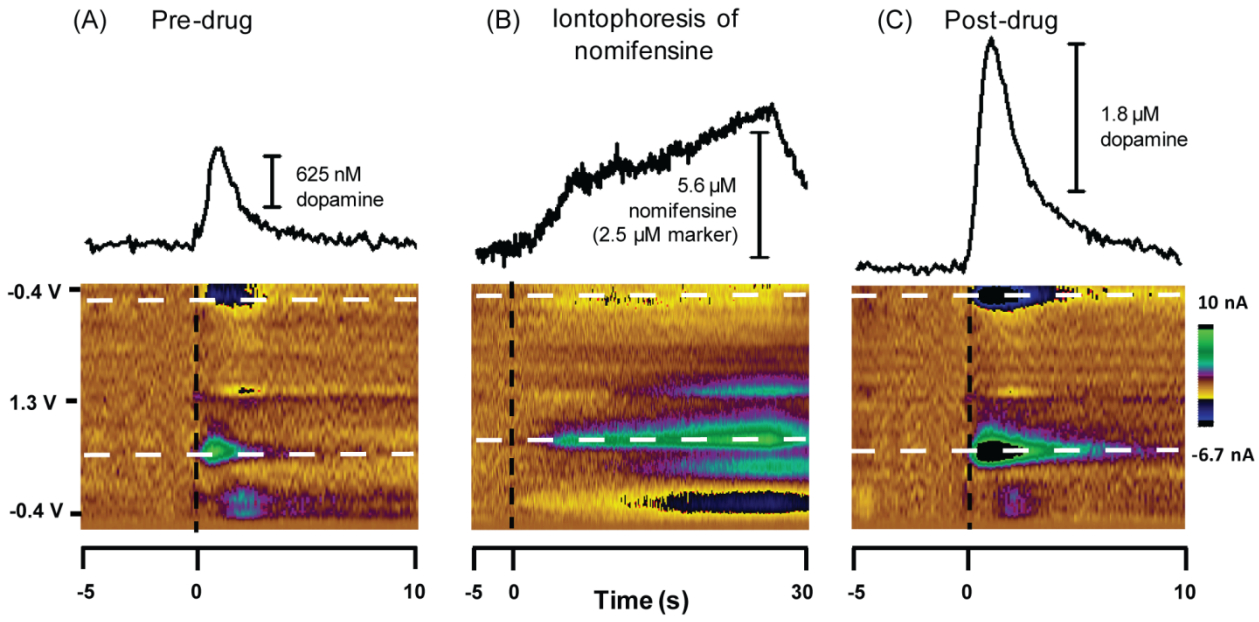

Figure 3.8. Stimulated dopamine release in an anesthetized animal before and after a localized ejection of solution containing both AP and nomifensine. The top panels show current as a function of time while the lower panels are two dimensional color plots where current is shown in false color on the potential vs. time axes. The white dashed lines on the color plots indicate the voltages at which oxidation (lower lines) and reduction (top lines) is occurring. (A) A representative baseline current trace and color plot for the stimulated release of dopamine. The black dashed line is the time to stimulation (B) Representation of iontophoretic ejection of AP and nomifensine. The black dashed line (t=0) indicates the application of a positive current to the barrel. Note that the measured signal is due solely to AP, and is used to estimate the concentration of nomifensine. Here, 2.5 µM AP is the average concentration across the electrode, and is equivalent to 5.6 µM nomifensine. (C) Current trace and color plot for stimulated release 120 s after ejection seen in B. At the time of stimulation (black dashed line), the concentration of AP has decreased to 2% of its original value, corresponding to a decrease in nomifensine concentration to 112 nM. The extracellular concentration of dopamine seen in C significantly increased and the clearance time is also increased, indicating a change in reuptake kinetics. In both A and C the time of stimulation is indicated by the black dashed line and t=0 for each trace.

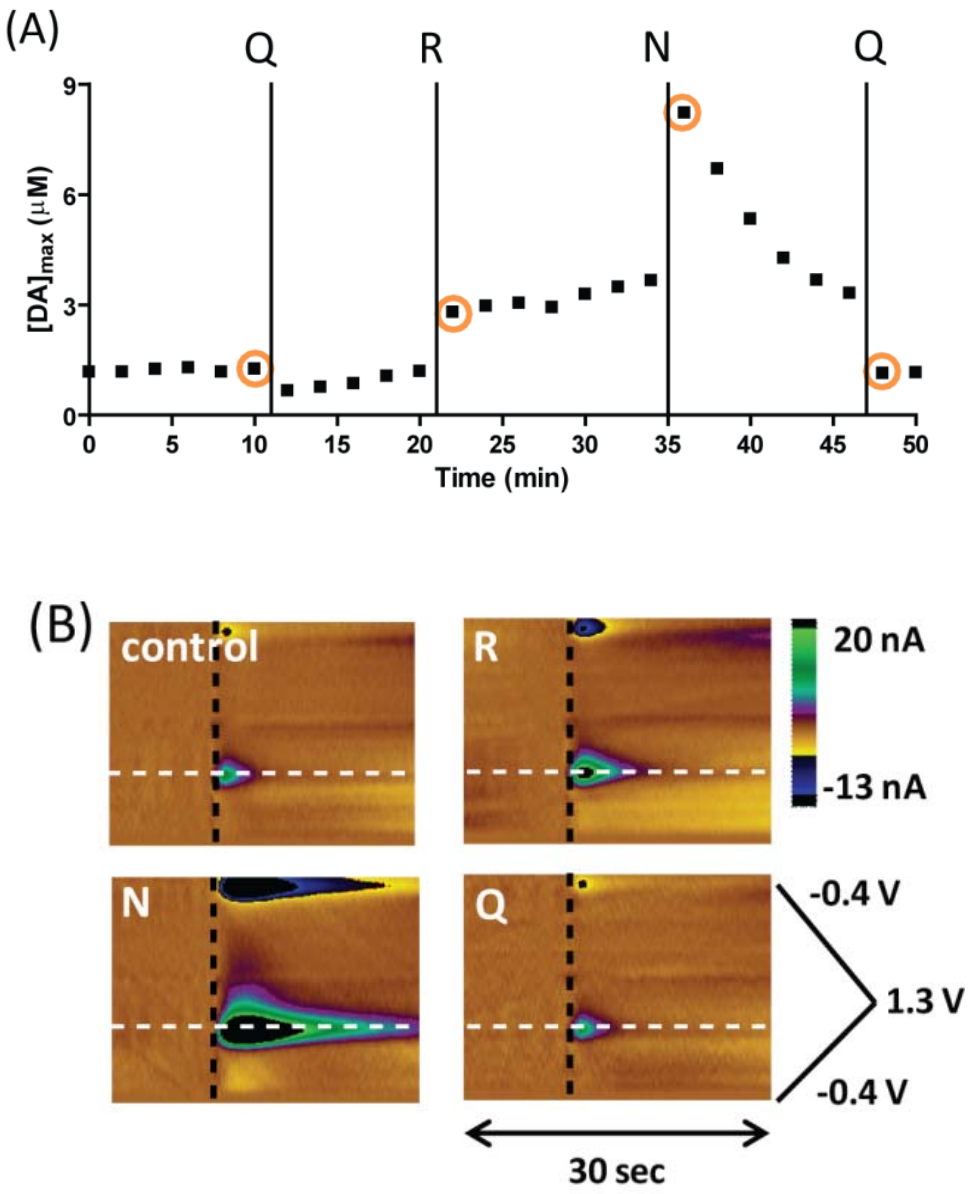

Figure 3.9. Rapid modulation of DA autoreceptors using quinpirole and raclopride and dopamine transporter using nomifensine. (A) Stimulated release of DA is recorded every 120 s and plotted is the maximum amount of dopamine overflow recorded from each stimulation. The circles denote the time points at which the color plots in B were taken. With the application of quinpirole (Q), raclopride (R) and nomifensine (N) at the time represented with the vertical dashed line, there was a change in DA signal seen at the next stimulation. (B) Color plots for the stimulated release of dopamine before application of any drugs and after the administration of each drug. The duration of the dopamine signal (white dashed line) after stimulation (black dashed line) is indicative of the re-uptake kinetics.

(Figure 3.8). The modulations observed due to localized application of all three drugs is consistent with those found for systemic injections (Kita et al., 2007).

Rapid modulation of dopamine release and uptake

One of the advantages of localized drug delivery is that drug effects are observed quickly. Figure 3.9 demonstrates rapid modulation of dopamine release and uptake by using a D2 agonist, D2 antagonist, and a dopamine reuptake blocker. Quinpirole, a D2 agonist, was delivered to attenuate dopamine release. As can be seen from Figure 3.9(A), a decrease in release is observed immediately after the 30 s ejection. In this representative experiment, the signal slowly returned to baseline over 10 min. Raclopride, a D2 antagonist, which blocks autoreceptors on dopamine terminals, quickly increased the amount of dopamine release observed by 3-fold. In contrast to quinpirole, this effect remained steady for over 10 min. To observe effects on dopamine uptake, we used the dopamine uptake inhibitor, nomifensine. As expected from previous findings, the uptake blocker increased the amount of dopamine release and slowed down uptake. This can be seen in the color plots shown at each point of modulation in Fig 9B. The dopamine signal apparent in the color plots has a longer duration once nomifensine is on board. This effect, however, is shorter lived than the raclopride effect, and over the course of 10 min, the signal returns to what it was before nomifensine ejection. To see if the raclopride and nomifensine effects could be reversed, quinpirole was re-applied, resulting in dopamine release returning back to the original baseline. In addition to demonstrating that iontophoresis can be used to quickly and robustly modulate dopamine release and uptake, it also gives insight into the different rates of unbinding for each of these drugs. The results show that nomifensine has a shorter-lasting effect than quinpirole and raclopride, consistent with studies that show nomifensine has the fastest

off rate from its binding site to striatal membranes (when adjusted for temperature) (Dubocovich and Zahniser, 1985; Dewar et al., 1989; Levant et al., 1992).

CONCLUSIONS

The results presented characterize and validate the use of an electroactive EOF marker for quantitative iontophoresis using carbon-fiber microelectrode assemblies. Nanomolar concentrations of raclopride, quinpirole, and nomifensine can be delivered by monitoring the co-ejection of the EOF marker. The effects of local delivery of these drugs can then be monitored by measuring electrically evoked dopamine release before and after drug. We show that a short, 30 s ejection is sufficient to affect autoreceptor regulation and reuptake of dopamine. Additionally, electrode placement can be verified by iontophoresis of a dye, such as pontamine sky blue. These experiments highlight the advantages of iontophoresis: quick, local, and selective receptor modulation. The use of carbon-fiber microelectrodes and an EOF marker enables real-time measurements of drug delivery, eliminating confounds from faulty ejections and differences in doses. These modifications improve the technique of iontophoresis for *in vivo* neuropharmacological experiments.

REFERENCES

Armstrong-James M, Fox K, Kruk ZL, Millar J (1981) Quantitative ionophoresis of catecholamines using multibarrel carbon fibre microelectrodes. J Neurosci Methods 4:385-406.

Axelsson J, Thesleff S (1959) A study of supersensitivity in denervated mammalian skeletal muscle. J Physiol 147:178-193.

Benoit-Marand M, Borrelli E, Gonon F (2001) Inhibition of dopamine release via presynaptic D2 receptors: time course and functional characteristics in vivo. J Neurosci 21:9134-9141.

Bloom FE (1974) To spritz or not to spritz: The doubtful value of aimless iontophoresis. Life Sciences 14:1819-1834.

Bradley PB, Candy JM (1970) Iontophoretic release of acetylcholine, noradrenaline, 5-hydroxytryptamine and D-lysergic acid diethylamide from micropipettes. Br J Pharmacol 40:194-201.

Cazes J (2001) Encyclopedia of chromatography. New York: Marcel Dekker.

Cheer JF, Aragona BJ, Heien ML, Seipel AT, Carelli RM, Wightman RM (2007) Coordinated accumbal dopamine release and neural activity drive goal-directed behavior. Neuron 54:237-244.

Crawford JM, Curtis DR (1964) The Excitation and Depression of Mammalian Cortical Neurones by Amino Acids. Br J Pharmacol Chemother 23:313-329.

Curtis DR, Eccles RM (1958) The excitation of Renshaw cells by pharmacological agents applied electrophoretically. J Physiol 141:435-445.

Curtis DR, Koizumi K (1961) Chemical transmitter substances in brain stem of cat. J Neurophysiol 24:80-90.

Curtis DR, Nastuk WL (1964) Micro-electrophoresis. In: Physical Techniques in Biological Research, pp 144-190. New York: Academic Press.

Curtis DR, Phillis JW, Watkins JC (1960) The chemical excitation of spinal neurones by certain acidic amino acids. J Physiol 150:656-682.

Del Castillo J, Katz B (1955) On the localization of acetylcholine receptors. J Physiol 128:157-181.

Del Castillo J, Katz B (1956) Localization of active spots within the neuromuscular junction of the frog. J Physiol 132:630-649.

Dewar KM, Montreuil B, Grondin L, Reader TA (1989) Dopamine D2 receptors labeled with [3H]raclopride in rat and rabbit brains. Equilibrium binding, kinetics, distribution and selectivity. The Journal of pharmacology and experimental therapeutics 250:696-706.

Dubocovich ML, Zahniser NR (1985) Binding characteristics of the dopamine uptake inhibitor [3H]nomifensine to striatal membranes. Biochemical pharmacology 34:1137-1144.

Freedman R, Hoffer BJ, Woodward DJ (1975) A quantitative microiontophoretic analysis of the responses of central neurones to noradrenaline: interactions with cobalt, manganese, verapamil and dichloroisoprenaline. British journal of pharmacology 54:529-539.

Herr NR, Kile BM, Carelli RM, Wightman RM (2008) Electroosmotic Flow and Its Contribution to Iontophoretic Delivery. Analytical Chemistry 80:8635-8641.

Hicks TP (1984) The history and development of microiontophoresis in experimental neurobiology. Prog Neurobiol 22:185-240.

Joseph JD, Wang YM, Miles PR, Budygin EA, Picetti R, Gainetdinov RR, Caron MG, Wightman RM (2002) Dopamine autoreceptor regulation of release and uptake in mouse brain slices in the absence of D(3) receptors. Neuroscience 112:39-49.

Kennedy RT, Jones SR, Wightman RM (1992) Dynamic observation of dopamine autoreceptor effects in rat striatal slices. J Neurochem 59:449-455.

Kita JM, Parker LE, Phillips PE, Garris PA, Wightman RM (2007) Paradoxical modulation of short-term facilitation of dopamine release by dopamine autoreceptors. Journal of neurochemistry 102:1115-1124.

Kiyatkin EA, Rebec GV (1996) Dopaminergic modulation of glutamate-induced excitations of neurons in the neostriatum and nucleus accumbens of awake, unrestrained rats. Journal of Neurophysiology 75:142-153.

Kiyatkin EA, Rebec GV (1997) Iontophoresis of amphetamine in the neostriatum and nucleus accumbens of awake, unrestrained rats. Brain Res 771:14-24.

Kiyatkin EA, Rebec GV (1999a) Modulation of striatal neuronal activity by glutamate and GABA: iontophoresis in awake, unrestrained rats. Brain research 822:88-106.

Kiyatkin EA, Rebec GV (1999b) Striatal neuronal activity and responsiveness to dopamine and glutamate after selective blockade of D1 and d2 dopamine receptors in freely moving rats. Journal of Neuroscience 19:3594-3609.

Kiyatkin EA, Rebec GV (2000) Dopamine-independent action of cocaine on striatal and accumbal neurons. The European journal of neuroscience 12:1789-1800.

Kiyatkin EA, Kiyatkin DE, Rebec GV (2000) Phasic inhibition of dopamine uptake in nucleus accumbens induced by intravenous cocaine in freely behaving rats. Neuroscience 98:729-741.

Kristensen EW, Wilson RL, Wightman RM (1986) Dispersion in flow injection analysis measured with microvoltammetric electrodes. Analytical Chemistry 58:986-988.

Krnjevic K, Laverty R, Sharman DF (1963a) Iontophoretic release of adrenaline, noradrenaline and 5-hydroxytryptamine from micropipettes. Br J Pharmacol Chemother 20:491-496.

Krnjevic K, Mitchell JF, Szerb JC (1963b) Determination of iontophoretic release of acetylcholine from micropipettes. J Physiol 165:421-436.

Levant B, Grigoriadis DE, DeSouza EB (1992) Characterization of [3H]quinpirole binding to D2-like dopamine receptors in rat brain. The Journal of pharmacology and experimental therapeutics 262:929-935.

Limberger N, Trout SJ, Kruk ZL, Starke K (1991) "Real time" measurement of endogenous dopamine release during short trains of pulses in slices of rat neostriatum and nucleus accumbens: Role of autoinhibition. Naunyn Schmiedebergs ArchPharmacol 344:623-629.

Miledi R (1960) The acetylcholine sensitivity of frog muscle fibres after complete or partial devervation. J Physiol 151:1-23.

Moquin KF, Michael AC (2009) Tonic autoinhibition contributes to the heterogeneity of evoked dopamine release in the rat striatum. Journal of neurochemistry.

Nastuk WL (1953) Membrane potential changes at a single muscle endplate produced by transitory application of acetylcholine with an electrically controlled microjet. Fed Proc 102.

Paxinos G, Watson C (2005) The rat brain in stereotaxic coordinates. Amsterdam ;Boston: Elsevier Academic Press.

Phillips PE, Hancock PJ, Stamford JA (2002) Time window of autoreceptor-mediated inhibition of limbic and striatal dopamine release. Synapse 44:15-22.

Purves R (1980a) Ionophoresis - Progress and Pitfalls. Trends in Neurosciences 3:245-247.

Purves RD (1977) The release of drugs from iontophoretic pipettes. J Theor Biol 66:789-798.

Purves RD (1979) The physics of iontophoretic pipettes. J Neurosci Methods 1:165-178.

Purves RD (1980b) Effect of Drug Concentration on Release from Ionophoretic Pipettes. Journal of Physiology-London 300:P72-P73.

Rebec GV (1998) Real-time assessments of dopamine function during behavior: single-unit recording, iontophoresis, and fast-scan cyclic voltammetry in awake, unrestrained rats. Alcoholism, Clinical and Experimental Research 22:32-40.

Rice ME, Nicholson C (1995) Diffusion and Ion Shifts in the Brain Extracellular Microenvironment and Their Relevance for Voltammetric Measurements. In: Voltammetric methods in brain systems Voltammetric methods in brain systems, p 27. Totowa, N.J.: Humana Press.

Simmonds MA (1974) Quantitative evaluation of responses to microiontophoretically applied drugs. Neuropharmacology 13:401-406.

Stone TW (1985) Microiontophoresis and Pressure Ejection. London: John Wiley & Sons.

Wu Q, Reith MEA, Walker QD, Kuhn CM, Carroll FI, Garris PA (2002) Concurrent Autoreceptor-Mediated Control of Dopamine Release and Uptake during Neurotransmission: An In Vivo Voltammetric Study. Journal of Neuroscience 22:6272-6281.

Chapter 4 :

In Vivo Electrochemical Monitoring of Electrically Evoked Extracellular Catecholamine in the Subregions of Bed Nucleus of the Stria Terminalis

INTRODUCTION

The bed nucleus of the stria terminalis (BNST) is a heterogeneous brain region that relays excitatory and inhibitory information from cortical, hippocampal and amygdalar nuclei to subcortical, hypothalamic and brainstem regions (Cullinan et al., 1993; Dong et al., 2000; Dong et al., 2001a; Dong et al., 2001b). Stemming from its anatomical positioning, various studies have explored the role of the BNST in mediating a host of behavioral responses ranging from fear and anxiety to addiction and reward (Epping-Jordan et al., 1998; Delfs et al., 2000; Erb et al., 2000; Cecchi et al., 2002; Sullivan et al., 2004; Fendt et al., 2005). Dopamine (DA) and norepinephrine (NE) project to the BNST and have demonstrated modulatory effects on signaling in this region (Forray and Gysling, 2004; Meloni et al., 2006; McElligott and Winder, 2009). Histochemical and behavioral experiments have suggested that noradrenergic and dopaminergic fibers are anatomically segregated in the BNST. However, the precise locations of their respective innervations within the subregions of the BNST are not entirely clear.

Historically, NE fibers are thought to be found mainly in the ventral BNST (Myers et al., 2005). However, emerging histochemical evidence suggests that both NE may be present in the dorsal lateral BNST (Egli et al., 2005), a subregion containing mostly

dopaminergic projections. A caveat of any histochemical study is that they do not establish if the projections stained for contain functional release sites. Microdialysis studies provide supporting evidence that DA and NE is found within the BNST (Carboni et al., 2000; Cecchi et al., 2002). However, the technique lacks the spatial resolution necessary to determine functional innervation of subnuclei. Despite the important roles of NE and DA in the regulation of behaviors, few studies have examined *in vivo* release and uptake of NE and DA in the subregions of the BNST. This is, in part, because BNST subregions containing appreciable amounts of NE or DA are often only a few hundred microns across, thus requiring techniques with high spatial resolution and sensitivity (Park, 2009). Additionally, BNST subnuclei reside is close proximity to the striatum, ventral pallidum (VP), and the preoptic areas (PA), all of which contain catecholamines (Figure 4-1).

Previously, Park *et al.* demonstrated that stimulus-evoked NE release in the *v*BNST can be distinctly measured utilizing *in vivo* fast-scan cyclic voltammetry (FSCV) at carbon-fiber microelectrodes (Park, 2009). A key advantage of this experimental approach is that it provides the spatial resolution necessary to selectively monitor catecholamines in small BNST subregions. In addition, rapid changes (subsecond) in the extracellular NE concentration can be monitored in real time, allowing critical differences in the dynamics of release and uptake amongst the BNST subregions to be probed.

Here, DA and NE are individually monitored in distinct subregions of the BNST using FSCV, with pharmacological verification and micro-lesioning of the recording site. Results show that the majority of functional noradrenergic projections are limited to the dorsomedial BNST with the largest projection innervating the subcommisural ventral BNST near the fusiform and parastrial subnuclei. Conversely, the dopaminergic projections are mainly distributed in the dorsolateral (*dl*) BNST near the oval subnucleus.

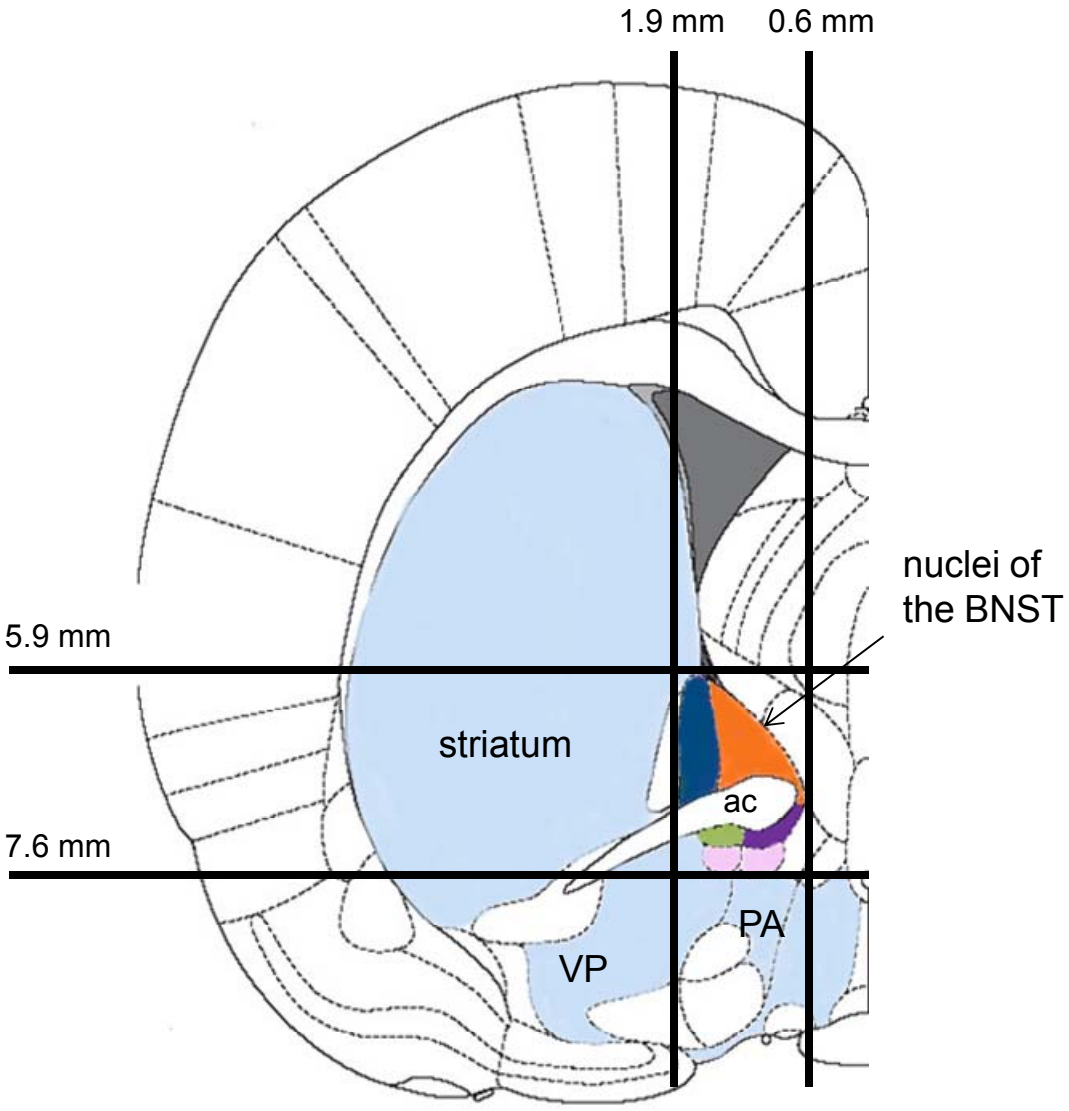

Figure 4.1. Anatomical location of BNST subnuclei. Shown is a depiction of a coronal slice of a rat brain. The BNST spans a little over 1 mm in the medial-lateral axis, and about 1.7 mm in the dorsal-ventral axis. It is divided into dorsal and ventral regions by the anterior commisure (ac). The subregions examined in this study are the *dl*BNST (orange), *dm*BNST (dark blue), and *mv*BNST (green). The *lv*BNST (purple) was not studied in this study, but does show some catecholamine release. Thus, the *mv*BNST will be referred to as the *v*BNST. Regions shown in light blue are neighboring sites that contain catecholamines and can confound results if the appropriate anatomical and pharmacological verifications are not done.

Using quantitative iontophoresis we compare the pharmacological effects of catecholaminergic receptor antagonists and uptake blockers administered i.p. with those delivered locally in the subregion of interest. Use of quantitative iontophoresis provided pharmacological evidence that modulation of release in the ventral-medial BNST occurs through presynaptic mechanisms, but modulation in the dorsal-medial occurs through a combination of mechanisms.

MATERIALS AND METHODS

Chemicals and drugs

Unless noted, all chemicals were purchased from Sigma-Aldrich (St. Louis, MO) and used as received. Chemical structures of the species used are shown in Appendix I. Solutions were prepared using deionized water. A physiological buffer solution, pH 7.4, (15 mM TRIS, 126 mM NaCl, 2.5 mM KCl, 25 mM $NaHCO_3$, 2.4 mM $CaCl_2$, 1.2 mM NaH_2PO4, 1.2 mM $MgCl_2$, 2.0 mM Na_2SO_4) was used in all calibration experiments.

Desipramine-HCl, raclopride-HCl, and idazoxan-HCl were dissolved in saline. GBR 12909-HCl was dissolved in double distilled water and then diluted with saline

Animals and surgery

Male Sprague-Dawley rats (225-350g; Charles River, Wilmington, MA) were anesthetized with urethane (1.5 g/kg, i.p.) and placed in a stereotaxic frame (Kopf, Tujunga, CA). Holes were drilled in the skull on the right hemisphere for the working and stimulating electrodes at coordinates selected from the atlas of Paxinos and Watson (Paxinos and Watson, 2005). An Ag/AgCl reference electrode was inserted in the left hemisphere. The carbon-fiber iontophoresis probe was placed either in the either the medial (+1.2 mm ML, 0 AP from bregma) or lateral BNST (+1.6 mm ML, 0 mm AP from

bregma). The stimulating electrode was placed in the VTA (+1.0 mm ML, -5.2 mm AP from bregma). The carbon-fiber and stimulating electrodes were individually adjusted in the dorsal-ventral coordinate to locate the optimal locations for stimulated NE release.

Electrical Stimulation

An untwisted bipolar stimulating electrode (Plastics One, Roanoke, VA) was used to stimulate catecholamine neurons using a pair of linear constant current stimulus isolators (model NL80A, NeuroLog System, Digitimer Ltd, UK). The stimulation train consisted of 40 biphasic pulses (± 300 μA, 2 ms/phase) applied at 60 Hz. The pulses were generated by a computer and applied between the cyclic voltammograms to avoid electrical interference.

Iontophoresis Probes

A glass capillary (Part # 624503, 0.60 mm o.d., 0.4 mm i.d., 4" long, A-M Systems, Sequim, WA) was loaded with a carbon fiber (T-650, Thornel, Amoco Corp., Greenville, SC) that served as the working electrode. This capillary containing the carbon fiber was then inserted into one barrel of a 4-barrel capillary (Part # 50644, 1 mm o.d., 0.75 mm i.d., 4barrel GF pipettes, 4" long, Stoelting Co., Wood Dale IL). The four barrel assembly contained glass filaments (GF) in each barrel that aid in filling the barrel by capillary action. The capillaries were bundled together with heat shrink and tapered to a sharp tip using a micropipette puller (Narashige, Tokyo, Japan) with a two-step pull process. The protruding carbon fiber was cut to a length between 30 and 50 μm by careful use of a scalpel under a 10X microscope objective. The resulting probe consists of a glass-encased carbon fiber that is 5-7 μm in diameter and 3 iontophoretic barrels each about 1 μm in diameter. Before use, the barrel containing the carbon fiber was backfilled with electrolyte (4 M potassium acetate, 150 mM potassium chloride) and fitted

with wires for electrical contact. The remaining barrels for iontophoresis were filled with solutions containing reagents to be ejected.

Electrochemical Data Acquisition and Presentation

Cyclic voltammograms were acquired using data-acquisition hardware and locally software written in LabVIEW (National Instruments, Austin, TX). The cyclic voltammetry waveform was generated and the voltammetric signal was acquired with a computer interface board, the PCI-6052E (National Instruments). A PCI-6711E D/A board (National Instruments) was used to synchronize waveform application, data acquisition, and to trigger the iontophoretic current applied and the loop injector in the flow injection apparatus. The voltammetric waveform was input into a custom-built instrument for application to the electrochemical cell and current transduction (University of North Carolina at Chapel Hill, Department of Chemistry Electronics Facility). After data collection, background subtraction, signal averaging, and digital filtering (low pass filtered at 2 kHz) were all done under software control.

For all experiments, a triangular waveform was applied with a scan rate of 400 V s^{-1} with a rest potential of -0.4 V versus a Ag/AgCl reference electrode between scans, a linear scan to 1.3 V, followed by a scan back to the rest potential. The scans were repeated every 100 ms, and collection was typically for 15- 60 s. This large amount of data is presented as a color plot, with the applied voltage plotted on the ordinate, time on abscissa, and measured current in false color.

Iontophoresis Ejections

Each barrel of the iontophoresis assembly was filled with the drug of interest and the EOF marker, usually AP, at concentrations of ~10 mM in 5 mM NaCl at pH 5.8. Injection currents were delivered by a constant current source designed for

iontophoresis (Neurophore, Harvard Apparatus, Holliston, MA). For each barrel, an ejection current (between 5 to 40 nA) was selected by evaluating ejections (30 s duration) that gave a measurable voltammetric signal for the EOF marker (average peak current of 5 to 30 nA at the peak potential in the voltammogram). A current of 0 nA was applied between ejections.

Calibrations

The response of the carbon fiber electrode was calibrated in a flow injection analysis system after *in vivo* use, unless the electrode was used for lesioning (Kristensen et al., 1986). The probe was positioned at the outlet of a six-port rotary valve. A loop injector was mounted on an actuator (Rheodyne model 7010 valve and 5701 actuator) that was used with a 12-V DC solenoid valve kit (Rheodyne, Rohnert Park, CA) to introduce the analyte to the surface of the electrode. The linear flow velocity (1.0 cm s^{-1}) was controlled with a syringe infusion pump (Harvard Apparatus model 940, Holliston, MA). The voltammetric current was measured at the peak potential for each analyte that was evaluated at 4 concentrations. For carbon-fiber microelectrodes used to lesion the brain (*see below*), we used a postcalibration factor (9.3 ± 0.5 nA/μM for dopamine, 6.0 ± 0.2 nA/μM for norepinephrine), based on the average response obtained from multiple electrodes as described in our previous study.

Capillary Electrophoresis Experiments

A home-built CE system equipped with an absorbance detector and a 30 kV power supply was employed. Absorbance traces were collected using a custom written LabVIEW program (Courtesy of Professor James Jorgensen, UNC-CH). Separations were carried out in a 50 μm diameter fused silica capillary, 96.0 cm in total length, with the UV detector placed 87.5 cm from the inlet. Experiments were done in cationic mode

(the anode at the inlet and cathode at the outlet). Samples were run at a concentration of 2 mM in 17 mM PBS (phosphate buffered saline, made up of 0.25% monosodium phosphate and 0.04% disodium phosphate) with a pH of 5.8 as in the iontophoresis experiments. UV detection was measured at 195 and 240 nm and electrophoretic mobilities were calculated as previously described (Herr et al., 2008).

Histology

At the end of experiments, electrode placements were verified by electrolytic lesions made with the carbon-fiber microelectrodes and killed with an overdose of urethane (2.0 g/kg) as described previously (Garris and Wightman, 1994; Park et al., 2009). A lesion was made at the recording site by applying constant current (20 μA for 10 s) to the carbon-fiber electrodes. Brains were removed from the skull and stored in 10 % formaldehyde for at least 3 days, and coronally sectioned into 40 μm thick slices with a cryostat. The sections mounted on slides were stained with 0.2 % thionin, and coverslipped before viewing under a light microscope.

RESULTS AND DISCUSSION

Catecholamine detection within the BNST

Figure 4.1 shows a coronal cross section of the BNST, highlighting the major subnuclei and the neighboring catecholaminergic sites. The BNST spans approximately 1 mm in the medial/lateral axis and approximately 1.5 mm on the dosal/ventral axis including the anterior commissure, which transects the BNST dividing it into dorsal and ventral portions. Although histochemical and microdialysis evidence exists indicating that DA an NE are present in regions of the BNST, mapping of the subregions using voltammetric techniques with high spatial resolution has not been done. In Figure 4.2, mapping of catecholamine release is shown for both ventral and dorsal regions in the

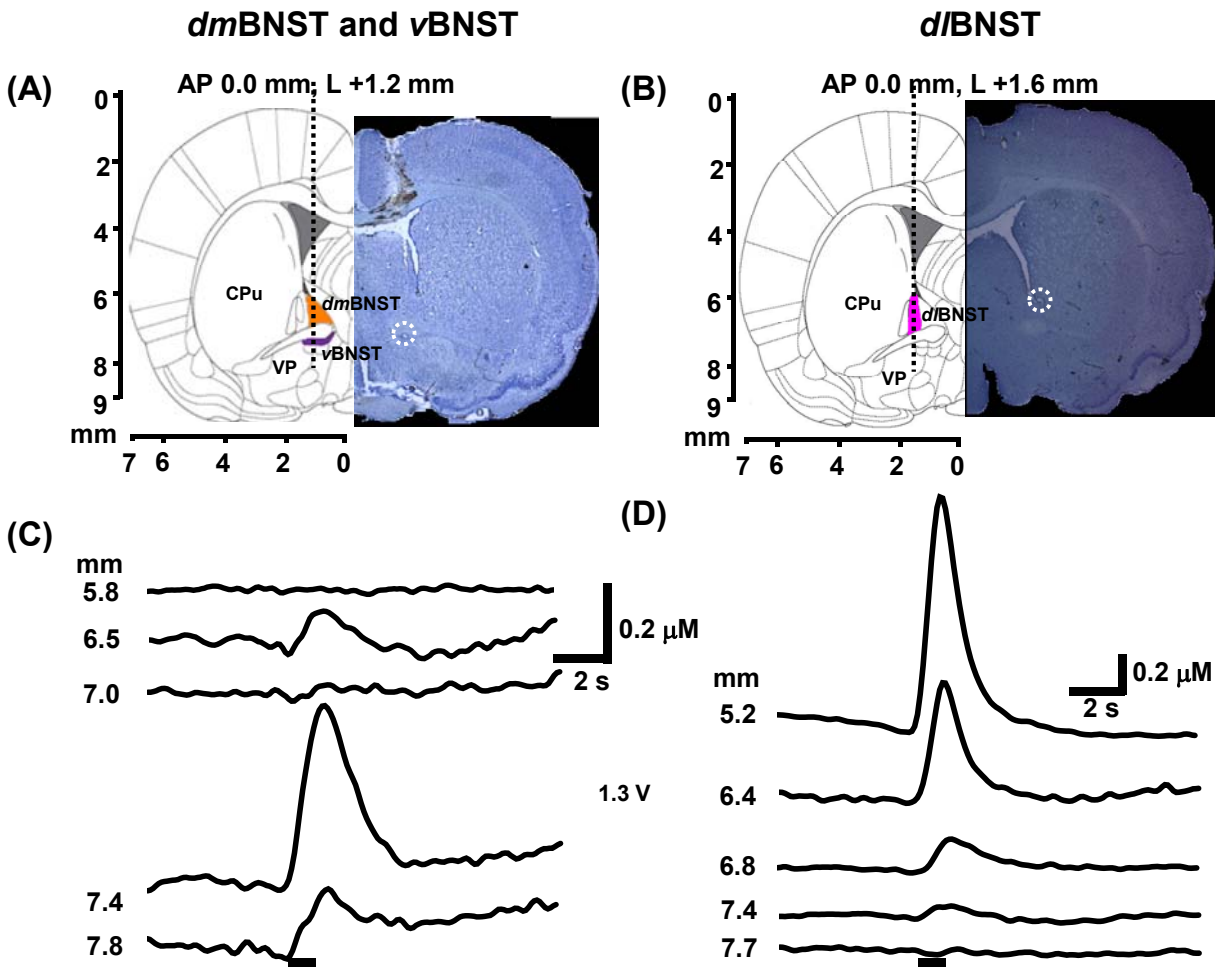

Figure 4.2 Anatomical mapping of catecholamine releasing sites in the medial and lateral BNST. (A, B). Electrical lesioning provides histological evidence that the electrode was positioned in the dorsomedial and ventral medial (A) or dorsolateral (B) BNST. (C,D) The BNST is divided into dorsal and ventral regions by the anterior commissure. Mapping of catecholamine release on the dorsal-ventral axis shows that in the medial BNST, the most robust signal is observed ventral to the commissure, although some catecholamine release is observed in the dorsal region. Conversely, in the lateral BNST, a measurable catecholamine signal is observed dorsal to the commissure.

BNST. Catecholamine release was evoked by lowering a bipolar stimulating electrode into the VTA/SN to stimulate dopamine cell bodies and passing noradrenergic fibers. A carbon-fiber microelectrode was lowered into either the medial (+1.2 mm ML, 0 AP from bregma) or lateral BNST (+1.6 mm ML, 0 mm AP from bregma) to measure release. Electrodes placed in the dorsomedial (*dm*) BNST revealed a slow rising current that appeared at approximately 6.0 mm from the skull surface, and was most robust in the ventral (*v*) BNST at approximately 7.5 mm from the skull near the parasagital and fusiform subnuclei. The current was not observed around 7.0 mm from the skull surface due to the electrode passing through the anterior commissure. Positioning the electrode in the dorsolateral (*dl*) BSNT revealed a characteristically distinct current from the medial position that was most robust at approximately +6.5 mm from the skull close to the oval and juxtacapsular subnuclei. This current showed a faster rise time, similar to signals observed when measuring DA in the striatum.

Pharmacological evidence for NE in the ventral BNST and DA in the dorsolateral BNST

The identity of the signals shown in Figure 4.3 cannot be determined based on qualitative assessment of the voltammetric signal. DA and NE exhibit similar electrochemical properties; thus their cyclic voltammograms are indistinguishable, as shown in Figure 4.3. However, selective NE or DA drugs can be used to distinguish the signals since pharmacology is an established criterion for determining the identity of a neurotransmitter. Idazoxan (IDA), an α_2-andrenergic antagonist and desipramine (DMI), a NET inhibitor were used to probe the contribution of NE to the signals measured. Conversely, raclopride, a D2 antagonist, and GBR 12909, a selective DAT inhibitor, were used to determine if the signal was dopaminergic or noradrenergic.

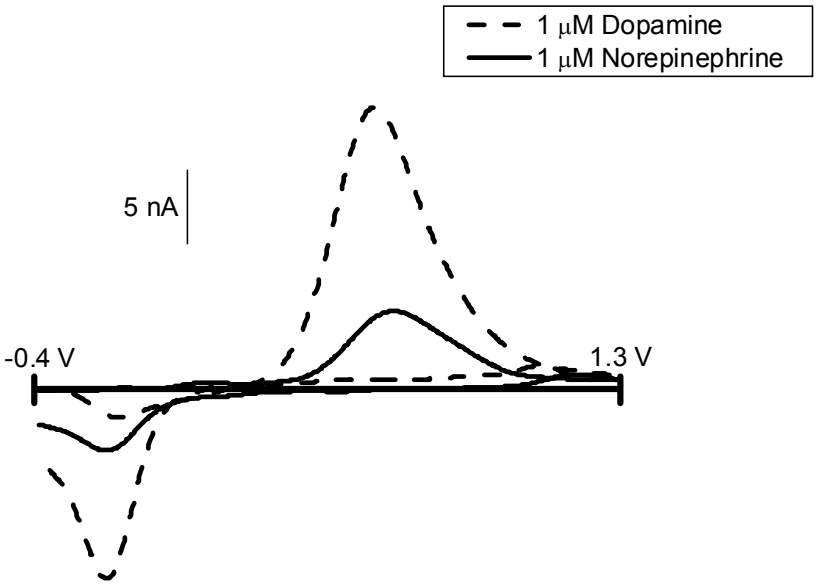

Figure 4.3. Cyclic voltammograms of dopamine and norepinephrine. Catecholamines are structurally and electrochemically similar. Cyclic voltammograms obtained for a 1 μM injection of DA (solid line) and NE (dashed line) are shown. While there is a slight offset between oxidation potential of DA and NE, it is not sufficient to qualitatively distinguish the signals. It is also important to note the differences in sensitivity for DA and NE. The current due to the oxidation of NE is nearly 4Xs less than that measured for DA oxidation. This significant decrease in sensitivity adds to the difficulty in monitoring NE *in vivo*.

The *v*BNST and *dl*BNST showed the greatest amount of catecholamine release, and thus these regions were chosen for pharmacological verification. After establishing reproducible catecholamine release, systemic injection (i.p.) of NE and DA drugs were given. NE drugs IDA (5 mg/kg) and DMI (15 mg/kg) increased the current and decay time (respectively) of stimulated catecholamine release in the *v*BNST but not in the *dl*BNST. Conversely, the DA drugs raclopride (2 mg/kg) and GBR 12909 (15 mg/kg) increased the current and half-life time ($t_{1/2}$), respectively, of stimulated catecholamine in *dl*BNST but not the *vm*BNST. The half-life of catecholamine uptake, $t_{1/2}$, was taken as the time to descend from its maximum value to half of that value. These data indicate that NE is the major catecholamine present in the *v*BNST, while DA is present in the *dl*BNST. The results from these experiments are shown in Figure 4.4.

Time course of catecholamine response within the BNST

A closer examination at the DA and NE signals measured in the BNST reveal interesting aspects about the nature of catecholamine release in this region. First, the $t_{1/2}$, which is indicative of re-uptake kinetics is approximately twice as long for NE release in the *v*BNST as compared to DA release in the *dl*BNST ($t_{1/2}$ norepineprhine: 1.36 $\pm$ 0.07; $t_{1/2}$ dopamine: 0.67 $\pm$ 0.05; n=6). Moreover, NE re-uptake in the *dm*BNST (2.37 $\pm$ 0.07, n = 5) is slower than in the *v*BNST. Surprisingly, following the onset of stimulation there is approximately a 260 ms time delay prior to the increase in current due to NE release that is not observed with DA (Figure 4.5). Neither the differences in the current decay time, nor the delay in stimulus onset can be attributed to the kinetics of the electrochemical reaction at the electrode surface as confirmed by *in* vitro experiments. Thus, the observed delay must have a physiological meaning that could reveal interesting and unique aspects of NE neurotransmission. While NE release and uptake *in vivo* are just beginning to be explored in the field, DA release and uptake have been

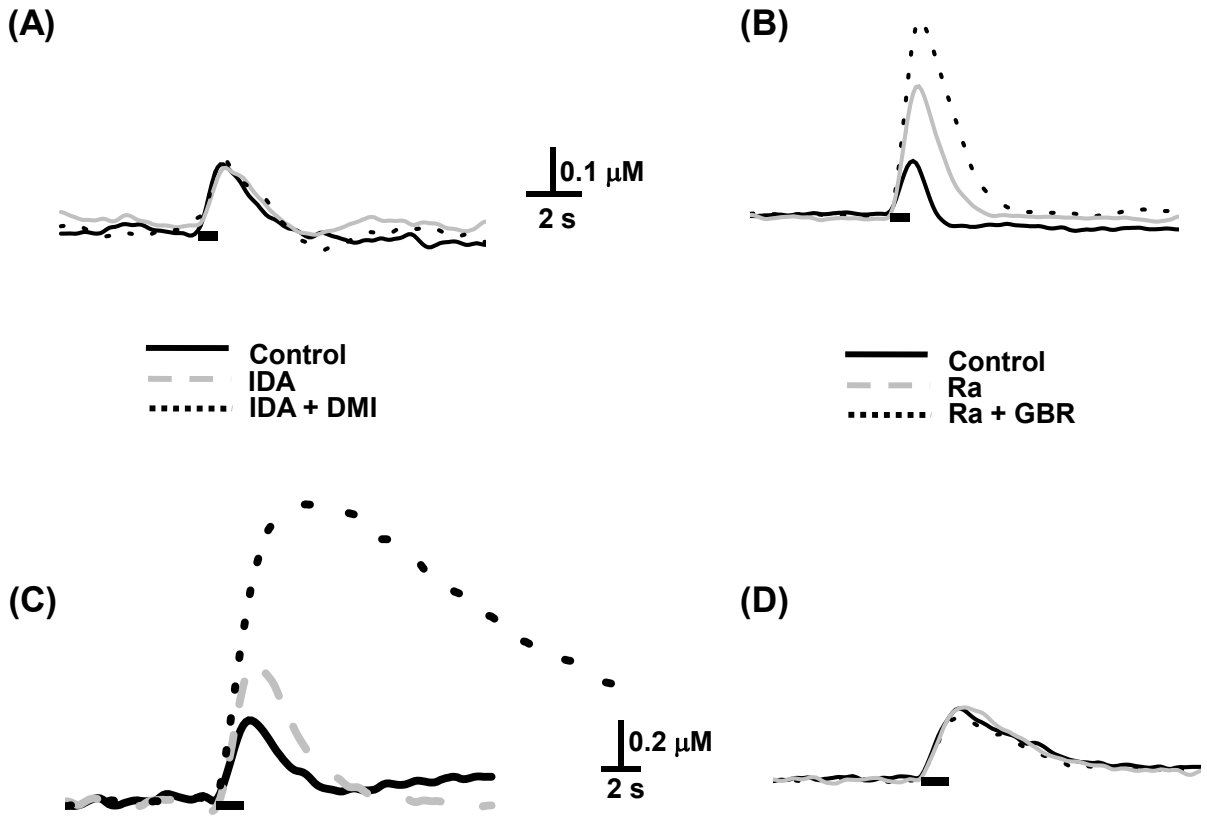

Figure 4.4. Identification of catecholamine signals with pharmacology. (A) NE drugs desipramine and idazoxan do not modulate electrically evoked catecholamine release in the dlBNST, but DA drugs raclopride and GBR12909 do modulate release in *dl*BNST (B). Conversely, NE drugs desipramine and idazoxan modulate release in the *vm*BNST (C) but not in the *dl*BNST (D). These data indicate the catecholamine signal measured in the *vm*BNST is NE, and DA in the d*l*BNST.

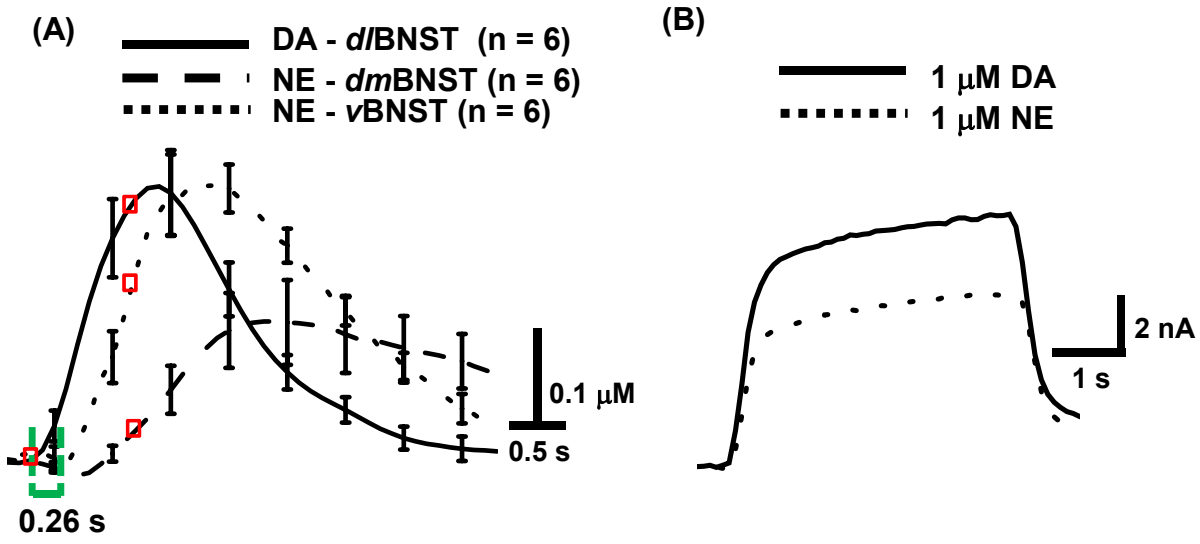

Figure 4.5. NE and DA show different rise times after electrical stimulation. Current versus time traces for NE and DA are shown in (A) due to electrical stimulation (red boxes indicate start and finish of stimulation). The green box indicates the delay in rise time present from NE traces. However, *in vitro*, NE and DA exhibit the same time-response at the electrode (B), thus the observed delay *in vivo* must have a physiological basis that may hint at signaling differences between NE and DA.

extensively studied in brain slice and in *in vivo*. The body of this work has shown that the shape of the current reveals important aspects of the kinetics of release and uptake. Thus, the characteristic differences in rise time and clearance of DA and NE may be indicative of differential modes of neurotransmission.

Local regulation of norepinephrine release in the BNST with quantitative iontophoresis

As demonstrated above, blocking NE's activation of the α_2-adrenergic receptors with a systemic injection of antagonist increases the observed concentration of NE release upon stimulation of noradrenergic fibers. This result fails to demonstrate, however, if the α_2-AR's control over noradrenergic transmission is at the synaptic terminals within the BNST or a global systemic effect. Although work done in BNST slices has shown that α_2-adrenergic receptors regulate NE release, presynaptic regulation of NE has not been demonstrated *in vivo*. Previous work has demonstrated that quantitative iontophoresis can be used to locally modulate dopaminergic release *in vivo* (Chapter 3). Thus, to examine presynaptic regulation of NE release, we used quantitative iontophoresis to locally apply selective NE drugs at BNST terminals. The *v*BNST and *dm*BNST, which show stimulus evoked NE release, were chosen as the target for these studies since both lie on the same anterior-posterior axis simplifying the experimental design.

Iontophoresis of acetaminophen has no effect on NE release in the medial BNST

Quantitative iontophoresis is accomplished by voltammetrically monitoring ejection of an electroactive neutral substance that serves as a marker for electroosmotic flow (EOF), the main source of variability in ionotophoretic ejections. Acetaminophen was chosen as the EOF marker for these experiments since it has been previously

shown to have no effect on neurotransmission in the striatum (see Chapter 2). However, the effects of acetaminophen iontophoresis into the BSNT have not been examined and thus needed to be tested before use with pharmacologically active drugs. Figure 4.6 shows that acetaminophen iontophoresis has no observable effect on the amplitude or kinetic of NE release in the BNST. As in the above experiments, the position of the carbon-fiber microelectrode was adjusted dorsal/ventrally to locate robust NE release. After establishment of a steady baseline, acetaminophen was iontophoretically delivered for 30 s. Confirmation and quantification of this ejection can be seen from the current v. time trace in Figure 4.6(B). After iontophoretic delivery was determined, 120s elapsed to allow to the electrochemical signal to return to baseline, at which stimulation was repeated. No observable change in the amplitude or kinetics of NE release was observed, establishing that acetaminophen can be used as an internal marker in the BNST for quantitative iontophoresis.

Quantification of iontophoretic delivery of electroinactive NE drugs

To determine the relative mobility of NE drugs IDA and DMI, capillary electrophoresis was used. As has been previously shown, electrophoretic mobilities obtained from capillary electrophoresis are positively correlated to the rate of iontophoretic transport relative to an electroosmotic flow (EOF) marker (Herr et al., 2008). Briefly, much like capillary electrophoresis, iontophoretic delivery is due to the combination of ion migration and EOF. Use of a neutral electroactive marker allows EOF to be directly monitored using carbon-fiber microelectrodes coupled to iontophoretic barrels. Differences in electrophoretic mobility indicate the relative rate of migration for ions within a single run. The rates of transport for DA and uric acid relative to acetaminophen have been previously determined in both capillary electrophoresis and iontophoresis (Herr et al., 2008). This data demonstrated that there is a positive

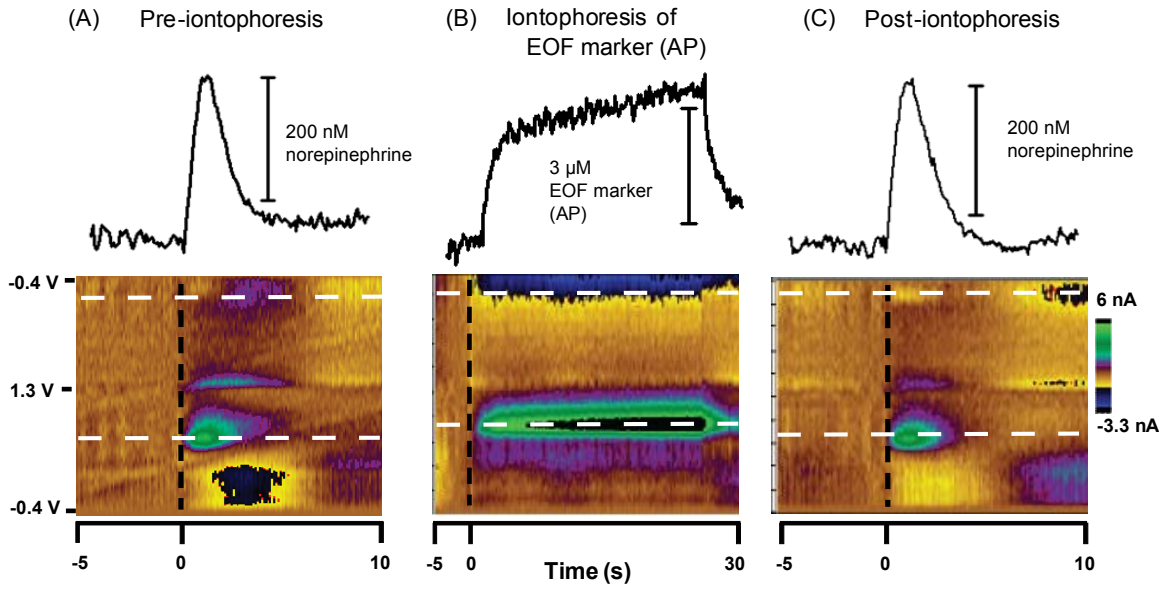

Figure 4.6. Effect of AP on stimulated NE release in the *v*BNST. The top panels show current as a function of time while the lower panels are two dimensional color plots where current is shown in false color on the potential vs. time axes. The white dashed lines on the color plots indicate the voltages at which oxidation (lower lines) and reduction (top lines) is occurring. (A) A representative baseline current trace and color plot for the stimulated release of dopamine. The black dashed line (t=0) indicates time of stimulation. (B) Representation of iontophoretic ejection of 3 µM AP. The black dashed line (t=0) indicates the application of a positive current to the barrel. (C) Current trace and color plot for stimulated release after ejection seen in B. The black dashed line (t=0) indicates time of stimulation. There is no change in the extracellular concentrations of NE seen in A and C elicited with a stimulation indicated by the black dashed line and t=0 for each trace.

correlation between the two. Thus, to quantify iontophoretic delivery of electroinactive drugs electrophoretic mobilities will be used to calculate the relative iontophoretic rate of delivery. The results from this experiment are shown in Figure 4.7. The data indicate that DMI and IDA are transported at rates that are 2.21 and 2.42 times as fast as the EOF marker, acetaminophen, respectively. These rates will be used to calculate the amount of IDA and DMI delivered when co-ejected with an EOF marker.

Iontophoresis of NE drugs in dorsal and ventral portions of the medial BNST

The effects of DMI and IDA were evaluated in the *dm*BNST and *v*BNST. Since iontophoresis allows for multiple drugs and sites to be evaluated in one animal, the effects of both drugs were first investigated in the *dm*BNST followed by the *v*BNST. Stimulated release of NE was first established in the *dm*BNST. Following pre-drug control measurements, IDA was iontophoretically applied for 30s. At steady state, the concentration of IDA at the electrode was 12 μM based on the measured acetaminophen concentration and the values obtained from Figure 4.7. Stimulation of noradrenergic fibers was repeated every 120s after iontophoretic application. Previous work has shown that 120s after the termination of ejection, the electrochemical signal observed due to ejection is diminished to ~2% of its steady-state value (Herr et al., 2008). Thus, at the time of stimulation the concentration of IDA present is ~ 240 nM. Identical experiments were done with DMI, after the IDA drug effect was evaluated and with both drugs in the vmBSNT. An example of these experiments is given in Figure 4.8 showing the effect of IDA on stimulated NE release in the *vm*BNST. Across animals in the *dm*BNST, neither IDA nor DMI had an effect on the amplitude of stimulated NE release. DMI did have an effect on re-uptake kinetics with an increase of 123 $\pm$ 3 % from the pre-drug value. Conversely, in the *v*BNST, both drugs had significant effects on the release and clearance of NE. Following IDA application, the measured NE overflow was 179 $\pm$ 25 %

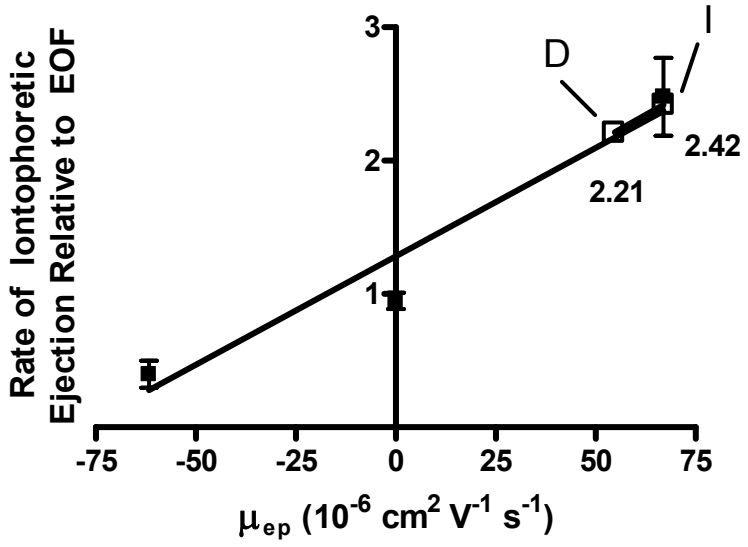

Figure 4,7. The electrophoretic mobilities of the electroactive compounds uric acid, AP, and DA (■) are positively correlated to previously reported iontophoretic rates. The linear regression from this correlation was used to determined iontophoretic rates relative to AP for desipramine (D) and idazaxon (I) (□) based on their electrophoretic mobilities calculated by capillary electrophoresis.

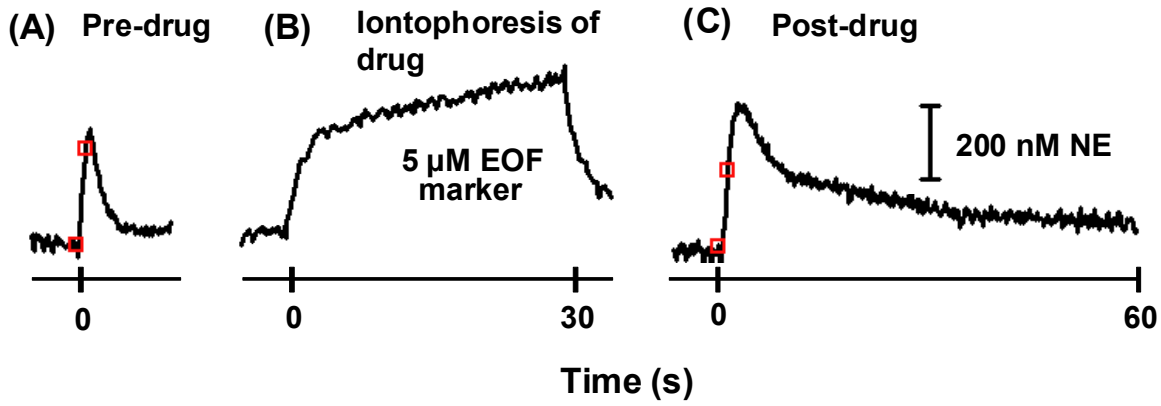

Figure 4.8. Stimulated NE release before and after a localized ejection of solution containing both AP and idazaxon. Shown is the current as a function of time at the oxidation potential for NE. (A) A representative baseline current trace for the stimulated release of NE. The red boxes indicate the beginning and end of stimulation (B) Representation of iontophoretic ejection of AP and idazoxan. The measured signal is due solely to AP, and is used to estimate the concentration of idazoxan. Here, 5 µM AP is the average concentration across the electrode, and is equivalent to 12 µM idazoxan. (C) Current trace for stimulated release 120 s after ejection seen in B. At the time of stimulation (red square), the concentration of AP has decreased to 2% of its original value, corresponding to a decrease in idazoxan concentration to 240 nM. The extracellular concentration of NE seen in C is significantly increased from that observed pre-drug.

of pre-drug value. DMI also increased stimulated NE release to 175 ± 21 % of the pre-drug value and had an effect on re-uptake giving an increase of 405 ± 145 % in $t_{1/2}$.

The dorsal and ventral portions of the BNST are differentially modulated by iontophoresis of desipramine and idazoxan

Drug effects of DMI and IDA on the *vm*BNST are consistent with drug effects following systemic (i.p.) injection. Interestingly, the average increase in NE release observed by iontophoretically and systemically delivered were not statistically different. This suggests that in our preparation regulation of NE by α_2-andrenergic receptors in the *v*BNST is controlled at the terminal regions. The effects of systemically delivered DMI increased NE release significantly more than iontophoretically applied DMI. However, this is likely due to the fact that systemically administered DMI followed systemic administration of IDA, which had not completely washed out. In contrast, iontophoresis drug effects are short-lived, with drug effects typically lasting only 10s of min. Thus, the effects of DMI iontophoresis were not compounded by application of IDA, and could explain the decreased effect observed.

The results from IDA iontophoresis in the *dm*BNST revealed no effect on NE release, in contrast to systemic (i.p.) injection of IDA which revealed a significant increase in release. This apparent contradiction of results could have several origins. First, it is possible that significantly different doses reached the receptors by systemic and iontophoretic delivery. Although we can accurate report the injected dose, it is difficult to know the dose present within the BNST following i.p. injection. Therefore, it is possible that the systemic dose at the receptors is significantly higher than that given iontophoretically. However, given the nature of iontophoretic delivery, this seems unlikely, since iontophoretic doses are traditionally on the high side as compared to EC_{50}'s determined through slice work (Herr et al., 2008). Indeed, the concentrations of

IDA achieved in the *dm*BNST were identical to those iontophoretically delivered in the *vm*BNST where significant increase in release was seen. An alternative and more likely explanation is that the observed drug effects from systemic i.p. injection are global and indicate that regulation of NE does not occur at terminal fields in the *dm*BNST. Instead, NE regulation may be due to activation of α_2-andrenergic receptors found on input neurons to the BNST that also modulate NE release (Shields et al., 2009). This is supported by the finding that α_2-andrenergic receptors are expressed ubiquitously in the brain, and are present on several brain regions that send inputs to the BNST.

Similar to the *vm*BNST, the effects of iontophoretically applied DMI are consistent with those observed due to systemic injection. This is not surprising since the role of NET is to control clearance locally and is not hypothesized to regulate release globally. Thus, the combination of systemic injections and iontophoresis suggest that NE release in the *vm*BNST is primarily controlled at the terminals by α_2-andrenergic receptors and NET. Control in the *dm*BNST appears to be more complicated, relying on a combination of terminal regulation by NET and possible global regulation by α_2-andrenergic receptors.

Iontophoresis as a diagnostic tool for the identification of catecholamine signals

During the course of the experiments it became apparent that iontophoresis could be used to quickly determine if the catecholamine signal being measured was noradrenergic or dopaminergic. In some animals, although the placement of the carbon-fiber iontophoresis probe was intended for the *vm*BNST, micro-lesioning after the experiment demonstrated that the electrode was partially placed in the striatum. Thus, the signal measured was a mixture, mostly containing DA. Iontophoresis of NE drugs in these animals caused no change in release. Due to the fast kinetics of the signal and

the ineffectiveness of NE drugs, DA contamination was suspected. This was verified by iontophoresis of DA drugs raclopride and GBR 12909 which significantly increased release. While this same pharmacological evaluation can be done with systemic drug injections, the advantage of using iontophoresis is 2-fold. First, iontophoretic drug delivery quickly modulates release. Drug effects are observed within a few minutes of delivery, and levels typically return to pre-drug values within 10-20 minutes. Second, and more importantly, the localized nature of iontophoretic drug delivery renders areas beyond ~100 μm from the release site drug-naïve. Therefore, if it is determined that there is contamination from other brain regions, the electrode can be adjusted, and the experiment continued without concern of lingering drug effects. Thus, although not the focus for this current study, this is a powerful use of iontophoresis, since a limiting factor in studying subregions in the BNST is the frequency with which the correct brain regions are targeted.

CONCLUSIONS

The results presented demonstrate that catecholamine release can be monitored in the subregions of the BNST *v*BNST, *dm*BNST, and *dl*BNST. Pharmacological characterization indicates that NE is the catecholamine found in *v*BNST and *dm*BNST while DA is in the *dl*BNST. Additionally, quantitative iontophoresis was used in the *v*BNST and *dm*BNST to demonstrate regulation of NE by α_2-andrenergic receptors and NET. The unique experimental approach of using quantitative iontophoresis coupled to fast-scan cyclic voltammetry revealed that regulation by α_2-andrenergic receptors is different in the *v*BNST than *dm*BNST. This interesting and novel result highlights the advantage of using iontophoresis to investigate terminal control of neurotransmission.

REFERENCES

Carboni E, Silvagni A, Rolando MT, Di Chiara G (2000) Stimulation of in vivo dopamine transmission in the bed nucleus of stria terminalis by reinforcing drugs. J Neurosci 20:RC102.

Cecchi M, Khoshbouei H, Javors M, Morilak DA (2002) Modulatory effects of norepinephrine in the lateral bed nucleus of the stria terminalis on behavioral and neuroendocrine responses to acute stress. Neuroscience 112:13-21.

Cullinan WE, Herman JP, Watson SJ (1993) Ventral subicular interaction with the hypothalamic paraventricular nucleus: evidence for a relay in the bed nucleus of the stria terminalis. J Comp Neurol 332:1-20.

Delfs JM, Zhu Y, Druhan JP, Aston-Jones G (2000) Noradrenaline in the ventral forebrain is critical for opiate withdrawal-induced aversion. Nature 403:430-434.

Dong H, Petrovich GD, Swanson LW (2000) Organization of projections from the juxtacapsular nucleus of the BST: a PHAL study in the rat. Brain Res 859:1-14.

Dong HW, Petrovich GD, Swanson LW (2001a) Topography of projections from amygdala to bed nuclei of the stria terminalis. Brain Res Brain Res Rev 38:192-246.

Dong HW, Petrovich GD, Watts AG, Swanson LW (2001b) Basic organization of projections from the oval and fusiform nuclei of the bed nuclei of the stria terminalis in adult rat brain. J Comp Neurol 436:430-455.

Egli RE, Kash TL, Choo K, Savchenko V, Matthews RT, Blakely RD, Winder DG (2005) Norepinephrine modulates glutamatergic transmission in the bed nucleus of the stria terminalis. Neuropsychopharmacology 30:657-668.

Epping-Jordan MP, Markou A, Koob GF (1998) The dopamine D-1 receptor antagonist SCH 23390 injected into the dorsolateral bed nucleus of the stria terminalis decreased cocaine reinforcement in the rat. Brain Res 784:105-115.

Erb S, Hitchcott PK, Rajabi H, Mueller D, Shaham Y, Stewart J (2000) Alpha-2 adrenergic receptor agonists block stress-induced reinstatement of cocaine seeking. Neuropsychopharmacology 23:138-150.

Fendt M, Siegl S, Steiniger-Brach B (2005) Noradrenaline transmission within the ventral bed nucleus of the stria terminalis is critical for fear behavior induced by trimethylthiazoline, a component of fox odor. J Neurosci 25:5998-6004.

Forray MI, Gysling K (2004) Role of noradrenergic projections to the bed nucleus of the stria terminalis in the regulation of the hypothalamic-pituitary-adrenal axis. Brain Res Brain Res Rev 47:145-160.

Garris PA, Wightman RM (1994) In vivo voltammetric measurement of evoked extracellular dopamine in the rat basolateral amygdaloid nucleus. J Physiol 478 239-249.

Herr NR, Kile BM, Carelli RM, Wightman RM (2008) Electroosmotic Flow and Its Contribution to Iontophoretic Delivery. Analytical Chemistry 80:8635-8641.

Kristensen EW, Wilson RL, Wightman RM (1986) Dispersion in flow injection analysis measured with microvoltammetric electrodes. Analytical Chemistry 58:986-988.

McElligott ZA, Winder DG (2009) Modulation of glutamatergic synaptic transmission in the bed nucleus of the stria terminalis. Prog Neuropsychopharmacol Biol Psychiatry 33:1329-1335.

Meloni EG, Gerety LP, Knoll AT, Cohen BM, Carlezon WA, Jr. (2006) Behavioral and anatomical interactions between dopamine and corticotropin-releasing factor in the rat. J Neurosci 26:3855-3863.

Myers EA, Banihashemi L, Rinaman L (2005) The anxiogenic drug yohimbine activates central viscerosensory circuits in rats. J Comp Neurol 492:426-441.

Park J, Kile BM, Wightman RM (2009) *In vivo* voltammetric monitoring of norepinephrine release in the rat ventral bed nucleus of the stria terminalis and anteroventral thalamic nucleus. Eur J Neurosci 30:2121-2133.

Park J, Kile, B.M., Wightman, R.M. (2009) *In vivo* voltammetric monitoring of norepinephrine release in the rat ventral bed nucleus of the stria terminalis and anteroventral thalamic nucleus. Eur J Neurosci *in press*.

Paxinos G, Watson C (2005) The rat brain in stereotaxic coordinates. Amsterdam ;Boston: Elsevier Academic Press.

Shields AD, Wang Q, Winder DG (2009) alpha2A-adrenergic receptors heterosynaptically regulate glutamatergic transmission in the bed nucleus of the stria terminalis. Neuroscience 163:339-351.

Sullivan GM, Apergis J, Bush DE, Johnson LR, Hou M, Ledoux JE (2004) Lesions in the bed nucleus of the stria terminalis disrupt corticosterone and freezing responses elicited by a contextual but not by a specific cue-conditioned fear stimulus. Neuroscience 128:7-14.

Chapter 5

Adaptation of quantitative iontophoresis to study neurotransmission during reward-seeking behaviors

INTRODUCTION

The positive reinforcing actions of drugs of abuse serve as the basis for many animal models of addiction. For example, animals can be trained to perform several tasks (e.g., pressing a lever) for drugs that have high abuse potential in humans (e.g., cocaine, amphetamine). The reinforcing properties of drug linearly correlate with how well animals perform the task, and how complex of a task they will perform (Koob, 1995). Similar to drugs of abuse, electrical stimulation of certain brain regions has positive reinforcing actions (Olds and Milner, 1954). In fact, self-stimulation by animals (termed intracranial self-stimulation (ICSS)) displays stronger reinforcement than some drugs of abuse, as indicated by the time it takes an animal to learn the behavior. Additionally, it has been shown to activate common pathways as drugs of abuse, and thus serves as a good model to study brain regions involved in reward-seeking.

Animals strongly support ICSS for dopamine (DA) neurons found in the ventral tegmental area (VTA) and its projection through the medial forebrain bundle (MFB), implicating this pathway in reward-seeking (Olds and Olds, 1963; Cooper and Breese, 1975; Wise, 2004). DA neurons from the VTA form synapses on medium spiny neurons (MSNs) in the nucleus accumbens (NAc), to form part of the mesolimbic DA system. Studies have shown that during reward-seeking behaviors, neurons in the VTA are

transiently activated and levels of DA in the NAc are increased (Phillips et al., 2003; Roitman et al., 2004; Cheer et al., 2007a; Day et al., 2007). However, what remains less clear is the exact role of DA during these behaviors, and the mechanisms by which DA modulates output signals from the NAc.

Electrophysiology data has shown that MSNs differentially respond in the NAc to reward and reward-related cues, suggesting that many mechanisms may be at play. For example, cues that predict the availability of a lever for ICSS or cocaine cause some NAc cells to increase in firing, while others decrease and some are unaffected (Carelli and Ijames, 2000; Cheer et al., 2007a). These dramatically different responses suggest that there are microenvironments within the NAc that may be differentially modulated during this behavior (Carelli and Wightman, 2004). Furthermore, using a combined electrochemical/electrophysiology technique, DA release from terminals has been correlated to measured changes in post-synaptic cell firing during ICSS and cocaine self-administration (Cheer et al., 2007a; Owesson-White et al., 2009). These results have found that in areas of the NAc where DA release is observed in connection to reward-related cues, post-synaptic cells exhibit phasic activation (either excitatory or inhibitory). Conversely, in areas where DA release was not observed, no activation of cells is seen. Thus, DA appears to play different modulatory roles in the phasic activation of post-synaptic cells during reward-seeking behavior.

To tease apart the apparent differing roles of DA, pharmacological agents that can target specific receptor subtypes are needed. Systemic injections and microinjection into the NAc of D1 antagonists have been shown to abolish ICSS behavior, while intervention with D2 antagonist does not (Cheer et al., 2007a). This suggests a role for D1 in mediating DA signaling in the NAc related to reward-seeking. However, since systemic drug injection affects the entire system, and microinjections

affect an entire brain region, local difference within the NAc cannot be identified. Iontophoresis can be used to investigate local differences, since iontophoresis ejections affect a small subset of the region being studied, usually less than 100 μm from the delivery site. This approach was used in combination with single-unit recordings to show that during ICSS, local application of the D1 antagonist, SCH23390, did not affect behavior but did decrease baseline and phasic firing in response to reward-related cues. Iontophoresis of the D2 receptor antagonist, raclopride, did not affect neuronal activity. These results suggest that DA signaling in the NAc during ICSS is at least partially under D1 receptor regulation (Cheer et al., 2007a). A caveat of this study is that iontophoresis is traditionally non-quantitative, and confirmation of a successful ejection is only obtained through positive results. Thus, if no effect is observed, it is difficult to definitively say whether the observed "no-effect" has physiological basis, or if a faulty ejection occurred. Although not documented, raclopride is thought of as "difficult to eject," primarily because effects of the drug are rarely reproducible.

Recent improvements to the technique enable real-time confirmation of drug ejection, and quantitation of drug delivery (See Chapter 3). Additionally, while the technique is traditionally coupled to electrophysiology, it has now been used to monitor and modulate pre-synaptic release events. These improvements will allow the role of DA in the NAc to be studied more definitively, and establish the involvement of D2 in DA signaling. In this chapter, the improvements made to iontophoresis in Chapters 2 and 3 will be adapted for experiments in awake and behaving animals. While iontophoresis has been successfully used in awake and behaving animals in the past, this was with electrophysiology only. Carbon-fiber microelectrodes can be used to simultaneously monitor release events and post-synaptic changes in cell firing. This combined technique will be combined with iontophoresis to allow for a more complete view of the

role of DA in the NAc. The main focus of this chapter will be on the adaptations done to date, and those still necessary to successfully transfer the use of quantitative iontophoresis for the studies described above.

EXPERIMENTAL METHODS

Animals and surgery

Male Sprague-Dawley rats (225-350g; Charles River, Wilmington, MA) were anesthetized with ketamine (10 mg/kg, i.p.) and xylazine (1 mg/kg, i.p.) and placed in a stereotaxic frame (Kopf, Tujunga, CA). A modified guide cannula (described in Results, Chapter 5, Bioanalytical Systems, West Lafayette, IL) was implanted above the NAc core (1.3 mm anterior, 1.3 lateral, coordinates relative to bregma) and a bipolar stimulating electrode (Plastics One, Roanoke, VA) was lowered to the substantia nigra/ventral tegmental area (VTA, 5.2 mm posterior, 1 mm lateral and 7.8 mm dorsoventral). The bipolar stimulating electrode tips were 1 mm apart. This tip separation allowed for centering in the VTA-region. These coordinates assure activation of the neurons projecting to the NAc core (Ikemoto, 2007). An Ag/AgCl reference electrode was placed in the contralateral hemisphere.

ICSS

Rats were trained to criterion on an FR-1 schedule, lever continuously presented. Following this rats were trained to lever press on a variable time-out (VTO) schedule, FR-1 (Figure 5.7). The VTO-schedule comprised of a maintenance and a maintenance-delay phase. When the animal depressed the lever, a stimulus train (24 biphasic pulses, 60 Hz, 125-150 μA, 2 ms per phase) was delivered to the stimulating electrode on average 150 ms later. In the maintenance phase the lever was presented with an audiovisual cue for 50 trials. In the maintenance-delay phase the audiovisual cue

preceded lever-out by 2 s (trials 51-200). Each trial finished after lever depression or if the animal failed to lever press after 15s. The inter-trial interval varied between 5 and 25 seconds.

Iontophoresis Probes

A glass tube (Part # 624503, 0.60 mm o.d., 0.4 mm i.d., 4" long, A-M Systems, Sequim, WA) was loaded with a carbon fiber (T-650, Thornel, Amoco Corp., Greenville, SC) that served as the working electrode. This tube containing the carbon fiber was then inserted into one barrel of a 4 barrel capillary (Part # 50644, 1 mm o.d., 0.75 mm i.d., 4barrel GF pipettes, 4" long, Stoelting Co., Wood Dale IL). The four barrel assembly contained glass filaments (GF) in each barrel that aid in filling the barrel by capillary action. The capillaries were bundled together with heat shrink and were tapered to a tip of about 1 μm in diameter using a micropipette puller (Narashige, Tokyo, Japan) with a two-step pull process. The protruding carbon fiber was cut to a length between 30 and 50 μm.

Iontophoresis probes were secured to the animal's head using a modified Biela manipulator that couples to the modified guide cannula placed in the NAc core. Prior to the start of the experiment, iontophoresis probes were prepared and loaded into the manipulator. Iontophoretic barrels were loaded with drug solution and fitted with electrical wires. Drug solutions were made up in 5 mM NaCl at a concentration of 10 mM at pH 5.8. The barrel containing the carbon fiber was backfilled with electrolyte (4 M potassium acetate, 150 mM potassium chloride) and also fitted with a wire for electrical contact.

Electrochemical Data Acquisition and Presentation

Cyclic voltammograms were acquired using data-acquisition hardware and locally software written in LabVIEW (National Instruments, Austin, TX). The cyclic voltammetry waveform was generated and the voltammetric signal was acquired with a computer interface board, the PCI-6052E (National Instruments). A PCI-6711E D/A board (National Instruments) was used to synchronize waveform application, data acquisition, and to trigger the iontophoretic current applied and the loop injector in the flow injection apparatus. The voltammetric waveform was input into a custom-built instrument for application to the electrochemical cell and current transduction (University of North Carolina at Chapel Hill, Department of Chemistry Electronics Facility). After data collection, background subtraction, signal averaging, and digital filtering (low pass filtered at 2 kHz) were all done under software control.

For all experiments, a triangular waveform was applied with a scan rate of 400 V s^{-1} with a rest potential of -0.4 V versus Ag/AgCl between scans, a linear scan to 1.3 V, followed by a scan back to the rest potential. The scans were repeated every 100 ms, and collection was typically for 15- 60 s. This large amount of data is presented as a color plot, with the applied voltage plotted on the ordinate, time on abscissa, and measured current in false color.

Iontophoresis Ejections

Ejection currents were delivered by a constant current source designed for iontophoresis (Neurophore, Harvard Apparatus, Holliston, MA). For each barrel, an ejection current (between 5 to 40 nA) was selected by evaluating ejections (30 s duration) that gave a measurable voltammetric signal for the EOF marker (average peak current of 5 to 30 nA at the peak potential in the voltammogram). A current of 0 nA was applied between ejections.

Calibrations.

The response of the carbon fiber electrode in the iontophoresis probe was calibrated in a flow injection analysis system after *in vivo* use (Kristensen et al., 1986). The probe was positioned at the outlet of a six-port rotary valve. A loop injector was mounted on an actuator (Rheodyne model 7010 valve and 5701 actuator) that was used with a 12-V DC solenoid valve kit (Rheodyne, Rohnert Park, CA) to introduce the analyte to the surface of the electrode. The linear flow velocity (1.0 cm s^{-1}) was controlled with a syringe infusion pump (Harvard Apparatus model 940, Holliston, MA). The voltammetric current was measured at the peak potential for each analyte that was evaluated at 4 concentrations.

RESULTS

Improvements to carbon-fiber iontophoresis probe construction

Several challenges exist with successfully combining electrochemistry, electrophysiology, and iontophoresis and behaving animals. There are many examples in the literature where electrophysiology and iontophoresis have been coupled for local modulation of cell firing (Kiyatkin and Rebec, 1996, 1997, 1999a, b; Kiyatkin et al., 2000; Kiyatkin and Rebec, 2000). However, few exist where electrochemistry and iontophoresis have been used together, and none exist where iontophoresis has been used to modulate release at terminals, except for in anesthetized preparations (Armstrong-James et al., 1981; Cheer et al., 2007b; Herr et al., 2008). The primary reason for this is that in order to obtain good, reproducible electrochemical signals, the integrity of the glass-carbon fiber seal must remain intact. Carbon-fiber iontophoresis probe suffer from significant more fragility than traditional carbon-fiber microelectrodes. Because the probes consist of multiple barrels bundled together, a long, thin tapered tip

must be made to reduce the size of the probe area entering the brain. This long, thin taper makes the tips very fragile, and in particular, the glass encasing the carbon-fiber is highly susceptible to breaking.

To reduce the fragility of the glass surrounding the carbon-fiber, an extra glass capillary was concentrically inserted into one barrel to provide extra structural support. The added glass capillary contains the carbon-fiber, and thus, the barrel that serves as the working electrode has extra structural support. In addition, this also greatly reduces electrical cross-talk that could be detected between the carbon-fiber and the iontophoretic barrels when currents switched from retaining to ejecting. Indeed, the commercially available multi-barrel pipettes are divided by thin glass wall that do not appear to have very good structural integrity. Figure 5.1 shows electrical cross-talk detected at the carbon-fiber due switching the current from 0 nA to 20 nA. The addition of a glass capillary to insulate the carbon-fiber has greatly reduced the occurrence of cross-talk, and has also generally led to more robust electrodes.

Modification to BAS guide cannula and Biela manipulator

Biela manipulators fabricated by Crist Instrument Co are designed to be used with multi-barrel probes. The manipulators fit probes that are 2 mm in diameter, making them ideal for iontophoresis probes made from 4-barrel glass, with each barrel being 1 mm in diameter. To couple the manipulator to the animal's brain, they sell threaded hubs to which the manipulator screws onto. The hubs are normally cemented onto the animal's head, directly above a hole that has been drilled above the brain region of interest. A major drawback of this approach is that during the animal's recovery from surgery, a scab forms over the hole, which will block passage of the electrode. Thus, before securing the manipulator to the animal's head, the inner diameter of the hub is cleaned out with heparin (a blood thinner that prevents clotting) to ensure clean passage

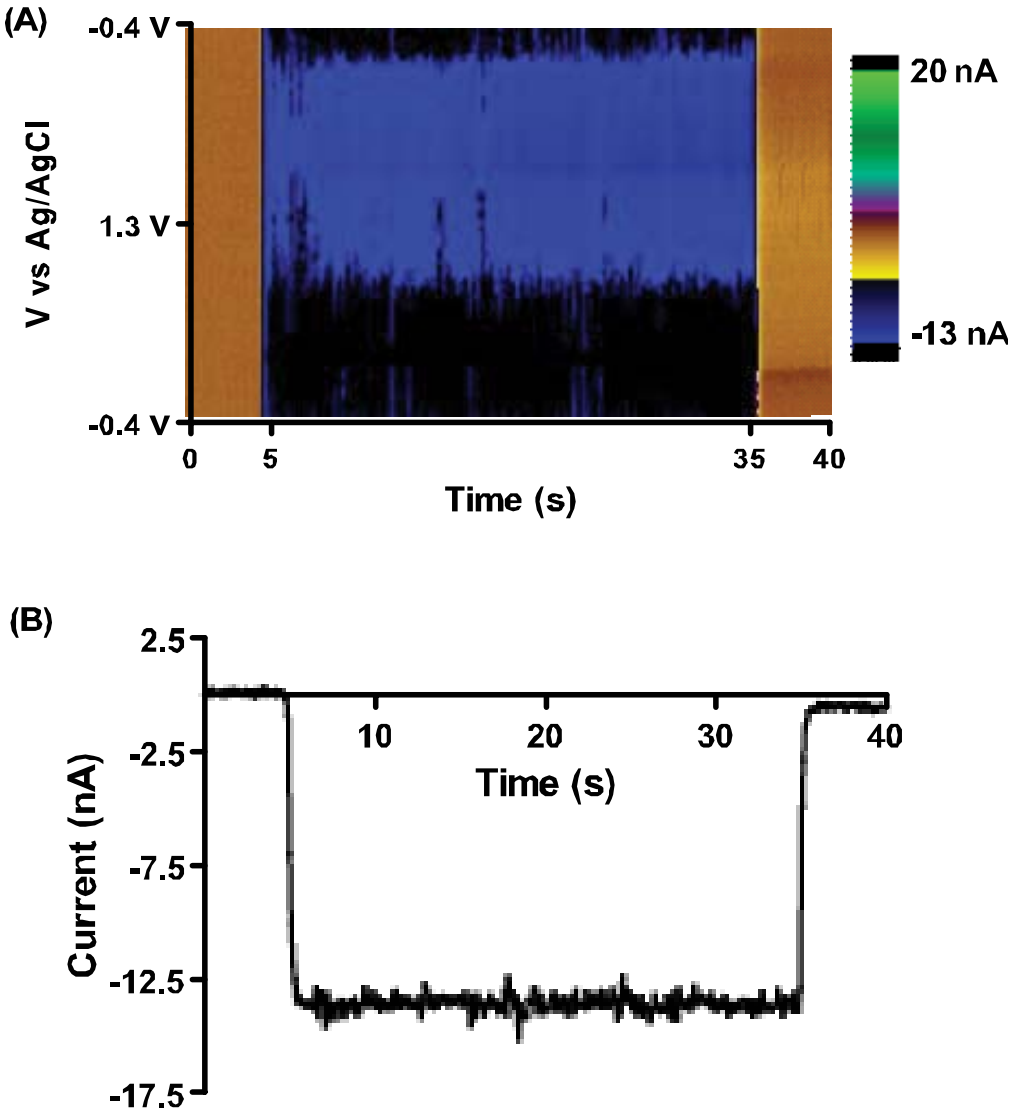

Figure 5.1. Electrical cross-talk from iontophoresis current. In some electrodes electrical cross-talk was detected at the carbon-fiber microelectrode as a large change in current when the ejecting current was switched on and off. (A) Color plot showing the large current change due to the change in current iontophoresis current from 0 nA to 20 nA at 5 s and 35 s. (B) Current vs time trace extracted from (A) at 0.6 V.

of the electrode. Often, animals will find the cleaning of the hub painful, as a scab has formed over the hole. Additionally, it is difficult to fully clean the hub, frequently causing electrodes to break during insertion. For these reasons it was determined necessary to modify the method by which the manipulator attached to the animal's head.

The Wightman lab routinely uses carbon-fiber microelectrodes to monitor DA release in awake and behaving animals. For these experiments an intracerebral guide cannula is inserted into the brain, aimed at the brain region of interest. Figure 5.2(A) shows a schematic of the canula which consists of a small diameter (~0.7 mm) polyimide tube attached to a hub that extends ~2 mm into the brain. The guide tubing serves the purpose of directing the electrode to the targeted brain region and prevents a scab from forming over the drilled hole. However, for iontophoresis probes, the guide tubing is too small. A modified version of the commercially available cannula was constructed with larger diameter polyimide tubing (0.041") to replace the smaller diameter tubing the cannulae are sold with. In addition, a bigger hole through the hub of the cannula was needed. These modifications can be done in-house, but have been contracted to the UNC Physics Machine shop to ensure that the polyimide tubing is cut to proper size and glued onto the hub as straight as possible.

The hub from the guide cannula in Figure 5.2 does not couple to the manipulator used for iontophoresis probes. Thus, the manipulator needed to be modified or a new canula that does couple to the manipulator needed to be designed and built. Both approaches were tried, although it was easier to modify the existing manipulator to couple with the cannula. Figure 5.3 shows a drawing of the Biela manipulator used for iontophoresis probes. As stated above, the manipulator screws onto a hub that is secured on the animal's head. To use the intracerebral guide cannula, an adapter piece

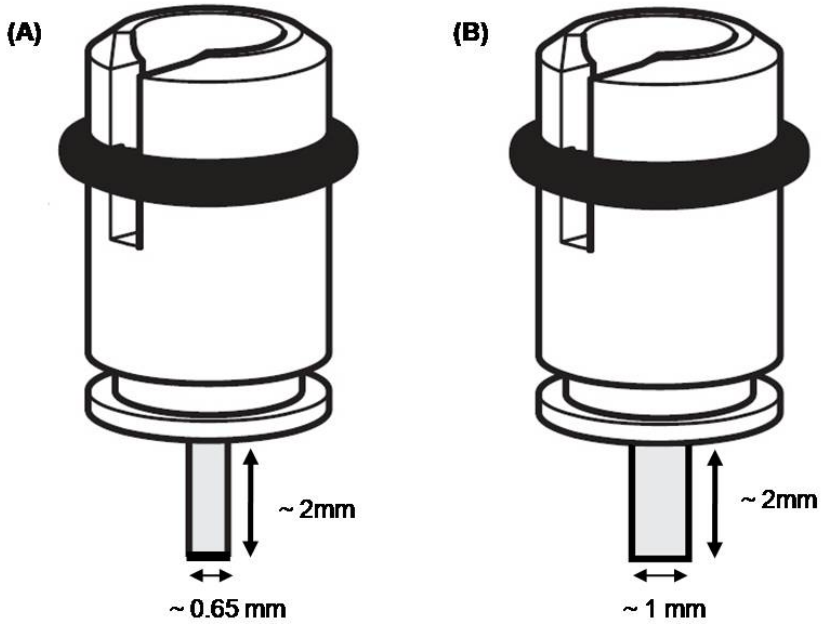

Figure 5.2. Intracerebral guide cannulae used for experiments with awake and behaving animals. (A) Commercially available cannula as sold from Bioanalytical Systems, Inc. (B) Modified cannula with wider tubing for iontophoresis probes. (Figure modified from http://www.basinc.com/products/iv/cannula.html)

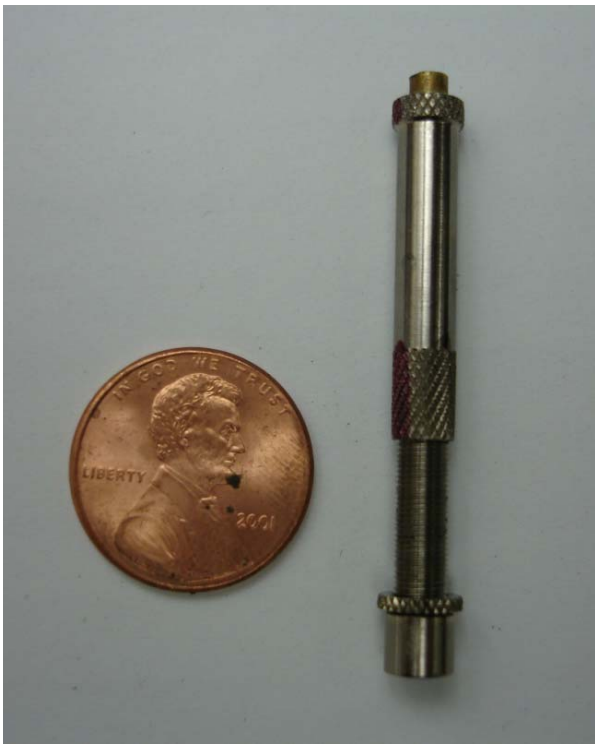

Figure 5.3. Manipulator from Crist Instruments for iontophoresis probes. The inner copper chamber is designed to fit 4-barrel glass micropipettes, like that used to construct iontophoresis probes. As the outer stainless steel chamber is rotated clock-wise, the electrode, which is secured to the inner copper chamber, moves down in a linear fashion, without turning. The manipulator has a traveling distance of 23 mm, which is ideal for experiments targeting the NAc core at ~7 mm from the skull. The bottom part of the manipulator is threaded and attaches to a threaded stainless steel hub secured onto the animal's head. To couple the manipulator to the modified guide cannula a piece that screws onto the bottom was machined as shown in Figure 5-4.

was machined by the UNC Physics Machine Shop that allows the manipulator to couple to the cannula hub. A schematic with dimensions is shown in Figure 5.4.

In addition, to minimize breakage of electrodes during insertion into the brain animals are lightly anesthetized with 2% isoflurane immediately before the electrode is lowered. The advantage of lightly anesthetizing animals with isoflurane is that they animals quickly wake up, usually within 1-2 minutes, and resume normal behavior. This approach has been used in other labs performing similar experiments, and has shown that once the effects of anesthesia have passed, there is no significant effect on the animal's ability to perform a trained behavior or on the measured DA release (Robinson and Carelli, 2008; Robinson et al., 2009).

The combination of these improvements has led to a higher success rate in inserting electrodes into the rat's brain without breaking. Challenges still exist with the detection of DA. Although DA is routinely measured in awake and behaving animals using traditional microelectrodes, DA detection appears more difficult with iontophoresis probes. There are a couple possible explanations for this. First, it is possible that while the iontophoresis tips appear to be unbroken as they are being lowered into the rat's brain, small cracks may be present that are not detectable by just observing the electrode's background current. Additionally, iontophoresis probes are cut to a length of ~20-50 μm to ensure that the site being measured from is within the sphere of influence of iontophoretically delivered drugs. However, signals in awake and behaving animals are much lower than those detected in anesthetized animals where strong electrical stimulations can be used (Chapters 3 and 4). Thus, the electrode length may need to be increased in order to measure the lower levels detected in awake animals.

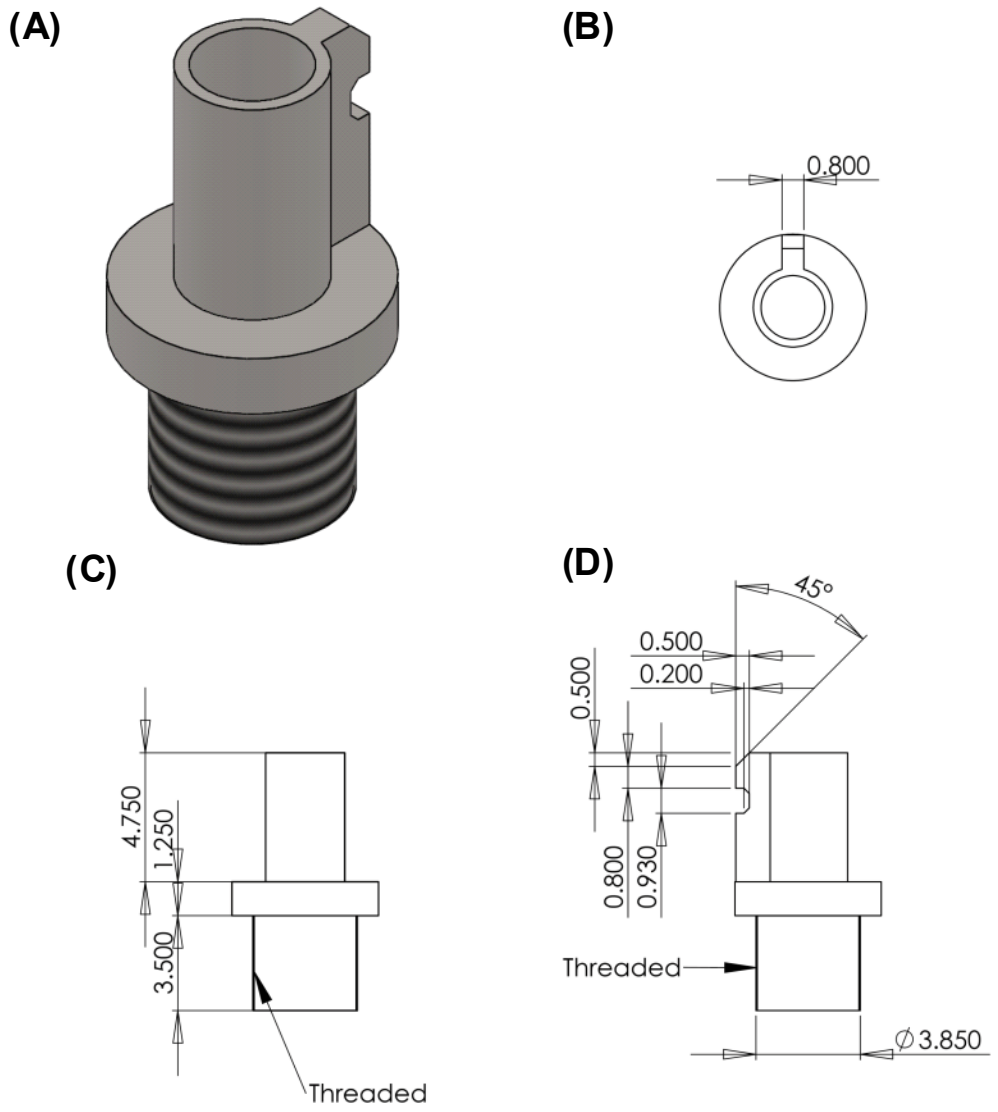

Figure 5.4. Machined piece to couple Biela manipulator to intracerebral guide cannula. (A) Schematic of the machined piece which screws onto the bottom of the Biela manipulator while the top portion couples directly to the guide cannula. (B-D) Dimensions of piece, given in mm. (B) Top view, (C,D) Side views. (Schematic courtesy of Matt Zachek.)

Modulation of DA release in awake, non-behaving animals using quantitative iontophoresis

Dopamine release from terminals in the striatum is regulated by D2-autoreceptors (Benoit-Marand et al., 2001). For these experiments we used raclopride, a D2-agonist, which has been shown to increase stimulated dopamine release. The position of the carbon-fiber/iontophoresis assembly was adjusted using a Biela manipulator to a location that showed robust stimulated DA release. After establishing reproducible stimulated release of DA, raclopride and acetaminophen was iontophoretically ejected from the same barrel for 30 sec. The local AP concentration was monitored by fast-scan cyclic voltammetry, and used to estimate the concentration of raclopride as described in Chapter 3. The stimulation was repeated 60 s after the iontophoretic delivery terminated.

Consistent with autoreceptor regulation, DA release was increased (representative example in Figure 5.5). Measurements were repeated in 3 different locations from 6.8 mm to 8.0 mm from the skull. The amount of raclopride ejected at each location was about the same, as indicated by the AP concentration measured during ejection. The average increase in release amplitude was 125 ± 3% (n = 4 locations) of its pre-drug value after 4 minutes. Figure 5.6(A) shows the average time-course of the drug effect for all locations. Interestingly, the increase in DA release is not significant when all locations are averaged. However, as shown in Figure 5.6(B), some of the locations show a significant increase in DA release, while other do not. The heterogeneity of the drug effect within a single animal is not entirely surprising given that DA release within the striatum is heterogeneous. When using a single working electrode, this form of drug effect heterogeneity can only be studied using iontophoresis since other forms of drug delivery will affect the entire brain region at once. Thus, by the

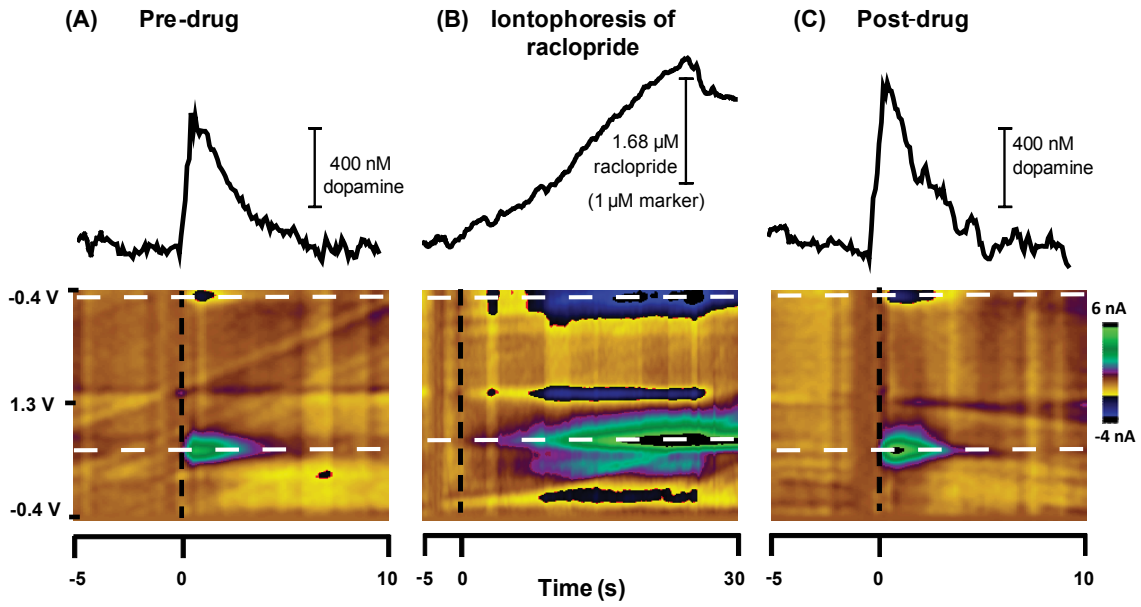

Figure 5.5. Stimulated dopamine release in an awake animal at rest before and after a localized ejection of solution containing both AP and raclopride. The top panels show current as a function of time while the lower panels are two dimensional color plots where current is shown in false color on the potential vs. time axes. The white dashed lines on the color plots indicate the voltages at which oxidation (lower lines) and reduction (top lines) is occurring. (A) A representative baseline current trace and color plot for the stimulated release of dopamine. The black dashed line indicates the time of stimulation (B) Representation of iontophoretic ejection of AP and quinpirole. The black dashed line (t=0) indicates the application of a positive current to the barrel. The measured signal is due solely to AP, and is used to estimate the concentration of quinpirole. Here, 1 µM AP is the average concentration across the electrode, and is equivalent to 1.68 µM raclopride. (C) Current trace and color plot for stimulated release 120 s after ejection seen in B. At the time of stimulation (black dashed line), the concentration of AP has decreased to 2% of its original value, corresponding to a decrease in raclopride concentration to 34 nM. The extracellular concentration of dopamine seen in C is significantly increased over that seen in A. In both A and C the time of stimulation is indicated by the black dashed line and t=0 for each trace.

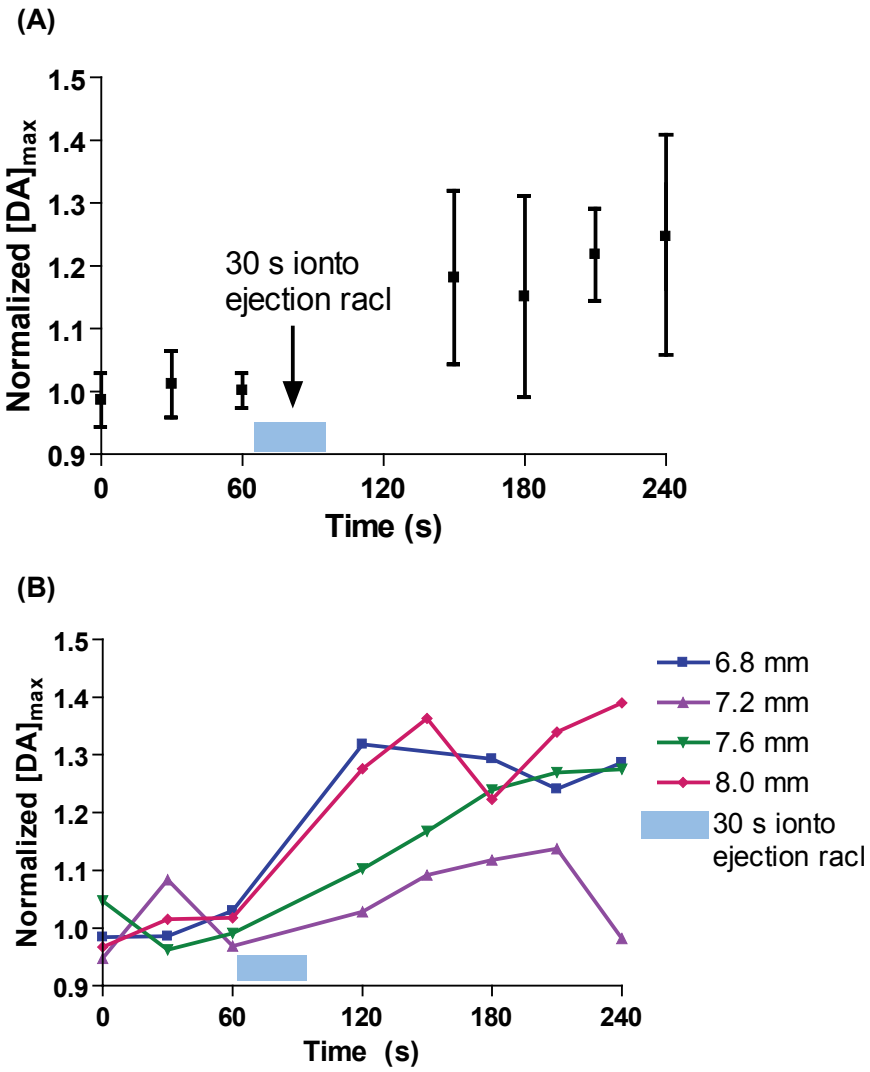

Figure 5.6. Time course of raclopride effect in an awake animal at rest. (A) Plotted is the maximal DA overflow measured due to electrical stimulation versus time at 4 separate locations within the same animal. At t = 65s, a 30s ejection of raclopride (light blue bar) was given. Stimulation was repeated 120s, and an increase in DA release was observed, although not statistically significant. The effect persists over the next 4 stimulations. (B) Time course at each individual location shows a similar pattern to that shown in (A), but it is apparent that at some locations, the drug effect is slower and causes less of an increase in stimulated DA release. This finding is not surprising given that DA release has been shown to be heterogeneous within the striatum.

time the electrode is moved to another position, the effects of the drug will have already begun. An alternative approach to studying drug-response heterogeneity is to use an array of electrodes while administering the drug systemically or locally with microinjection.

Effects of raclopride on reward-related DA release

Animals were trained to lever press for an electrical stimulation. A cue was associated with the reward, and came to predict the availability of the lever. Figure 5.7 shows a timing diagram of the experiment and the corresponding DA signal measured during the behavior. As can be seen, a transient increase in DA is detected at the electrode in response to the cue that predicts the reward and the reward itself. The Wightman lab has shown that the increase in response to the cue increases overtime, can be extinguished by removing the reward, and is reinstated once the reward is returned (Owesson-White et al., 2008). Additionally, they have shown that when the time between trials is fixed, a DA transient can be seen before the cue, indicating that the animals have learned to predict the cue before it is presented. Thus, a variable timeout (time between trials) is used so that the measured DA transient is due only to the presentation of the cue. In this experiment, the variable time-out was increased from the traditional 5-25 s to 30-40 s to allow time for iontophoresis ejections in between trials.

The role of D2 was examined in this paradigm by using localized delivery with iontophoresis. Systemic drug injections of D2 antagonists such as raclopride abolish ICSS behavior, and thus only by using localized drug delivery can the role of D2 be studied. Figure 5.8 shows that local application of raclopride causes an increase in cue-related DA transients. Interestingly, a single 30s dose of raclopride is sufficient to cause the observed increase, and subsequent doses do not appear to further increase DA

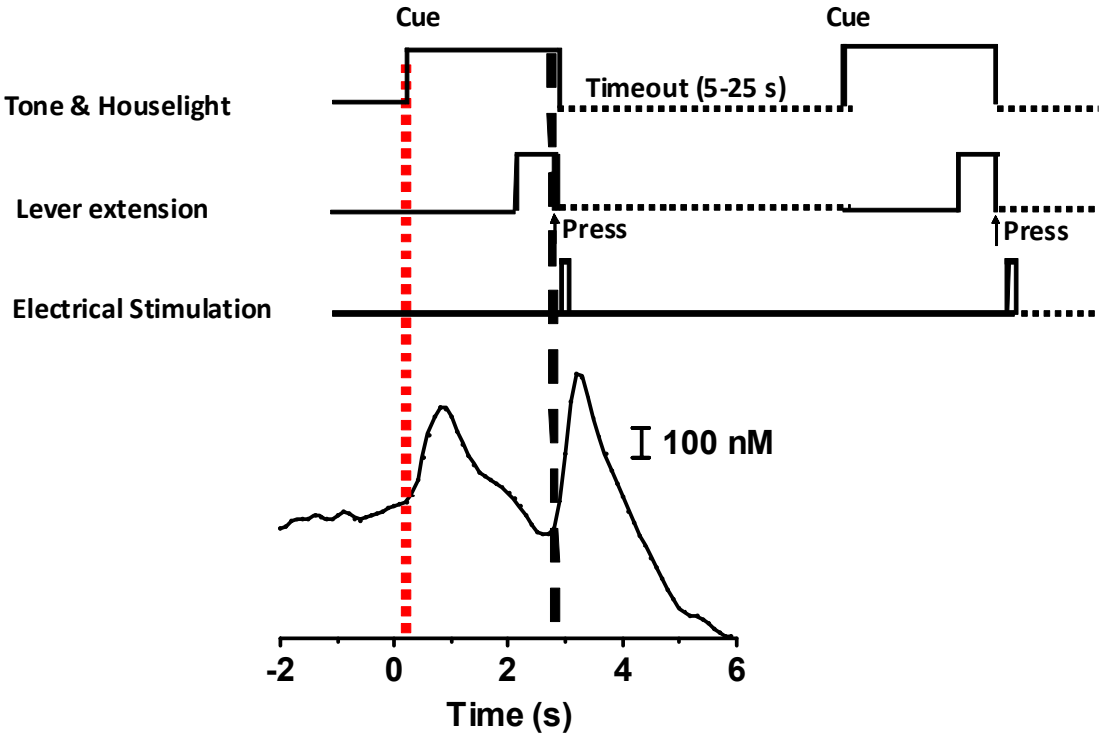

Figure 5.7. Timing diagram and corresponding increases in DA release during ICSS. Animals are trained to press a lever for an electrical stimulation to the VTA. The electrical stimulation is delivered 200 ms after the lever press. Immediately preceding lever extension, a houselight and tone come on that serve as a cue for the reward. A variable timeout period is used because previous experiments showed that animals are able to predict when the lever will be presented when the cycle is repeated a regular interval. The bottom traces show transient increases in DA release in response to the cue and the reward (electrical stimulation).

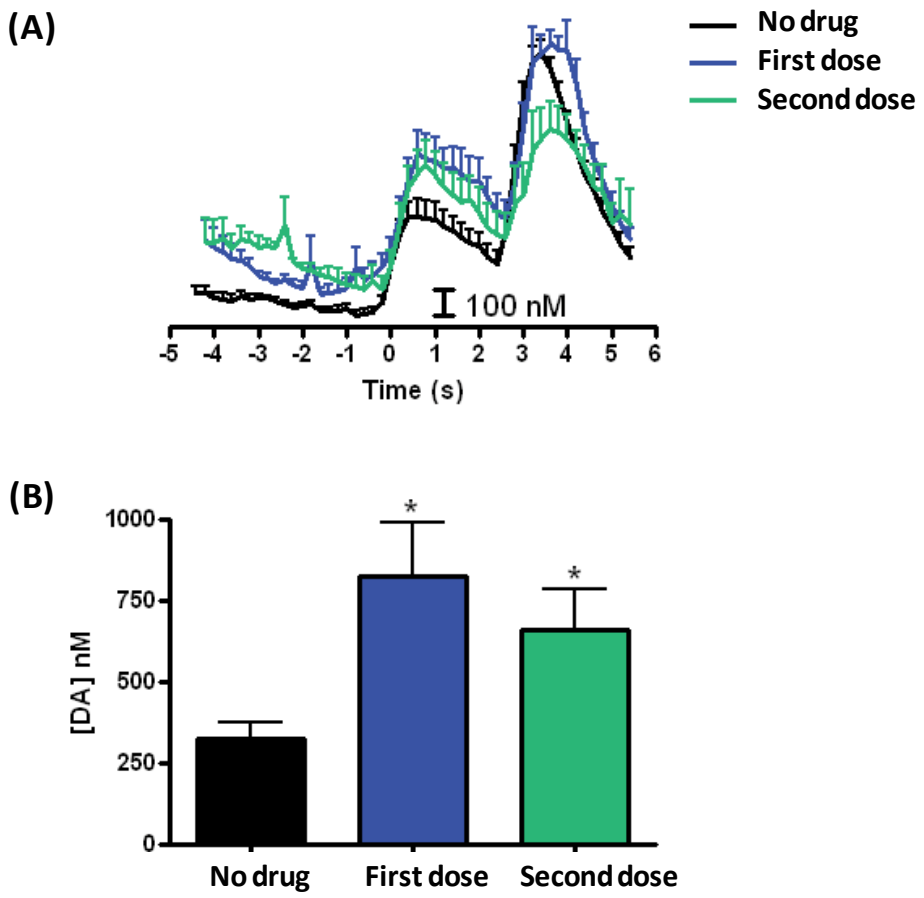

Figure 5.8. Increase in dopamine signal due to cue and lever presentation. (A) Average current v. time trace for 30 trials when no drug is on board, after a single 30 s iontophoretic application of raclopride, and after a second 30 s application. An increase in cue-related DA release is seen after the first application, but no further increase is detected after a second application. DA release in response to the electrical stimulation is not affected over the average of 30 trials by either drug application. (B) Increases in cue-related DA release over the first 5 trials. Since iontophoresis is a localized drug delivery tool, with fast onset of drug effect, we suspected that the majority of the drug effect occurred over the first few trials. As shown, cue-related DA release is significantly increased after both application, but the first application shows a greater increase despite both doses being the same. Additionally, the increase observed over the first 5 trials is greater than over the average of 30 trials, indicating that the majority of the drug effect occurs within the first few trials.

release. Also, the increase in DA is most dramatic in the first 5 trials following application. While this experiment is only n = 1, it shows the utility of the experimental approach and provides interesting results related to dosing. Consistent with anesthetized work in Chapter 3 and 4, drug effects occur quickly after a single, short dose. However, it is interesting that subsequent doses do not further increase the effect. This appears to be a phenomenon true only for experiments in awake animals, as dosing experiments have been done in anesthetized animals. Thus, while in the work of Cheer *et al. 2007* drugs were iontophoretically delivered for 10's of min, a short 30 s ejection appears to be responsible for the majority of the drug effect observed.

Conclusions and future directions

The work presented in this chapter demonstrates the challenges with using quantitative iontophoresis for electrochemical monitoring of dopamine signaling in awake and behaving animals. Improvements on probe construction and modifications to intracerebral guide cannulae and iontophoresis manipulators have increased the success rate of lowering an electrode into the animal's brain without breaking. However, detection of DA release remains a challenge, and may be due to the length of the electrodes used. Future directions for this project include overcoming the challenges preventing routine DA detection with iontophoresis probes in awake and behaving animals. Possible approaches may include further strengthening the tip of the probes using an insulating polymer, although care will be required to prevent the iontophoresis tips from being clogged.

Once the technique is improved sufficiently to routinely detect DA release, characterization of the role of D1 and D2 receptors in goal-directed behavior can begin. The main goal of this characterization would be to correlate differences in DA release and response to D1 or D2 drugs to the different populations of cells that have been

identified by electrophysiology (Carelli et al., 2000). However, many other receptors and neurotransmitters are involved in striatal signaling, and directly or indirectly affect the role of DA in the striatum. Thus, to fully understand dopaminergic signaling in the striatum, the roles of glutamate and acetylcholine, and their respective receptors must also be studied. Iontophoresis is uniquely poised for these types of experiments since multiple drugs may be evaluated within a single animal. The improvements described in this chapter will help further our use of iontophoresis in awake and behaving animals, and hopefully lead to a better understanding of dopaminergic signaling. In addition, the technology can be extended to other neurotransmitter systems, such as norepinephrine and serotonin, and other behaviors, such as natural reward seeking.

REFERENCES

Armstrong-James M, Fox K, Kruk ZL, Millar J (1981) Quantitative ionophoresis of catecholamines using multibarrel carbon fibre microelectrodes. J Neurosci Methods 4:385-406.

Benoit-Marand M, Borrelli E, Gonon F (2001) Inhibition of dopamine release via presynaptic D2 receptors: time course and functional characteristics in vivo. J Neurosci 21:9134-9141.

Carelli RM, Ijames SG (2000) Nucleus accumbens cell firing during maintenance, extinction, and reinstatement of cocaine self-administration behavior in rats. Brain Res 866:44-54.

Carelli RM, Wightman RM (2004) Functional microcircuitry in the accumbens underlying drug addiction: insights from real-time signaling during behavior. Curr Opin Neurobiol 14:763-768.

Carelli RM, Ijames SG, Crumling AJ (2000) Evidence that separate neural circuits in the nucleus accumbens encode cocaine versus "natural" (water and food) reward. J Neurosci 20:4255-4266.

Cheer JF, Aragona BJ, Heien ML, Seipel AT, Carelli RM, Wightman RM (2007a) Coordinated accumbal dopamine release and neural activity drive goal-directed behavior. Neuron 54:237-244.

Cheer JF, Aragona BJ, Heien ML, Seipel AT, Carelli RM, Wightman RM (2007b) Coordinated accumbal dopamine release and neural activity drive goal-directed behavior. Neuron 54:237-244.

Cooper BR, Breese GR (1975) A role for dopamine in the psychopharmacology of electrical self-stimulation. Natl Inst Drug Abuse Res Monogr Ser:63-70.

Day JJ, Roitman MF, Wightman RM, Carelli RM (2007) Associative learning mediates dynamic shifts in dopamine signaling in the nucleus accumbens. Nat Neurosci 10:1020-1028.

Herr NR, Kile BM, Carelli RM, Wightman RM (2008) Electroosmotic Flow and Its Contribution to Iontophoretic Delivery. Analytical Chemistry 80:8635-8641.

Ikemoto S (2007) Dopamine reward circuitry: Two projection systems from the ventral midbrain to the nucleus accumbens-olfactory tubercle complex. Brain Res Rev.

Kiyatkin EA, Rebec GV (1996) Dopaminergic modulation of glutamate-induced excitations of neurons in the neostriatum and nucleus accumbens of awake, unrestrained rats. Journal of Neurophysiology 75:142-153.

Kiyatkin EA, Rebec GV (1997) Iontophoresis of amphetamine in the neostriatum and nucleus accumbens of awake, unrestrained rats. Brain Res 771:14-24.

Kiyatkin EA, Rebec GV (1999a) Striatal neuronal activity and responsiveness to dopamine and glutamate after selective blockade of D1 and d2 dopamine receptors in freely moving rats. Journal of Neuroscience 19:3594-3609.

Kiyatkin EA, Rebec GV (1999b) Modulation of striatal neuronal activity by glutamate and GABA: iontophoresis in awake, unrestrained rats. Brain research 822:88-106.

Kiyatkin EA, Rebec GV (2000) Dopamine-independent action of cocaine on striatal and accumbal neurons. The European journal of neuroscience 12:1789-1800.

Kiyatkin EA, Kiyatkin DE, Rebec GV (2000) Phasic inhibition of dopamine uptake in nucleus accumbens induced by intravenous cocaine in freely behaving rats. Neuroscience 98:729-741.

Koob GF (1995) Animal Models of Drug Addiction In: Psychopharmacology : the fourth generation of progress (Bloom FE, Kupfer DJ, eds). New York: Raven Press.

Kristensen EW, Wilson RL, Wightman RM (1986) Dispersion in flow injection analysis measured with microvoltammetric electrodes. Analytical Chemistry 58:986-988.

Olds J, Milner P (1954) Positive reinforcement produced by electrical stimulation of septal area and other regions of rat brain. J Comp Physiol Psychol 47:419-427.

Olds ME, Olds J (1963) Approach-avoidance analysis of rat diencephalon. J Comp Neurol 120:259-295.

Owesson-White CA, Cheer JF, Beyene M, Carelli RM, Wightman RM (2008) Dynamic changes in accumbens dopamine correlate with learning during intracranial self-stimulation. Proc Natl Acad Sci U S A 105:11957-11962.

Owesson-White CA, Ariansen J, Stuber GD, Cleaveland NA, Cheer JF, Wightman RM, Carelli RM (2009) Neural encoding of cocaine-seeking behavior is coincident with phasic dopamine release in the accumbens core and shell. Eur J Neurosci 30:1117-1127.

Phillips PE, Stuber GD, Heien ML, Wightman RM, Carelli RM (2003) Subsecond dopamine release promotes cocaine seeking. Nature 422:614-618.

Robinson DL, Carelli RM (2008) Distinct subsets of nucleus accumbens neurons encode operant responding for ethanol versus water. Eur J Neurosci 28:1887-1894.

Robinson DL, Howard EC, McConnell S, Gonzales RA, Wightman RM (2009) Disparity between tonic and phasic ethanol-induced dopamine increases in the nucleus accumbens of rats. Alcohol Clin Exp Res 33:1187-1196.

Roitman MF, Stuber GD, Phillips PE, Wightman RM, Carelli RM (2004) Dopamine operates as a subsecond modulator of food seeking. J Neurosci 24:1265-1271.

Wise RA (2004) Dopamine, learning and motivation. Nat Rev Neurosci 5:483-494.